

A NONLINEAR DYNAMIC ANALYSIS OF
LINE STRUCTURAL MEMBERS

Thesis for the Degree of Ph. D.
MICHIGAN STATE UNIVERSITY
JOHN G. JANSSEN

1968

1968-12



This is to certify that the

thesis entitled

A NONLINEAR DYNAMIC ANALYSIS OF
LINE STRUCTURAL MEMBERS

presented by

John G. Janssen

has been accepted towards fulfillment
of the requirements for

Ph. D. degree in Civil Engineering

R. K. Wen

Major professor

Date Aug. 1, 1968







ABSTRACT

A NONLINEAR DYNAMIC ANALYSIS OF LINE STRUCTURAL MEMBERS

by John G. Janssen

A general numerical procedure for the dynamic analysis of line structural members in which both geometric and material nonlinearities are considered is presented. A lumped mass and lumped flexibility model is formulated by discretizing both the length and the cross-sections of the member. Thus, the method can take into account the effects of axial force-bending moment interactions, large displacements, inelasticity, as well as initial crookedness, residual stresses, initial static loadings, and movements of the supports, if any.

The numerical procedure is based upon a step-by-step numerical integration of the equations of motion. A computer program was written in Fortran for use on Michigan State University's CDC 3600 computer.

The reliability of the numerical approach is demonstrated by comparing solutions obtained from the present analysis with a variety of known solutions. From the comparison it was concluded that the method

of analysis presented does produce results sufficiently accurate for engineering purposes.

Solutions to problems heretofore unsolved are then obtained to demonstrate the usefulness and versatility of the method. These problems include the inelastic dynamic snap-through of arches and the effects of strain hardening and residual stresses on the critical snap load. The failure of an inelastic axially loaded column subjected to transverse support motion was also studied.

A NONLINEAR DYNAMIC ANALYSIS OF
LINE STRUCTURAL MEMBERS

by

John G. Janssen

A THESIS

Submitted to
Michigan State University
in partial fulfillment of the requirements
for the degree of

DOCTOR OF PHILOSOPHY

Department of Civil Engineering

1968

C 521.1
1972

ACKNOWLEDGMENTS

The author would like to express his deep gratitude and appreciation to his advisor, Dr. R. K. Wen, whose guidance and assistance were invaluable throughout the author's graduate program and especially during the course of this investigation. Thanks are also due the other members of the author's guidance committee, Dr. C. E. Cutts, Chairman of the Department of Civil Engineering, Dr. J. S. Frame, and Dr. L. E. Malvern, for their encouragement and inspiration.

Special thanks are extended to the National Science Foundation for their support of this investigation through Grant #GK-590, and to the Division of Engineering Research. Also, the personnel of the computer laboratory deserve thanks for their advice and cooperation during the course of this study.

The author will forever be indebted to his wife, Susan, whose help and encouragement have made his work immeasurably easier.

TABLE OF CONTENTS

	Page
ACKNOWLEDGMENTS	ii
LIST OF TABLES	v
LIST OF FIGURES	vi
Chapter	
I. INTRODUCTION	1
1.1 General	1
1.2 Related Works	2
1.3 Organization of Report	4
1.4 Notation	4
II. DISCRETE MODEL	7
2.1 Introduction	7
2.2 Subelement Arrangements Investigated	8
2.3 Formal Element Adopted	10
2.4 Spring System Representation of Flexibility	12
2.4.1 General	12
2.4.2 Deformation of Springs	13
2.4.3 Spring Force-Deformation Relation	14
2.4.4 Internal Spring Force Resultants	15
III. METHOD OF ANALYSIS	16
3.1 Introduction	16
3.2 Geometric Considerations	16
3.3 Equations of Motion	18
3.4 Support Conditions	19
3.5 Initial Residual Stresses	20
3.6 Arches and Initial Crookedness	22
3.7 Initial Static Loads	23
IV. NUMERICAL PROCEDURE AND COMPUTER PROGRAM	24
4.1 Introduction	24
4.2 Numerical Integration Procedure	24
4.3 Step-By-Step Numerical Solution	25
4.4 Stability of the Numerical Solution.	27

Chapter	Page
4.5 Computer Program	29
4.6 Energy and Impulse-Momentum Check	31
4.6.1 General	31
4.6.2 Energy Check	32
4.6.3 Impulse-Momentum Check	34
V. COMPARISON STUDIES	35
5.1 Introduction	35
5.2 Fixed-Fixed Elastic Beam	36
5.3 Elastic Circular Arch	37
5.4 Imperfect Elastic Column	38
5.5 Simply Supported Inelastic Beam	39
VI. NUMERICAL EXAMPLES	41
6.1 Introduction	41
6.2 Dynamic Snap Through of Arches	41
6.2.1 Inelastic Arches	41
6.2.2 Effect of Strain Hardening on the Critical Dynamic Snapping Load	42
6.2.3 Effect of Residual Stresses on the Critical Dynamic Snapping Load	44
6.2.4 Effect of Model Bias	44
6.2.5 Comparison with Static Arch Buckling	46
6.3 Effects of Support Motion on a Column	47
VII. CONCLUSIONS	49
BIBLIOGRAPHY	52
TABLES	57
FIGURES	58
APPENDIX. COMPUTER PROGRAM	76

LIST OF TABLES

Table	Page
1. Comparison Study of Elastic Circular Arch .	57
2. Effect of Strain Hardening and Residual Stresses on the Critical Dynamic Snapping Load, P_s , of a Pin-ended Arch	57

LIST OF FIGURES

Figure		Page
2.1	Spring System Representation of Lumped Flexibility	58
2.2	Model Element Assemblies	59
2.3	"Formal" and "Modified" Models	60
2.4	Bilinear Stress-Strain Relation	61
3.1	Portion of Deformed Model	61
3.2	Free-Body Diagrams of a Mass Point and a Massless Panel	61
3.3	Treatment of Boundary Conditions Involving Prescribed Support Rotation . . .	62
3.4	Residual Stress Representation	63
4.1	Flow Diagram for One Step of Integration . .	64
5.1	Response History for Center Displacement . .	65
5.2	Response History for Quarter Point Displacement	66
5.3	Elastic Circular Arch	67
5.4	Large Displacements of a Column	68
5.5	Comparison of Large and Small Deflection Solutions for a Small Deflection Problem . .	69
5.6	Comparison of Large and Small Deflection Solutions for a Large Deflection Problem . .	70
6.1	Snap-Through of an Arch ($N = 10$)	71
6.2	Dynamic Snap-Through Loads of a Shallow Arch	72

Figure	Page
6.3 Evaluation of Model Bias	73
6.4 Maximum End Displacement vs. Peak Support Motion	74
6.5 Permanent Lateral Set at ζ vs. Axial Load . .	75

CHAPTER I

INTRODUCTION

1.1 General

There has been much interest in the study of structures subjected to earthquake or blast loadings. Under these loading conditions the ultimate strength and the associated deformations are of interest to the engineer. In order to determine these sufficiently accurately, an inelastic, large deflection (i.e., geometric nonlinearities considered) analysis is usually required.

This thesis is concerned with the dynamic inelastic analysis of line structures (i.e., structures in which the length is much greater than either the depth or the breadth) which includes beams, columns, and arches. The study is limited to response contained in one of the principal planes of bending.

In this investigation a lumped mass and lumped flexibility model is used to approximate a line member of arbitrary shape and cross-section. The cross-section of the member as well as its length is discretized so that the moment-thrust interaction is implicitly considered in the model. The equations of motion of the masses are

integrated numerically. Large deflections are considered even though the deformation of each lumped flexible joint is assumed to be small. This analysis also takes into account the effects of axial inertia, residual stresses, inelasticity, and support motion.

1.2 Related Works

The work of Newmark (32)* in obtaining a numerical solution of the buckling load for an elastic beam-column is well known. Salvadori (38) solved the same problem by finite difference techniques. Eppink and Veletsos (10) studied the dynamic response of elastic circular arches by using a lumped mass, lumped flexibility model instead of directly applying finite difference techniques to the differential equations for the continuum structure.

Wen and Toridis (51) studied three discrete models for elasto-inelastic beams without considering geometrical nonlinearity and axial loads. The models studied were: model A, lumped flexibility and continuous mass; model B, lumped mass and lumped flexibility; and model C, lumped mass and continuous flexibility. Beylerian (6) also used a lumped parameter model to study the effects of shear deformations on the response

*Numbers refer to references listed in the Bibliography.

of inelastic beams. In the study the interaction of bending moment and shear on the elasto-plastic response was taken into account.

Analytical studies of the response of an elastic column with a small sinusoidal imperfection under the dynamic loading condition that one end of the column is forced toward the other were made by Hoff (18) and Sevin (40, 41). Sevin considered the effect of axial inertia while Hoff did not. Bailey (2) improved upon the works of Hoff and Sevin by taking into account the effects of large deflections as well as axial inertia.

In studying the inelastic static behavior of wide flange steel beam-columns Ketter, Kaminsky, and Beedle (22) developed a series of moment-thrust interaction curves. Galambos and Ketter (14) used these interaction curves to determine the inelastic critical load (i.e., the load at which Newmark's numerical procedure, when applied to the inelastic member, would just fail to converge). They also considered the effects of residual stresses on the moment thrust interaction curves and the aforementioned critical load.

The static behavior in the inelastic range of line members with rectangular cross-sections was studied by Malvick and Lee (28) and Lee and Murphy (26). Both straight columns with small initial deflections and circular arches were studied in the small deflection range.

A feature of their analyses is the discretization of the cross-section into a finite number of subareas.

1.3 Organization of Report

In Chapter II a basic element is formulated of which the model of the continuous member is constructed. Chapter III concerns the derivation of the equations governing the behavior of the model. The treatment of the support conditions, residual stresses, initial crookedness and static loadings are also considered in this chapter. In Chapter IV the numerical solution of the governing equations is presented. In the same chapter a section on the computer program used in this study is also included along with the impulse-momentum and energy checks on the numerical solution. The credibility of the model is examined in Chapter V by comparing its numerical results for certain problems with solutions that have been presented in the literature. In Chapter VI the dynamic behavior of several arches, including the "snapping through" phenomenon, is depicted. The failure of a column subjected to a lateral motion of one of the supports is also considered.

1.4 Notation

The symbols listed below have been adopted in this investigation.

A	= area of the continuous cross-section;
A_{ij}	= j th lumped area of the i th discrete cross-section;
Amp	= rise of sinusoidal arch;
d_{ij}	= deformation of the j th spring in the i th spring system;
dh_i	= relative displacement of the i th spring system;
E	= Young's modulus;
E_p	= inelastic modulus;
f_{ij}	= force in the j th spring of the i th spring system;
$Flex_i$	= lumped flexibility at the i th joint;
$flex(s)$	= distributed flexibility;
h_i	= deformed length of the i th element;
h_o	= initial element length;
i	= subscript referring to joints or panels;
I	= moment of inertia of the continuous cross-section;
j	= subscript referring to parameters dealing with the j th subarea;
L	= length of the member as measured along the centroidal axis;
m	= mass per unit length of the continuous member;
m_i	= i th lumped mass;
M_i	= moment at the i th joint;
n	= number of elements in the discrete model;
P_i	= longitudinal load lumped at the i th joint;
P_y	= $A\sigma_y$;
P_a	= magnitude of asymmetric loading;

- p_b = magnitude of uniformly distributed loading;
 q_i = transverse load lumped at the i th joint;
 R = radius of circular arch;
 R_{sh} = strain hardening parameter, E_p/E ;
 r = radius of gyration of the continuous cross-section about the axis of bending;
 s = distance measured along centroidal axis of the member;
 T_i = axial force in the i th panel;
 $T_f = \frac{2L^2}{\pi} \sqrt{\frac{m}{EI}}$;
 t & t_i = time, the subscript referring to a particular instant;
 Δt = time increment;
 u_i = displacement in the x -direction of the i th mass;
 v_i = shear in the i th panel;
 v_i = displacement in the y -direction of the i th mass;
 x_i = x -coordinate of the i th mass;
 x_{o_i} = initial x -coordinate of the i th mass;
 y_i = y -coordinate of the i th mass;
 y_{o_i} = initial y -coordinate of the i th mass;
 z_{ij} = distance of A_{ij} from the neutral axis;
 ϕ_{o_i} = rotational correction factor applied to the i th joint;
 ϕ_i = relative rotation of the i th joint;
 ρ = density of member material;
 σ_y = yield stress of the member material;
 θ_i = angle between i th element and the x -axis.

CHAPTER II

DISCRETE MODEL

2.1 Introduction

The model considered in this work has both the flexibility and the mass of the line structure lumped at discrete points along its length. This approach was hinted by the results of Wen and Toridis (51) which showed that a seemingly more accurate approach (either model A or C) would not necessarily lead to a more accurate solution.

The model for the entire member is composed of a series of elements joined together. Each element is made up of subelements. These subelements are rigid panels, lumped mass points (rotatory inertia not included) and lumped flexible systems. Each of the subelements represents the corresponding properties of length (geometry), mass, and flexibility for a portion of the continuous member.

The flexible systems are composed of a finite number of parallel springs located between two rigid parallel faces that are perpendicular to the adjacent panels (see Fig. 2.1). In order to determine the

deformation and the force in each spring of a flexible system, the rotation and compression distortion of the flexible system are required. Hereafter the flexible systems will be referred to as "spring systems."

In this chapter three types of elements based on different arrangements of the subelements will be considered. The reason for adopting one in favor of the others will be discussed. In addition the manner of lumping the flexibility into spring systems will be described.

2.2 Subelement Arrangements Investigated

In Fig. 2.2 are shown the elements and their corresponding assemblies considered in this chapter. The element, B-1, in Fig. 2.2a consists of a lumped mass at either end and two spring systems contiguous to the masses. A rigid massless panel connects the spring systems. In this configuration the lumped masses and flexibilities represent the mass and flexibility of the continuous member corresponding to one-half of the panel length.

Due to its symmetric arrangement, this element has a strong intuitive appeal. However, it has one serious drawback. The model assembled from this element is kinematically indeterminate, i.e., it is not possible to determine the distortions of each spring

system entirely from considerations of the kinematics of the displacements of the mass points alone. Consideration of any joint (see Fig. 2.2a for definition) reveals that, given the total relative rotation of that joint, it is necessary to proportion this rotation between the two spring systems located at that joint. Since the mass lumped at the joint is assumed to possess no rotational inertia, it is required that the moments generated by the two spring systems be equal. An equilibrium condition must therefore be satisfied.

Similarly by considering the relative displacements of the two masses at the ends of an element, it is seen that the total compression in this element must be appropriately proportioned between the two spring systems at the two ends to satisfy the equilibrium condition that the axial forces generated by these two spring systems be equal. It should be noted that these two equilibrium conditions are coupled among the successive joints and panels.

It is possible, given the boundary conditions of the problem, to write a set of simultaneous equations which incorporates both the geometric and the equilibrium conditions of the problem. A solution of this set of equations would yield the spring system distortions, provided that the solution exists and is unique, which would be true in the linearly elastic case. It is,

however, easily conceivable that in a nonlinear problem in which yielding takes place, the solution of these equations would be very difficult, if not impossible, to find.

In Fig. 2.2b is shown element B-2. By lumping the flexibility at only one end of the element the difficulties associated with element B-1 are eliminated. In this case the spring distortions can be uniquely determined directly from the mass point coordinates without the necessity of solving a set of simultaneous equations. This greatly simplifies the analysis. This element, however, lacks the appealing symmetry of element B-1.

It is possible to obtain a symmetric element different from B-1, by lumping the flexibility at the center as shown in Fig. 2.2c. It turns out that this element B-3, leads to a model which may or may not be kinematically determinate depending upon the boundary conditions. Even in the cases where the boundary conditions lead to a kinematically determinate model, a set of nonlinear simultaneous equations must be solved in order to determine the spring system distortions.

2.3 Formal Element Adopted

Due to the complications which would arise in the utilization of element B-1 and B-3, they were not

used. Element B-2, in spite of its asymmetry, was adopted in this investigation because it makes the analysis manageable. The individual elements B-2 are then assembled to form a formal model of the continuous member as illustrated in Fig. 2.3a. In this case the model represents a beam-column with one end fixed and the other end simply supported as shown at the top of the figure. The coordinate axes are shown as well as the numbering of the masses, the flexible systems, and the massless rigid panels. The flexibilities are lumped in the following manner:

$$\begin{aligned} \text{Flex}_1 &= \int_0^{h_0} \text{flex}(s) \, ds \\ \text{Flex}_i &= \int_{s_i}^{s_{i+1}} \text{flex}(s) \, ds \quad \dots (2-1) \\ \text{Flex}_{n+1} &= 0 \end{aligned}$$

where Flex_i denotes the lumped flexibility at the i th joint, $\text{flex}(s)$ the flexibility distributed along the length, and s the distance along the member axis.

An inspection of the "formal" model in Fig. 2.3a reveals that it is asymmetric; there is a spring system adjacent to the left support but not the right. As will be shown later, the error introduced by approximating the continuum member with this model would be aggravated in this case if one or both of the ends of the member were

fixed. In order to alleviate this difficulty, a slight variation of the formal model is introduced. The modified model is shown in Fig. 2.3b. The difference between the formal model and the "modified" model lies in the manner of defining what portion of the continuous member each spring system represents. In contrast to Eqs. (2-1), the following equations define the lumped flexibilities for the modified model.

$$\text{Flex}_1 = \int_0^{h_o/2} \text{flex}(s) \, ds$$

$$\text{Flex}_i = \int_{s_i - h_o/2}^{s_i + h_o/2} \text{flex}(s) \, ds \quad \dots (2-2)$$

$$\text{Flex}_{n+1} = \int_{L - h_o/2}^L \text{flex}(s) \, ds$$

It should be noted in passing that for a prismatic member the amount of flexibility lumped at an interior joint is the same for both the formal and modified models.

2.4 Spring System Representation of Flexibility

2.4.1 General.--The flexibility of the member is lumped in spring systems at discrete points along the member as described in the previous sections. In this section the discretization of the flexibility over the cross-section of the member is considered. This discretization is

consistent with the philosophy of the discretization of the mass and flexibility along the length of the member.

As mentioned earlier the spring systems are each represented by a collection of parallel springs connected to two rigid faces. The cross-sectional area of the continuous member is divided into an appropriate number of subareas of some appropriate shape. In Fig. 2.1 is shown a spring system which represents the cross-section of a wide flanged member. A_{ij} represents the j th subarea of the i th cross-section, and z_{ij} is the distance from the neutral axis of the member to the centroid of A_{ij} . The positive direction of z_{ij} is opposite to that of y .

Each spring in a spring system represents the axial flexibility of a prismatic bar whose length, h_o , is that of the rigid panel and whose cross-sectional area is that of the corresponding subarea. The spring is located at the same distance from the neutral axis as that of the centroid of the subarea to which it corresponds.

2.4.2 Deformation of Springs.--In order to calculate the force in each of the springs in a spring system, it is necessary to determine the deformation in each spring. There are two parameters which uniquely determine the deformation of every spring in the spring system. These two parameters are the relative rotation, ϕ_i , and the relative displacement, dh_i , of the faces of the spring system.

Referring to Fig. 2.1 and assuming ϕ_i is small, the deformation of the j th spring in the i th spring system is given by:

$$d_{ij} = dh_i + \phi_i z_{ij} \quad \dots (2-3)$$

Spring deformations are considered positive if they are compressed, and positive rotations are those which cause compression in the springs with $z_{ij} > 0$.

2.4.3 Spring Force-Deformation Relation.--Once the deformation of a spring has been determined, the force in it can be found from the force deformation relation for that spring. The force deformation relation for any particular spring is dependent upon the stress-strain relation of the continuous member material, the length discretization, and the area which that spring represents. For each spring the force deformation diagram is obtained by respectively multiplying the scales of the stress and strain axes of the stress-strain diagram by the subarea, A_{ij} and by the panel length, h_o .

Used in this work is the bilinear stress-strain relation in which hysteresis and strain hardening are taken into account as shown in Fig. 2.4. Of course, the method of analysis as presented is not restricted to this type of stress-strain relation. More general types such as trilinear or curvilinear relations may be employed.

2.4.4 Internal Spring Force Resultants.--Once the spring forces are known, the internal force resultants can be calculated by the familiar equations of mechanics. The moment is given by:

$$M_i = \sum_j f_{ij} z_{ij} \quad \text{.....(2-4)}$$

and the thrust is given by:

$$T_i = \sum_j f_{ij} \quad \text{.....(2-5)}$$

where f_{ij} is the force in the j th spring of the i th spring system.

CHAPTER III

METHOD OF ANALYSIS

3.1 Introduction

Up to now the main topic under consideration has been the formulation of the model used to approximate the actual continuum structure. Once the model has been established, the next step is to derive the equations which govern its behavior.

3.2 Geometric Considerations

In Fig. 3.1 is shown a portion of the deformed structure. The deformed length of the i th element including the spring system, is given by

$$h_i = \sqrt{(x_{i+1} - x_i)^2 + (y_{i+1} - y_i)^2} \quad \dots (3-1)$$

where x_i and y_i are the x and y coordinates of the i th mass. The compression in the i th spring system is

$$\Delta h_i = h_0 - h_i \quad \dots (3-2)$$

where h_0 was defined previously as the initial panel length. The angle that the i th panel makes with the

x-axis is not explicitly needed in the computations. However the sine and cosine of this angle are. They are given by

$$\sin\theta_i = \frac{y_{i+1} - y_i}{h_i} \quad \text{..... (3-3)}$$

and

$$\cos\theta_i = \frac{x_{i+1} - x_i}{h_i} \quad \text{..... (3-4)}$$

Denoting the angles of the adjacent panels by θ_{i-1} and θ_i , the relative rotation of the spring system is given by

$$\phi_i = \theta_{i-1} - \theta_i \quad \text{..... (3-5)}$$

Taking the sine of both sides of Eq. (3-5) and using the appropriate trigonometric identity and finally taking the arcsine of both sides, the required relative rotation is found to be

$$\begin{aligned} \phi_i = \arcsine(\cos\theta_i \sin\theta_{i-1} \\ - \sin\theta_i \cos\theta_{i-1}) \end{aligned} \quad \text{..... (3-6)}$$

Since the relative rotation of a spring system is assumed to be small, the multi-valuedness of Eq. (3-6) is inconsequential. Note that the limitation of smallness of the

relative rotation of the spring systems does not preclude large rotations of the panels.

3.3 Equations of Motion

In Fig. 3.2 are shown a free-body diagram of a mass point and of an adjacent massless panel. The forces acting on this typical mass and panel are shown in their positive sense. For simplicity the external loads are assumed to act at the mass points.

The equations of motion for this mass point are obtained by applying Newton's second law of motion.

$$\begin{aligned} m_i \ddot{u}_i &= T_{i-1} \cos \theta_{i-1} + V_{i-1} \sin \theta_{i-1} \\ &\quad - T_i \cos \theta_i - V_i \sin \theta_i - p_i \end{aligned} \quad \text{..... (3-7)}$$

$$\begin{aligned} m_i \ddot{v}_i &= T_{i-1} \sin \theta_{i-1} - V_{i-1} \cos \theta_{i-1} \\ &\quad - T_i \sin \theta_i + V_i \cos \theta_i + q_i \end{aligned} \quad \text{..... (3-8)}$$

where m_i is the i th lumped mass, \ddot{u}_i and \ddot{v}_i are the accelerations in the x and y directions respectively, V_i is the shear in the i th panel, and q_i and p_i are the external loads.

Since the shears cannot be determined directly from the deformations which are being considered, it is necessary to determine them in some other manner. By writing an equation of moment equilibrium



about one end of a massless panel it is possible to find the shear resultant in terms of the end moments of the panel. This relationship is given by

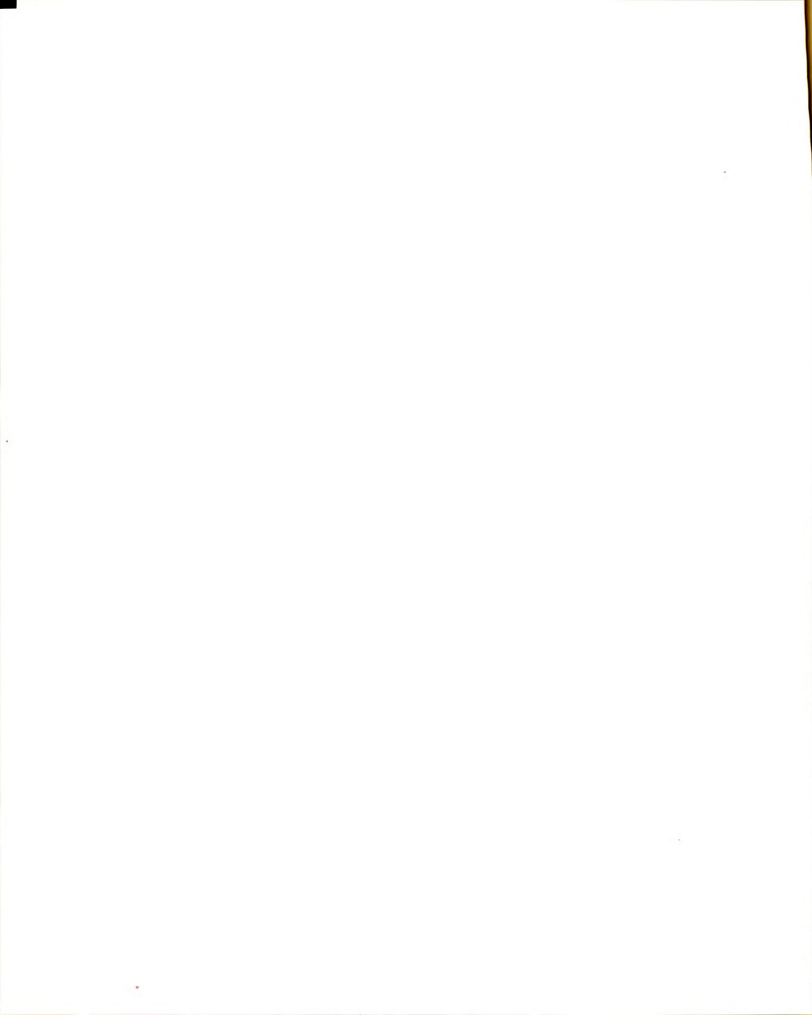
$$V_i = \frac{1}{h_i} (M_{i+1} - M_i) \quad \dots (3-9)$$

It should be pointed out that the element length h_i in the above relation is not constant; it depends on the linear deformations of the spring system.

3.4 Support Conditions

For a continuum member, three boundary conditions may be imposed at each end of the member by prescribing either the displacement or the corresponding reaction for each of the coordinates: u , v , and ϕ . The standard support conditions of "free," "roller," "hinged," and "fixed" are special cases of the preceding.

In general the interpretation of the boundary conditions for the model is obvious and need not be discussed except in the case where the rotation of the support is prescribed in the continuum problem. If there is no spring system at the support point (as at the right end of the formal model), the rotation of the adjacent rigid bar should be taken to be the same as the prescribed support rotation since the bar is fixed to it. If there is a spring system at the support (as at the

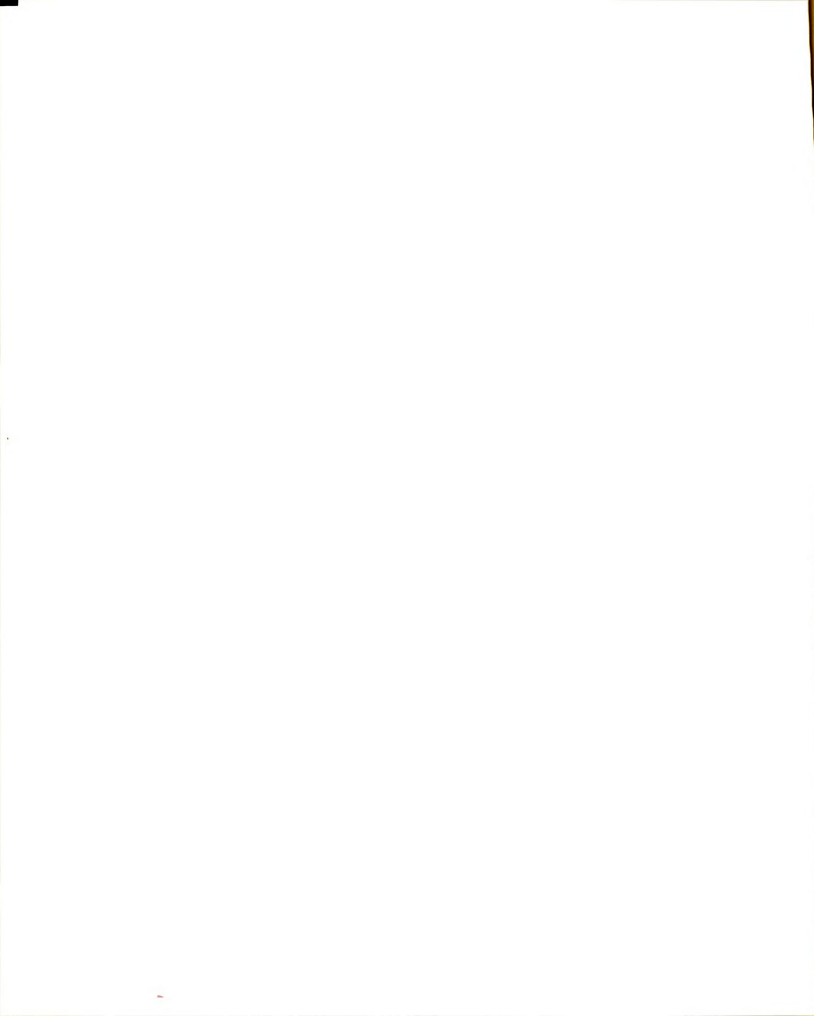


left end of the formal model and both ends of the modified model) the appropriate face of the spring system is fixed to the support as shown in Fig. 3.3; and the adjacent rigid bar is allowed to rotate. The relative rotation of the spring system is then determined by finding the rotation of the rigid bar relative to the support.

In the use of the modified model for prismatic members, the flexibilities of the spring systems lumped at the supports are half that of the interior systems. It is convenient from a computational point of view to consider all spring systems to possess the same flexibility and double the relative rotations of the spring systems at the supports. This has the same effect of halving the flexibility at the support as the model is formulated.

3.5 Initial Residual Stresses

In certain cases of rolled steel sections there may be self-equilibrating residual stresses distributed over the cross-section due to the forming and subsequent cooling process. These stresses would influence the response of the member in the inelastic range. In this study it is assumed that the distribution of residual stresses remains constant along the length of the member (14).

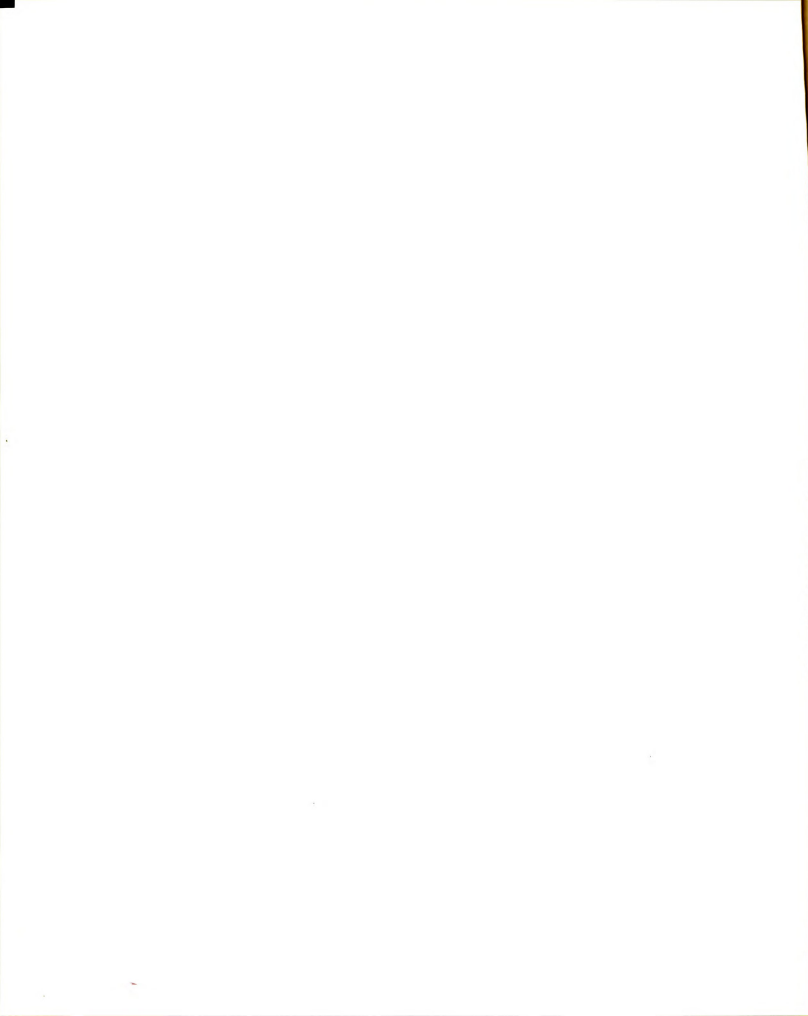


The cross-section of the member is divided in a manner that would allow a reasonable approximation to the residual stress pattern. In dividing the flange areas, it may be necessary to lump at least two areas in order to consider the variation of the residual stresses there. For example, in a wide flanged member both tension and compression stresses exist in each flange (14). In this case it is necessary to consider at least two lumped areas to represent each flange, one area for tension and one for compression as shown in Fig. 3.4. The lumped area corresponding to the compression residual stresses in the flange represents the two exterior portions of the flange away from the web while the lumped area corresponding to the tension residual stresses represents the remaining interior area of the flange.

The problem is initialized by pre-setting the force intercepts of the force deformation diagrams accordingly. They are pre-set in such a way that the force due to zero spring deformation is given by

$$f_{ij} = \int_{A_{ij}} \sigma_r dA \quad \dots (3-10)$$

where σ_r is the residual stress acting over the subarea A_{ij} .



3.6 Arches and Initial Crookedness

Since the procedure is developed within the framework of large displacement theory, it is capable of treating structural members with initial shapes other than the perfectly straight. These would include arches which may be considered to have "alignments" which are far removed from perfectly straight or members with slight imperfections or crookedness as occasionally imparted to rolled steel sections during manufacture.

A method of handling these initial "misalignments" consists of describing the initial coordinates of the mass points such that they approximate the shape under consideration. The sum of the lengths of the massless panels which make up the model may be taken to be the length of the member. Each panel is assumed to be straight. The manner of computing the initial coordinates may consist of prescribing the value of the y-coordinate for each mass of the model, and then computing the x-coordinate in such a manner that the distance between two adjacent masses is equal to the length of the massless panel, h_0 , i.e.,

$$x_{o_i} = \sqrt{h_0^2 - (y_{o_i} - y_{o_{i-1}})^2} + x_{o_{i-1}} \quad \dots (3-11)$$

where x_{o_i} and y_{o_i} are respectively the initial x and y coordinates of the ith mass.

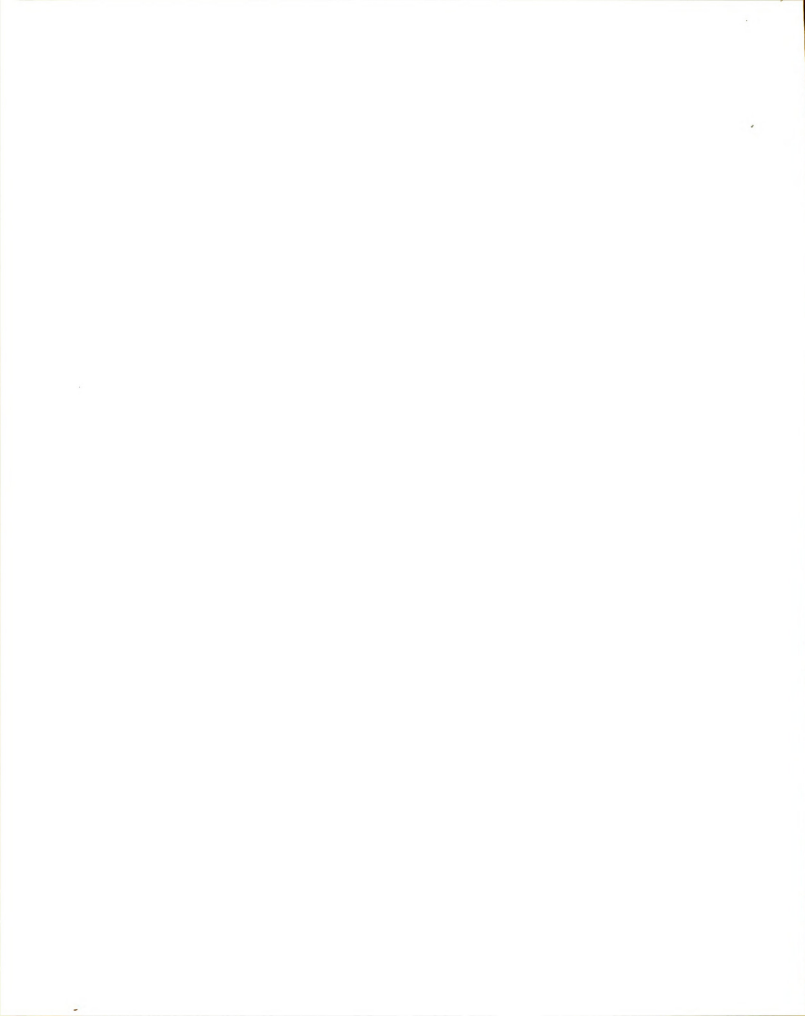


It should be noted that for an initially non-straight member there exists at each spring system some initial rotation which must be accounted for in the computation of the deformation of the spring systems. This may be done by applying to Eq. (3-5) a correction factor ϕ_{0_i} , taken equal to the negative of the initial relative joint rotation. In this manner any bending rotations computed are relative to the initial configuration of the model. Thus Eq. (3-5) takes the form:

$$\begin{aligned} \phi_i = & \arcsine(\cos\theta_i \sin\theta_{i-1} \\ & - \sin\theta_i \cos\theta_{i-1}) + \phi_{0_i} \quad \dots\dots(3-12) \end{aligned}$$

3.7 Initial Static Loads

In order to make the treatment of one dimensional structural members more complete, the effects of the initial static loadings should be considered. This can be accounted for by setting the initial values of the displacements and forces to those called for by static equilibrium requirements.



CHAPTER IV

NUMERICAL PROCEDURE AND COMPUTER PROGRAM

4.1 Introduction

In the preceding chapters a nonlinear model of a line structural member and the equations governing its behavior have been developed. In this chapter the numerical procedure used to calculate the model's response is presented. This numerical procedure includes the adaptation of a numerical integration technique to a step-by-step solution of the governing equations of motion. A computer program based on the method developed was written. This program is briefly discussed along with its capabilities and limitations.

4.2 Numerical Integration Procedure

The particular numerical technique adopted for this study is from the class of self-starting single step marching integration methods studied by Tung and Newmark (49) and Newmark (33). In particular the method used in this work is the so-called $\beta = 0$ method. This method has the advantage of being non-iterative if the accelerations are not explicitly dependent on the velocities of



the mass points. This is the case in the problem at hand since damping is not considered.

Let the acceleration, velocity, and displacement of a mass, say, the i th mass, in the x -direction be given by \ddot{u}_i , \dot{u}_i , and u_i respectively. Then the $\beta = 0$ method prescribes the velocity and displacement at time $t_j + \Delta t$ in terms of the displacement, velocity, and acceleration of the mass point by the following relations:

$$\begin{aligned} u_i(t_j + \Delta t) &= u_i(t_j) + \Delta t \dot{u}_i(t_j) \\ &\quad + \frac{1}{2} \Delta t^2 \ddot{u}_i(t_j) + O(\Delta t^3) \end{aligned} \quad \text{.....(4-1)}$$

$$\begin{aligned} \dot{u}_i(t_j + \Delta t) &= \dot{u}_i(t_j) + \frac{1}{2} \Delta t \left[\ddot{u}_i(t_j) \right. \\ &\quad \left. + \ddot{u}_i(t_j + \Delta t) \right] + O(\Delta t^2) \end{aligned} \quad \text{.....(4-2)}$$

A similar set of equations is obtained for the y -direction by substituting v for u in the above relations. The manner in which these equations are employed in the solution process is explained in the following section.

4.3 Step-By-Step Numerical Solution

The general procedure involved in extending the solution from time t_j to $t_j + \Delta t$ is briefly explained below. A generalized flow diagram of a single step is presented in Fig. 4.1, in which the boxes represent

intermediate stages in the completion of the step and the arrows represent advancements.

It is necessary at the start of the problem to establish the initial values of the quantities relevant to the solution. These, for example, include displacements, velocities, and accelerations of the mass points. In addition, the force deformation relation for each spring must be pre-set to its initial state.

Once the relevant quantities have been initialized the fundamental problem is to determine these quantities one increment or step into the time domain. Once this fundamental problem has been solved it is only necessary to reapply the solution of the single step repeatedly to advance the solution of the given problem the desired distance into the time domain.

At the beginning of each step, for example, the step starting at time t_j , all the relevant quantities are known. The first advancement in the step is the determination of the displacements $u_i(t_j + \Delta t)$ and $v_i(t_j + \Delta t)$. These are either prescribed or computed by numerical integration of the equations of motion as the case may be. In general, the interior masses are free to move and are governed by the equations of motion while the end masses may be either case, depending upon the boundary conditions. Once the displacements of the mass points are known their coordinates are given by:



$$x_i(t_j + \Delta t) = x_{0i} + u_i(t_j + \Delta t) \quad \dots\dots(4-3)$$

$$y_i(t_j + \Delta t) = y_{0i} + v_i(t_j + \Delta t) \quad \dots\dots(4-4)$$

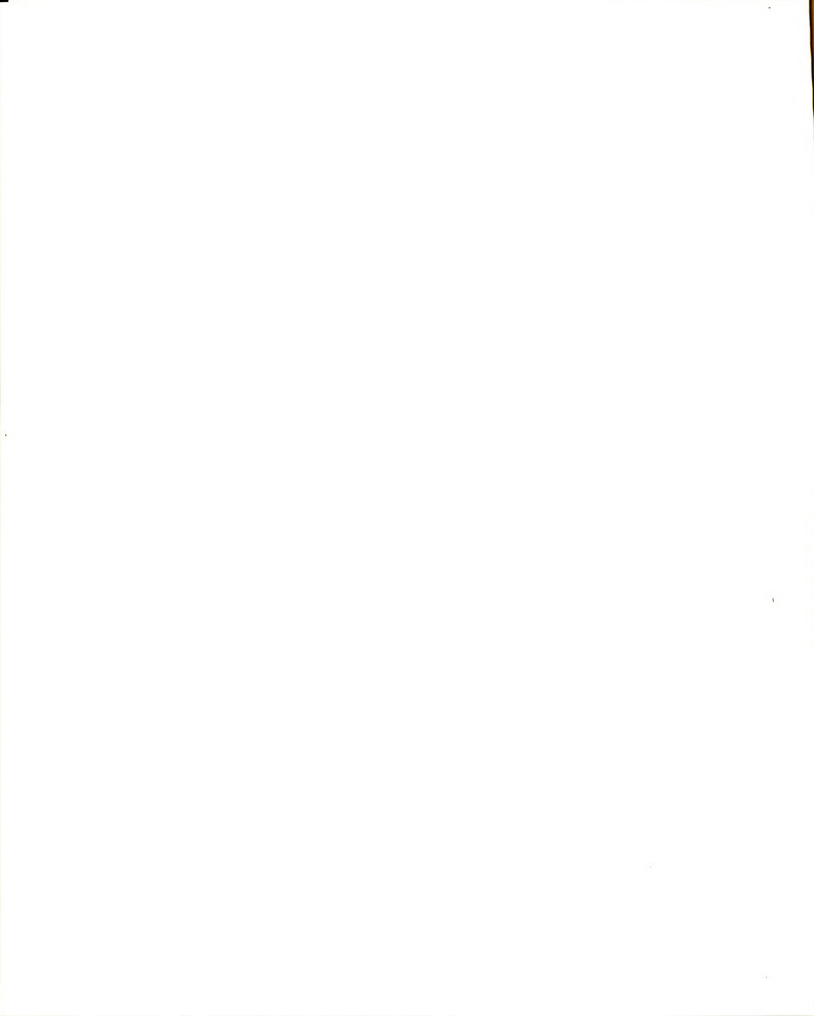
From these coordinates the spring deformations are computed from the geometric relations derived in Chapters II and III.

The second advancement in the step is the determination of the spring forces from the spring deformations. From these forces the internal force resultants are obtained from Eqs. (2-4) and (2-5). These forces along with any externally applied forces and considerations of the geometry changes of the structure obtained in the first advancement are then used to compute the accelerations of the mass points in the third advancement. Once the accelerations are determined, the velocities of each mass point can be found by applying Eq. (4-2).

At this intermediate stage in the step, all the relevant quantities have been established for the next time, $t_j + \Delta t$. The fourth and final advancement consists of incrementing the time such that $t_j + \Delta t$ becomes t_{j+1} and the situation is similar to that at the beginning of the previous step. In this manner the equations of motion may be integrated along the time axis as far as desired.

4.4 Stability of the Numerical Solution

Tung and Newmark (49) have shown that stability of the numerical integration method, $\beta = 0$, requires that the

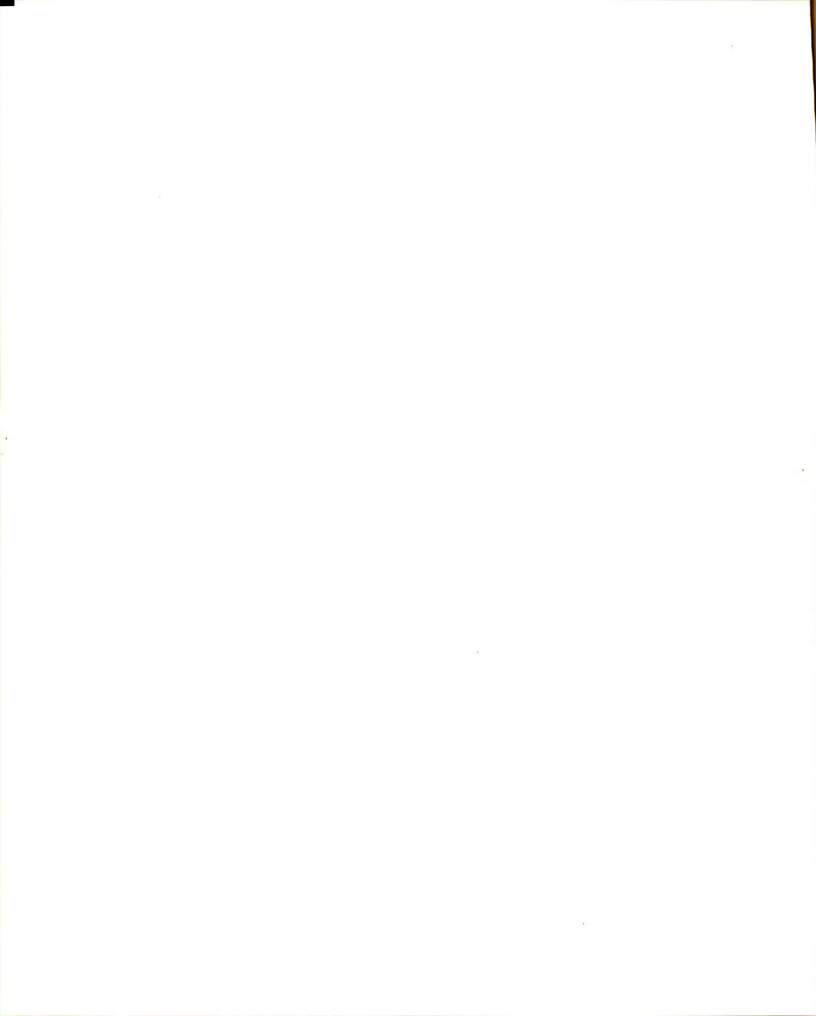


maximum time increment be less than $\frac{1}{\pi}$ times the smallest period of elastic vibration of the system under consideration. In general it is not convenient nor necessary to exactly determine this period in order to choose a time increment. It is only necessary to estimate the value of the smallest period of vibration and then take a fraction of it to insure that the time increment is less than the critical value.

For the model under consideration there are two basic types of motion, transverse or bending vibrations and longitudinal or axial vibrations. The time increment is selected by first finding the n th (where n is the number of rigid massless panels in the model) elastic bending period of vibration of a simply supported span which possesses the same length L , modulus of elasticity E , moment of inertia I , area A , and distributed mass m as the continuum structural member under consideration. The n th elastic axial period of vibration of a column with both ends fixed is similarly computed. The time increment is then taken as $1/10$ of the smaller of these two values as shown below.

$$\Delta t = \min. \left[\frac{1}{10} \frac{2L^2}{\pi n^2} \sqrt{\frac{m}{EI}} ; \frac{1}{10} \frac{2L}{n} \sqrt{\frac{m}{EA}} \right] \quad \dots (4-5)$$

This approach of choosing a time increment was used by Wen and Toridis (51) with considerable success, although



in their case they only needed to consider bending vibrations.

In order to test the stability of the numerical solution based upon the above method of time increment selection, the response of a particular member was calculated by using several values for the increments. The time increments used in the solution were multiples of the "standard increment" as given by Eq. (4-7). The particular system studied is the fixed-fixed uniformly loaded elastic beam (with $n=10$) presented in section 5.2.

The following multipliers of the standard time increment were considered: $1/2$, 1, 3, 4, and 10. The response of the beam for multipliers $1/2$, 1, and 3 varied by less than 1%. However, the response of the beam for the multiplier 4 was different from the above three by 150%. The response for multiplier 10 was erratic and obviously unstable. The stability limit for the problem under consideration thus seems to lie between 3 and 4 times the standard time increment, as expected.

4.5 Computer Program

The numerical method presented in the foregoing was programmed for solution on the Michigan State CDC 3600 computer system using 3600 Fortran. The program can consider a model with up to 40 panels and 10 discrete cross-sectional areas. In order to simplify the program, however,

it has been limited to prismatic members with bilinear stress-strain relations. Two versions of the program have been developed; one considers circular arches, the other straight members with sinusoidal imperfections of the form

$$y_{o_{i+1}} = \text{Amp} \cdot \sin \frac{i\pi}{n} ; i = 0, 1, \dots, n \quad \dots (4-6)$$

Both versions of the program solve the problem in exactly the same manner. Only the schemes in which the geometric properties and the loadings are input and initialized are different. The program for the circular arch is presented in the Appendix.

The input for the program consists of the geometric and material properties of the member, the support conditions, the external loadings, prescribed motions, if any, of the supports, the strains due to existing static loadings, the strain intercepts for residual stresses, if any, the number of panels used, interval to be covered by the solutions, and the number of print requests per unit time. At periodic intervals of time, as specified in the input, the computer prints out a graphic display of the displaced member, the coordinates of the mass points, the spring deformations and the corresponding spring forces, the joint rotations and the element compressions, the moments and thrusts, and the energy check parameters (to be discussed in section 4-6). At the end of each problem, the computer

also presents a graphic display of the response history of the center mass point.

In problems in which support motion is a factor, the following restriction exists. Support motion may not be prescribed for either rotational degree of freedom. In addition, of the four remaining translational degrees of freedom only one may have a prescribed motion. This restriction could be removed, if necessary, without a great deal of reprogramming.

The compiling time on the CDC 3600 computer for the program is about 1 min. and 15 sec. The run time will depend mainly upon the number of panels and the length of time for which the solution is sought. For a typical problem with 10 panels, 4 discrete areas in the cross-section, and a total problem time of 3 fundamental elastic bending periods of vibration, a run time of 4 minutes is about average.

4.6 Energy and Impulse-Momentum Check

4.6.1 General.--In the analysis and the computer program presented there are at least four sources of error. The first source arises from the discrete approximation of a continuum member (the effectiveness of this approximation is studied in Chapter V by comparing results with known continuum solutions). The second source arises from the truncation of the numerical integration formulas, Eqs. (4-1) and (4-2). The third source, round off error, occurs

in the numerical computations associated with the problem. The fourth source of error is the mistakes which may occur in programming the method of solution on the computer.

The energy and impulse-momentum checks incorporated in the program are intended to indicate programming errors and unacceptable round off errors. Since these checks must necessarily be based upon the numerical solution to the equations governing the behavior of the model, they cannot suggest the error of approximating the continuum member by a discrete model nor measure the truncation error of the numerical integration formulas. These checks may be easily removed from the program to decrease run time.

4.6.2. Energy Check.--For a system initially at rest the input energy (the energy due to external loads and support motions) is balanced by the strain energy absorbed by the springs and the kinetic energy. The concept of input and absorbed energies is that of force moving through a distance, while kinetic energy is the typical $mv^2/2$. Since the velocity for each mass point is known at the end of every step, it is easy to compute the kinetic energy at each instant of time. On the other hand, the input and absorbed energies must be accumulated throughout the duration of the problem. Since the force varies during the time interval, the average value is used in the computations of either the input or absorbed energies.

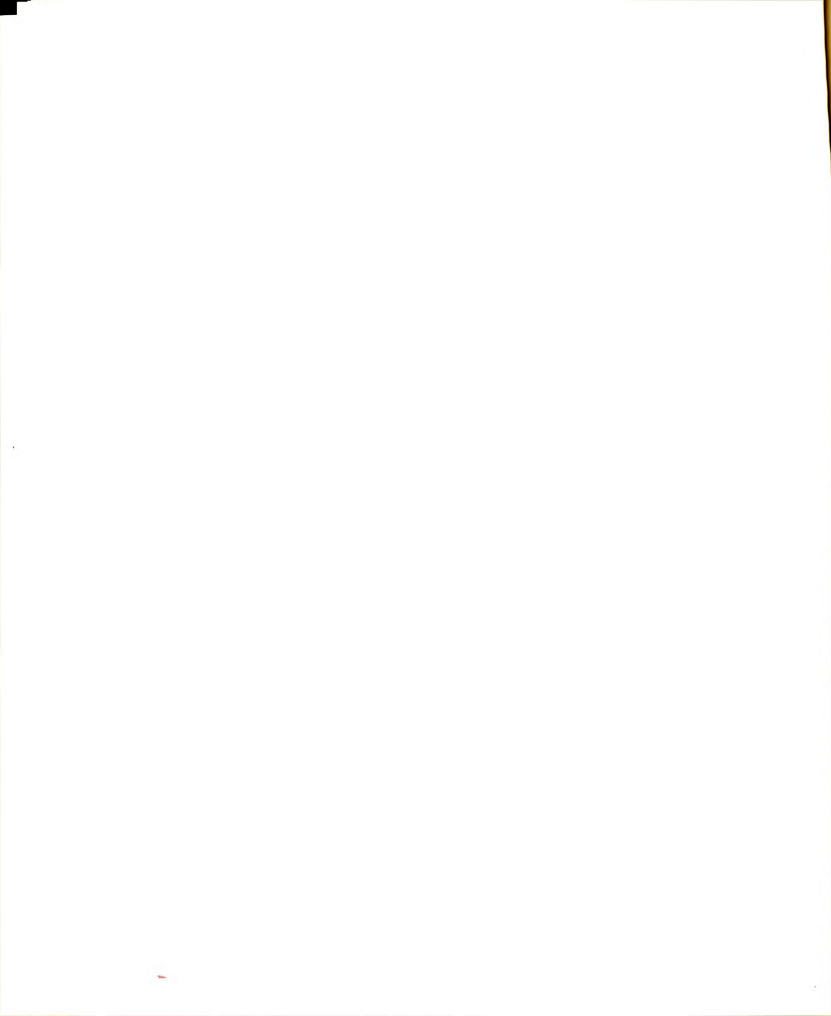
Conceptually the input and absorbed energies can be computed as follows:

$$\begin{aligned}
 E_g &= \int_0^t F(\tau) \frac{\partial S}{\partial \tau} d\tau \\
 &\approx \frac{1}{2} \sum_{i=1}^n \{ [F(t_i) + F(t_{i-1})] \\
 &\quad \cdot [S(t_i) - S(t_{i-1})] \} \dots (4-7)
 \end{aligned}$$

where E_g represents energy, F is force, which may represent load, reaction, or spring force, and S is displacement, which may represent deflections, support motion, or spring deformations, and t denotes time.

By observing inconsistencies in the energy check several programming errors were detected. These errors would have been overlooked without this check as their effects on the numerical results were quite small. For example, an error existed in the initialization of the numerical integration procedure which, for a step loading, induced a small initial velocity to the mass points. Results obtained with the erroneous programs were however, not all discarded since the difference in the maximum response was only 1/2% (less than that obtained by varying the time increment) from the corrected solutions.

Once the errors were corrected, the difference between the input energy and the absorbed and kinetic energies was consistently less than 0.001% of the total input energy.



4.6.3 Impulse-Momentum Check.--This is in reality two independent checks, one in the x-direction, and the other in the y-direction. The vector components in the x and y directions of the external loads and the reactions are numerically integrated in the time domain, in a similar fashion to that for energy calculations, to form the impulses applied to the mass system. These impulses are compared to their respective momentums, which like the kinetic energy, are computed at the end of every time interval. Any differences which may exist are noted. In general, the differences obtained from the check were of the order of 0.000001% depending on the problem and the length of time the solution had progressed into the time domain.

CHAPTER V

COMPARISON STUDIES

5.1 Introduction

In the preceding chapters the model representation of the continuous member and the analysis of the model have been presented. In order to obtain numerical results, this analysis has been programmed on the Michigan State University CDC 3600 computer. The purpose of this chapter is to compare the results obtained from this analysis with known solutions in order to judge the accuracy and dependability of the present numerical procedure (as well as the correctness of the computer program prepared).

Four problems for which the solutions are known are examined. The scope of these extends from an elastic small displacement problem to an inelastic large displacement one. Taken together these problems contain: four types of support conditions including support motion, initial crookedness, elasticity and inelasticity, and small and large displacements. The comparisons made between known solutions and the numerical results obtained show that the procedure presented here does, in fact, produce reliable results.

5.2 Fixed-Fixed Elastic Beam

The results of an elastic continuum fixed-fixed beam subjected to a uniform step loading (i.e., suddenly applied constant load) are compared with results using the model under consideration. The parameters were selected to insure small deflections in order that the two solutions could be compared. Solutions were obtained for both the formal and modified model (see section 2.3).

In Fig. 5.1 the response of the center of the beam is shown for all three solutions corresponding to the formal and modified models with 20 panels and the continuum with 20 terms taken in the series solution. With respect to the first peak response of the continuum solution, the response of the modified model was in error by 2% while that of the formal model was in error by 1%. With respect to the time corresponding to that response the modified model was in error by 1.1% while the formal model by .25%.

In Fig. 5.2 the response of the mass point at the quarter point of the beam is shown for all three cases. For the formal model the responses of both the right and left sides of the beam are shown since the model is asymmetric. It should be noted that in the elastic case under symmetric conditions the modified model yields symmetric response. Therefore, as in the continuum case, the response of only one quarter point

is needed. It can be seen that in this case the modified model gives the better results. The formal model was in error by 12% and by 15% for the left and right sides, respectively, while the modified model was in error by only 3%.

It is of interest to note that convergence of the modified model to the continuum solution's response is slower for the fixed-fixed support conditions than for the simply supported conditions. For 10 panels, the response of the model differs from the continuum solution in the simply supported case by 0.7% while in the fixed-fixed case the difference is 7%. A probable reason for the difference in the two cases is that, for a simply supported beam, all boundary conditions are exactly satisfied, while for a fixed-fixed beam the rotational displacement boundary conditions are only approximately satisfied.

5.3 Elastic Circular Arch

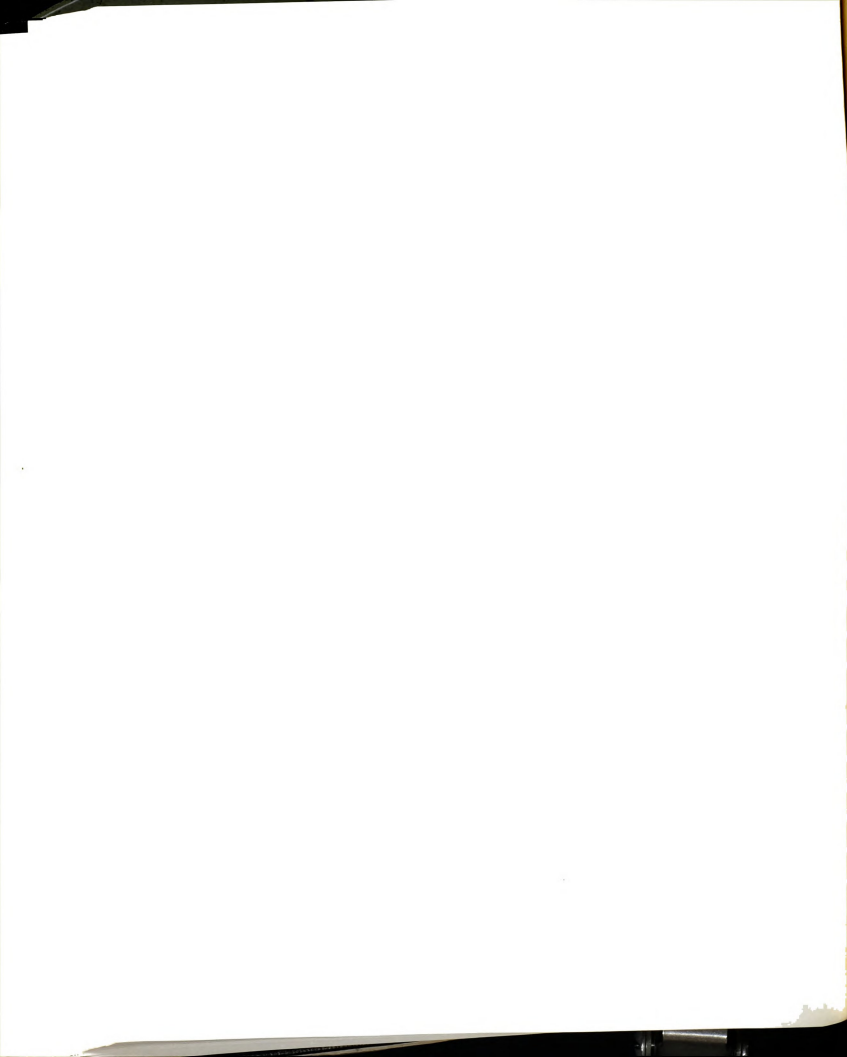
To compare the responses of a structure with a large "initial crookedness," an elastic arch problem studied by Eppink and Veletsos (10) is solved. The problem consists of a two hinged circular arch of dimensions and properties as shown in Fig. 5.3. A uniform step loading normal to the structure is applied. The magnitude of the loading is such that the displacements would be small. Eppink and Veletsos used a discrete model and

obtained results using both a direct numerical integration of the equations of motion and a modal analysis applied to their model. The comparison of the numerical results is shown in Table 1. All the results are based upon a discrete model with 12 panels. It is seen that the results of the present method agree closely with those obtained by Eppink and Veletsos. The maximum difference with respect to the results of the modal analysis is 3%, while the average difference is 1.2%.

5.4 Imperfect Elastic Column

Bailey (2) has studied the large elastic displacement behavior of a slender pin-ended column with a sinusoidal initial crookedness as shown in Fig. 5.4. The right end of the column is forced toward the left end at a constant velocity of 0.001 times the velocity of sound in the material. Bailey's solution is a finite difference solution of the continuum equations with a mesh size of $L/16$. In the corresponding solution obtained with the present model 16 panels were also used.

The results of both solutions are shown in Fig. 5.4. Both solutions predict a bimodal (one complete wave) response of the column, although quantitatively there is a slight discrepancy. One point of difference is that Bailey's results did not indicate any horizontal displacement of the right support when in reality there should be a displacement



to the left. There is, otherwise, good general agreement of the results.

5.5 Simply Supported Inelastic Beam

Wen and Toridis (51) investigated the dynamic response of a simply supported beam using a small displacement, lumped mass, lumped flexibility model. Their beam was subjected to a uniformly distributed blast loading which decreased exponentially with time. In the small displacement range, the model considered in the present work should yield similar results.

In this comparison study, the present analysis considered so-called "ideal" or "sandwich" beams in order that the bilinear stress strain relation used in the present work will produce a bilinear moment rotation relation that was used in (51). Two sets of data are presented in Fig. 5.5 and Fig. 5.6 corresponding to, respectively, a small displacement problem and a large displacement one. In each figure the solution obtained from Ref. (51) is compared with that obtained by the present model.

It is seen that for the small displacement problem in Fig. 5.5 both solutions agree well. However, for the large displacement problem in Fig. 5.6 the two solutions are appreciably different; the maximum mid-span deflection yielded by the small displacement analysis of Ref. (51) is 13% larger than that by the present large displacement

analysis. This is thought to be due to the "cable action" in the beam in the large displacement range. This mechanism is included in the large displacement analysis but not in the small displacement one.



CHAPTER VI

NUMERICAL EXAMPLES

6.1 Introduction

In order to demonstrate the usefulness and versatility of the method of analysis presented in this thesis, two categories of problems are considered, namely arch and column problems. Each individual problem is concerned with demonstrating how the procedure developed could be applied to study a particular type of problem that heretofore had not been analyzed.

The arch problem indicates how the method could be applied to problems which consider strain hardening and residual stresses. The second category, column problems, complements the first by considering ground motion and initial static axial loadings. Both categories, of course, involve material as well as geometric nonlinearities.

6.2 Dynamic Snap Through of Arches

6.2.1 Inelastic Arches.--The problem consists of a circular pin-ended arch that subtends an arc of 90 degrees with a radius of 136 inches. The material has a modulus of elasticity of 5,000,000 psi, a yield stress of 6000 psi,

and a strain hardening parameter, R_{sh} , of 0.02. The cross-section has the shape of a wide flange 8WF31 section with the web in the plane of the deformation. The cross-section is divided into four areas, symmetrically located about the centroidal axis, one area representing each flange and two areas representing the web. A uniform step loading normal to the centroidal axis is applied to the member. A length discretization of ten panels is used.

By trying various magnitudes of the loading, the critical (lowest) dynamic snapping load was found to lie between 300 and 400 ppi. For the 400 ppi. loading the arch readily snapped and this "snap" is shown in stop action in Fig. 6.1. The time at which the arch configuration was captured is shown in the upper left of each picture. For this particular arch and loading, the failure shape corresponds to one and a half waves with two interior nodes, or briefly "tri-modal." Also in this particular case the arch snapped in a symmetric fashion about the center line of the arch. It should be mentioned here that on account of the asymmetry of the model, the response of the arch was not perfectly symmetric, and the vertical deflections of symmetrically located masses were not exactly the same. However, the difference is small--of the order of 3% with respect to the rise of the arch.

6.2.2 Effect of Strain Hardening on the Critical Dynamic Snapping Load.--Problems concerning initial

crookedness need not be limited to circular arches as above, but may consider other shapes as well. Consider for example the pin-ended arch subjected to a uniform step vertical load as shown in Fig. 6.2. The shape of the structure approximates a half sine wave as computed by Eq. (4-6) and its cross-sectional shape is the same as the previous arch problem. The material properties are: $E = 30,000,000$ psi, $\sigma_y = 30,000$ psi, and $R_{sh} = 0.0$. The magnitude of the load is increased with each trial until the arch snaps. In this way the upper and lower bounds of the critical dynamic snapping load may be determined.

Also in Fig. 6.2 the maximum vertical crown displacement (within the range of time covered by the solution, i.e., $1.5 T_f$) is plotted against the load magnitude for each trial. The upper bound on the snapping load for the $R_{sh} = 0.0$ case is 962 ppi and the lower bound is 935 ppi.

Working the same problem for a strain hardening material with $R_{sh} = 0.03$, the critical snapping load increased to an upper bound of 1229 ppi, and a lower bound of 1202 ppi. This is an increase of about 25% over that obtained from the no strain hardening case. It is of interest to note that at dynamic loads less than 800 ppi. there is no appreciable difference in the response of the two cases.

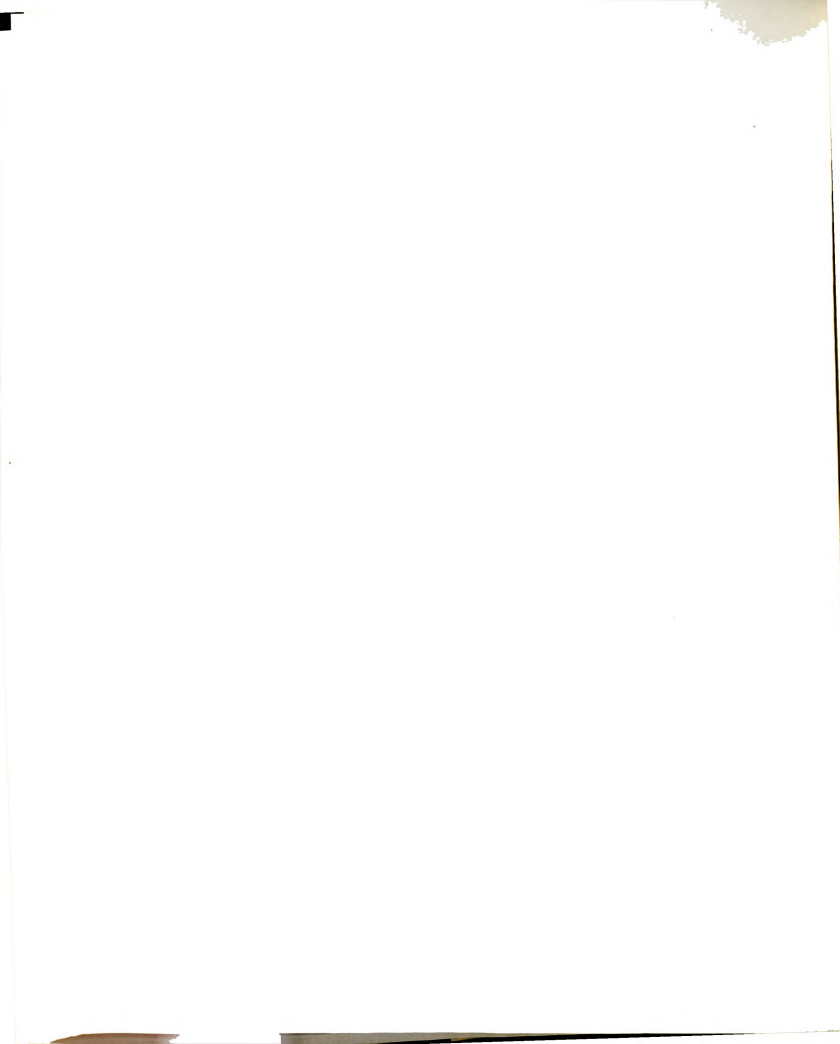
6.2.3 Effect of Residual Stresses on the Critical Dynamic Snapping Load.

--The above two cases of section 6.2.2 (with $R_{sh} = 0.0$ and 0.03) were reworked considering the existence of residual stresses. The residual stress pattern used here was shown in Fig. 3.4. The magnitudes of the residual stresses varied from $0.3\sigma_y$ (compressive) in the flanges to $0.312\sigma_y$ (tensile) in the central portion of the flanges and the web. This residual stress pattern was assumed to be constant along the length of the member.

The results of the analysis are shown in Table 2. It can be seen that for the problems considered, the effect of residual stresses on the critical dynamic snapping load is much less than that of strain hardening. This is of course due to the fact that residual stresses affect only initial yielding. Once that has taken place the material behaves just as though there were no residual stresses. Hence residual stresses would have a significant influence on the response if the inelastic strains are small. On the other hand, the effect of strain hardening persists even for large strains. In the problems considered the strains are large. Hence, the previously noted observations obtain.

6.2.4 Effect of Model Bias.

--As pointed out in Chapter II, the model used in this analysis is asymmetric. Therefore, it would produce "biased" results when used to



approximate a continuum member. In order to investigate the influence of the bias, the following method was employed. The problem considered in section 6.2.2 with $R_{sh} = 0.0$ was modified in such a way that superimposed on the uniform vertical load, p_b , was a full sine wave distributed load the magnitude of which p_a could be varied. This additional loading was increased until the asymmetry of the response had been reflected about the centerline of the arch. This is shown in Fig. 6.3.

A measure of the bias can be obtained by comparing the amount of asymmetric loading needed to cause the response to reflect about the centerline. In Fig. 6.3d is shown the deformed arch with $p_b = 990$ ppi and $p_a = 0$ at $t = 1.5T_f$. In Fig. 6.3e is shown the deformed arch with $p_a = 27$ ppi at the same values of p_b and t as in Fig. 6.3d. It is seen that with this addition of p_a the deformation pattern has been reversed. In this particular case the ratio of p_a to p_b is 0.03 and this may be taken as a measure of the "bias."

These results are for a length discretization of ten panels. It seems clear that as the discretization of the length becomes finer the effect of this bias would decrease. The preceding discussions and the fact that the bias did not prevent the model from predicting an overall symmetric response as can be seen in Fig. 6.1 would indicate that the effect of the bias is small.

It may be noted in passing that the shape of the load distribution has an effect upon the snapping shape of the arch. In the case of a half sine wave vertical step loading, the arch failed symmetrically while, under a uniform step loading, its failure shape is asymmetric.

6.2.5 Comparison with Static Arch Buckling.--

Recently Lee and Murphy (26) have published some data on the static buckling load of shallow arches. It was thought that it would be of some interest to compare their data to the dynamic solution.

The particular problem considered corresponds to their Arch No. 3 which has a radius of 50 inches and subtends an arc of 40 degrees. The depth of its rectangular cross-section is 1/2 inch and the width is 1 inch. The arch material is aluminum alloy 3003-0 which possesses a curvilinear stress strain relation. To approximate this with a bilinear relation the following material properties were used: $E = 5,000,000$ psi, $\sigma_y = 6000$ psi. and a strain hardening factor $R_{sh} = 0.075$.

For the present analysis the model was divided into 10 panels and the cross-section into 4 equal discrete areas. The critical dynamic snap-through loading was found to be between 36.25 psi. and 37.5 psi. Lee and Murphy found the static critical load to be slightly above 41.2 psi. It seems reasonable to expect that the dynamic critical load be smaller than the static critical load. In addition,

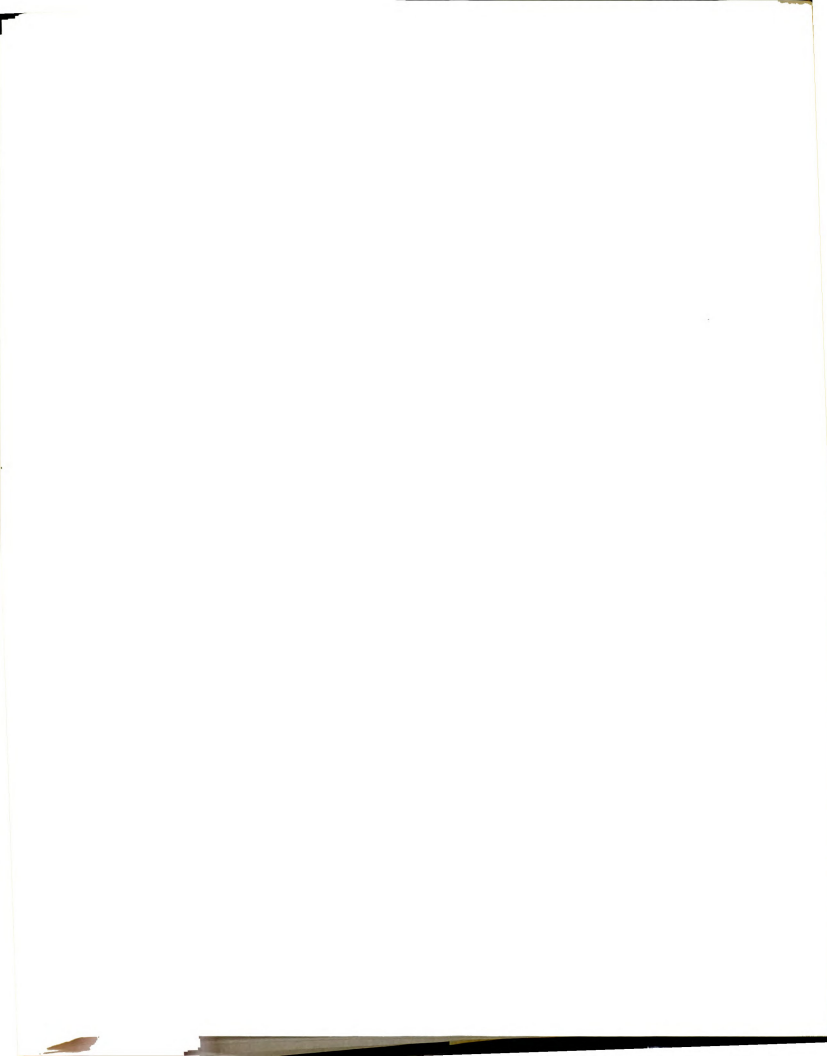
they observed that an asymmetric buckling mode developed from a symmetric displacement pattern as the loading on the arch increased. From the dynamic solutions obtained for the present study, an asymmetric snapping mode shape was also seen to develop from a symmetric displacement pattern as the magnitude of the loading is increased.

6.3 Effects of Support Motion on a Column

Consider a vertical column fixed at each end under a constant vertical load initially acting through the centroidal axis as shown in Fig. 6.4. For the particular column considered, the axial yield load of the column is far less than the Euler load ($P_{\text{Euler}} = 3.65P_y$). This column is then subjected to a horizontal support motion at the base which may idealize an earthquake. Two cases are considered. For case I, the vertical load is held constant at one half the yield load (based on the cross-sectional area). The problem is solved for support motions with various amplitudes but a fixed duration.

The maximum longitudinal end displacement of the column is plotted against the amplitude of the support motion. It is seen that the displacement increases rapidly with the amplitude of motion. At an amplitude equal to $0.075L$ the column failed.

For case II, consider the support motion to have a constant magnitude of $0.015L$. The vertical load is then



increased. In Fig. 6.5 is shown a plot of the permanent transverse displacement at the column mid-height versus the axial load on the structure. It is seen that the permanent displacement increases rapidly with an increase in the axial load. Failure occurs at $P = 0.9P_y$.

An interesting feature of the response is the reversal of the direction of the permanent set as the collapse load is approached. As the column fails the mid-point of the column actually bows to the left whereas the support motion was to the right.

CHAPTER VII

CONCLUSIONS

In this thesis a method of analyzing the dynamic response of line structural members has been presented. A discrete model was used for the analysis in which both the length and the cross-section were discretized. In constructing the model, an asymmetric element was chosen, as the symmetric ones considered would lead to complications not easily resolved.

In the formulation of the analysis, both material and geometric nonlinearities have been included. Thus the method can take into account the effects of axial-force bending-moment interactions, large displacements, inelasticity, as well as initial crookedness, residual stresses, initial static loadings, and movement of the supports, if any. A computer program has been prepared incorporating most of the capabilities mentioned. Impulse-momentum and energy checks were found to be useful in detecting programming errors. They should also indicate unacceptable round-off errors.

Using the program developed, a number of problems have been solved. These problems fall into two categories: problems which have been solved by other researchers and

problems which have not. The first category is used to check the reliability of the method and the correctness of the computer program. The second is used to exhibit the usefulness and versatility of the method. The first category problems included a fixed-fixed elastic beam, an elastic circular arch, an imperfect elastic column and a simply supported inelastic beam. By comparing the model's response with known solutions of these problems, it was demonstrated that the method presented here is sufficiently accurate for most engineering purposes.

In the second category, two types of problems were considered: the snap-through behavior of elasto-inelastic arches, and the failure of an axially loaded column subjected to transverse support motions. In studying the snapping phenomenon of a shallow arch, it was found that strain hardening significantly increased the critical dynamic snapping load while residual stresses did not affect it appreciably.

Because of the asymmetric nature of the model, the numerical solutions indicated a certain amount of "bias." However, it is shown that the corresponding error is relatively small (of the order of 3% for 10 panels).

In conclusion it may be said that a discrete model approach is a feasible and powerful method for studying the dynamic response of nonlinear (both geometric and material) line structural members. In the present study this model

is limited to motion in one plane. As a possible extension of this study, the general case of motion in space may be considered. In this case, however, torsional deformation appears to be a significant factor. Consequently, the model would have to have a mechanism to incorporate shear deformations. This would seem to be a major and challenging problem.

BIBLIOGRAPHY

1. Augusti, G. "Experimental Rotation Capacity of Steel Beam Columns," Journal of the Structural Division, ASCE, Vol. 90, No. ST6, Proc. Paper 4175, December 1964, pp. 171-188.
2. Bailey, H. R. "Dynamic Bending of Elastic Columns," Journal of the Structural Division, ASCE, Vol. 89, No. ST4, Proc. Paper 3585, August 1963, pp. 95-114.
3. Baker, J. F., Horne, M. R., and Heyman, J. The Steel Skeleton. Cambridge, England: Cambridge University Press, Vol. II, 1956.
4. Beedle, L. S., and Tall, L. "Basic Column Strength," Journal of the Structural Division, ASCE, Vol. 86, No. ST7, Proc. Paper 2555, July 1960, p. 139.
5. Beedle, L.S., et al. Structural Steel Design. New York: The Ronald Press Co., 1964.
6. Beylerian, B. N. "Elastic-Plastic Response of Beams Including the Effect of Shear and Rotatory Inertia," Ph.D. Thesis, Dept. of Civil Engineering, Michigan State University, June 1965.
7. Bleich, F. Buckling Strength of Metal Structures, Engineering Societies Monographs, McGraw-Hill, 1952.
8. Chu, K. H., and Pabarcus, A. "Elastic and Inelastic Buckling of Portal Frames," Journal of the Engineering Mechanics Division, ASCE, Vol. 90, No. EM5, Proc. Paper 4094, October 1964, pp. 221-249.
9. Cox, H. L., and Denke, P. H. "Stability and Free Vibrations of Non-uniform Beams Continuous Across Flexible Supports," Journal of the Aeronautical Sciences, Vol. 21, #8, August 1954, pp. 572-573.
10. Eppink, R. T., and Veletsos, A. S. "Dynamic Analysis of Circular Elastic Arches," Conference Papers of 2nd Conference on Electronic Computation, ASCE, Sept. 8-9, 1960, Pittsburgh, Pa., pp. 477-502.



11. Evan-Iwanowski, R. M. "On the Parametric Response of Structures," Applied Mechanics Reviews, Vol. 18, No. 9, September 1965, pp. 699-702, 85 references given on the subject.
12. Fenves, S. J. "Guide to Development and Use of Electronic Computer Programs: Introduction," Journal of the Structural Division, ASCE, Vol. 90, No. ST6, Proc. Paper 4151, December 1964, pp. 1-5.
13. _____. "Guide to Development and Use of Electronic Computer Programs: Program Planning," Journal of the Structural Division, ASCE, Vol. 90, No. ST6, Proc. Paper 4153, December 1964, pp. 19-24.
14. Galambos, T. V., and Ketter, R. L. "Columns Under Combined Bending and Thrust," Transactions, ASCE, Vol. 126, Part I, 1961, p. 1.
15. Galambos, T. V. "Strength of Round Steel Columns," Journal of the Structural Division, ASCE, Vol. 91, No. ST1, Proc. Paper 4219, February 1965, pp. 121-140.
16. Goldberg, J. E., Bogdanoff, J. L., and Glauz, W. D. "General Computer Analysis of Beams," Journal of the Engineering Mechanics Division, ASCE, Vol. 90, No. EM3, Proc. Paper 3943, June 1964, pp. 135-146.
17. Hauck, G. F., and Lee, S. L. "Stability of Elasto-Plastic Wide Flanged Columns," Journal of the Structural Division, ASCE, Vol. 89, No. ST6, Proc. Paper 3738, December 1963, pp. 297-324.
18. Hoff, N. J. "The Dynamics of the Buckling of Elastic Columns," Journal of Applied Mechanics, Trans. 18, 1 (1951), pp. 68-74.
19. Horne, M. R. "The Stability of Elastic-Plastic Structures," Progress in Solid Mechanics, Vol. II, Edited by I. N. Sneddon and R. Hill. Amsterdam: North Holland Publishing Co., 1961.
20. Huddleston, J. V. "Analysis of an Inelastic Column," Journal of the Engineering Mechanics Division, ASCE, Vol. 90, No. EMD4, Proc. Paper 3992, August 1964, pp. 1-21.
21. Jennings, P. C. "Earthquake Response of a Yielding Structure," Journal of the Engineering Mechanics Division, ASCE, Vol. 91, No. EM4, Proc. Paper 4435, August 1965, pp. 41-68.

22. Ketter, R. L., Kaminsky, E. L., and Beedle, L. S. "Plastic Deformation of Wide-Flange Beam Columns," Transactions, ASCE, Vol. 120, 1955, p. 1028.
23. Lay, M. G. "The Yielding of Uniformly Loaded Steel Members," Journal of the Structural Division, ASCE, Vol. 91, No. ST2, Proc. Paper 4580, December 1965, pp. 49-66.
24. Lay, M. G., and Galambos, T. V. "Inelastic Steel Beams Under Uniform Moment," Journal of the Structural Division, ASCE, Vol. 91, No. ST6, Proc. Paper 4566, December 1965, pp. 67-93.
25. Lay, M. G. "Flange Local Buckling in Wide Flange Shapes," Journal of the Structural Division, ASCE, Vol. 91, No. ST6, Proc. Paper 4554, December 1965, pp. 95-116.
26. Lee, L. H. N., and Murphy, L. M. "Inelastic Buckling of Shallow Arches," Journal of the Engineering Mechanics Division, ASCE, Vol. 94, No. EM1, Proc. Paper 5804, February 1968, pp. 225-239.
27. Lu, L. W. "Inelastic Buckling of Steel Frames," Journal of the Structural Division, ASCE, Vol. 91, No. ST6, Proc. Paper 4577, December 1965, pp. 185-214.
28. Malvick, A. J., and Lee, L. H. N. "Buckling Behavior of an Inelastic Column," Journal of the Engineering Mechanics Division, ASCE, Vol. 91, No. EM3, Proc. Paper 4372, June 1965, pp. 113-127.
29. Massey, C., and Pitman, F. S. "Inelastic Lateral Stability Under a Moment Gradient," Journal of the Engineering Mechanics Division, ASCE, Vol. 92, No. EM2, Proc. Paper 4779, April 1966, pp. 101-111.
30. Miranda, C., and Ojalvo, M. "Inelastic Lateral-Torsional Buckling of Beam Columns," Journal of the Engineering Mechanics Division, ASCE, Vol. 91, No. EM6, Proc. Paper 4563, December 1965, pp. 21-37.
31. Neal, B. G. The Plastic Methods of Structural Analysis. London: Chapman & Hall, Ltd., 1956.
32. Newmark, N. M. "Numerical Procedures for Computing Deflections, Moments, and Buckling Loads," Transactions, ASCE, Vol. 108, 1943, p. 1161.



33. Newmark, N. M. "A Method of Computation for Structural Dynamics," Transactions, ASCE, Vol. 127, 1962, p. 1406.
34. Onat, E. T., and Prager, W. "The Influence of Axial Forces on the Collapse Load of Frames," Proceedings of the First Midwest Conference on Solid Mechanics, University of Illinois, Urbana, Illinois, 1953, pp. 40-42.
35. Osgood, W. R. "The Double Modulus Theory of Column Action," Civil Engineering, Vol. 5, No. 3, March 1935, pp. 173-175.
36. Pfrang, E. O., and Siess, C. P. "Predicting Structural Behavior Analytically," Journal of the Structural Division, ASCE, Vol. 90, No. ST5, Proc. Paper 4110, October 1964, pp. 99-111.
37. Rosenbluth, E., and Herrera, I. "On a Kind of Hysterical Damping," Journal of the Engineering Mechanics Division, ASCE, Vol. 90, No. EMD4, Proc. Paper 3999, August 1964, p. 37.
38. Salvadori, M. G. "Numerical Computation of Buckling Loads by Finite Difference," Proceedings, ASCE, Vol. 75, December 1949.
39. Schreyer, H. L., and Masur, E. F. "Buckling of Shallow Arches," Journal of the Engineering Mechanics Division, ASCE, Vol. 92, No. 4, Proc. Paper 4875, August 1966, pp. 1-19.
40. Sevin, E. "Digital Computer Solutions of the Dynamic Column Buckling Equations" Proceeding of the First Conference on Electronic Computation, ASCE, 1958, pp. 237-256.
41. ———. "On the Elastic Bending of Columns Due to Axial Inertia," Journal of Applied Mechanics, ASME, Vol. 27, No. 1, 1960, pp. 125-131.
42. Shanley, F. R. "The Column Paradox," Journal of the Aeronautical Sciences, Vol. 13, No. 12, December 1946, p. 678.
43. ———. "Inelastic Column Theory," Journal of the Aeronautical Sciences, Vol. 14, No. 5, May 1947, pp. 261-267.

44. Shinozuka, M., and Henry, L. "Random Vibration of a Beam Column," Journal of the Engineering Mechanics Division, ASCE, Vol. 91, No. EM5, Proc. Paper 4510, October 1965, pp. 123-143.
45. Thurlimann, B. "New Aspects Concerning the Inelastic Instability of Steel Structures," Journal of the Structural Division, ASCE, Vol. 86, No. ST1, Proc. Paper 2485, January 1960, p. 99.
46. Timoshenko, S. P. History of Strength of Materials. New York: McGraw-Hill, 1953.
47. Timoshenko, S. P., and Gere, J. M. Theory of Elastic Stability, Engineering Societies Monographs, McGraw-Hill, New York, 1961, 2nd ed.
48. Tong, A. L. "Elasto-Plastic Analysis by Numerical Procedures," Journal of the Engineering Mechanics Division, ASCE, Vol. 86, No. EM6, Proc. Paper 2690, December 1960, pp. 73-88.
49. Tung, T. P., and Newmark, N. M. "A Review of Numerical Integration Methods for Dynamic Response of Structures," Technical Report to Office of Naval Research, Contract N6 ori-071 (06), Task Order VI Project NR-064-183, Department of Civil Engineering, University of Illinois, Urbana, Illinois March 1954.
50. Van Kuren, R. C., and Galambos, T. V. "Beam Column Experiments," Journal of the Structural Division, ASCE, Vol. 90, No. ST2, Proc. Paper 3876, April 1964, pp. 223-256.
51. Wen, R., and Toridis, T. "Discrete Dynamic Models for Elasto-Inelastic Beams," Journal of the Engineering Mechanics Division, ASCE, Vol. 90, No. EM5, Proc. Paper 4081, October 1964, pp. 71-102.
52. Wood, R. H. "The Stability of Tall Buildings," Proceedings, Institution of Civil Engineers, Vol. 11, 1958 (Sept.-Dec.), p. 69.



Table 1.--Comparison Study of Elastic Circular Arch

Time	Vertical Crown Displacement/(pR^2/AE)		
$t/2\pi R\sqrt{\frac{\rho}{E}}$	Model Response	Eppink and Veletsos	
		Numerical	Modal
0.5	2.130	2.128	2.128
1.0	2.021	2.024	2.029
1.5	2.073	2.061	2.057
2.0	0.916	0.902	0.890
2.5	1.064	1.075	1.088
3.0	1.704	1.698	1.697

Table 2.--Effect of Strain Hardening and Residual Stresses on the Critical Dynamic Snapping Load, P_s , of a Pin-Ended Arch

Number of Panels	$R_{sh} = E_p/E$	Residual Stresses Present?	Bounds on the Critical Snapping Load, P_s .
5	0.0	No	$962\text{ppi} < P_s < 989\text{ppi}$
10	0.0	No	$935\text{ppi} < P_s < 962\text{ppi}$
		Yes	$908\text{ppi} < P_s < 935\text{ppi}$
	0.03	No	$1202\text{ppi} < P_s < 1229\text{ppi}$
		Yes	$1202\text{ppi} < P_s < 1229\text{ppi}$



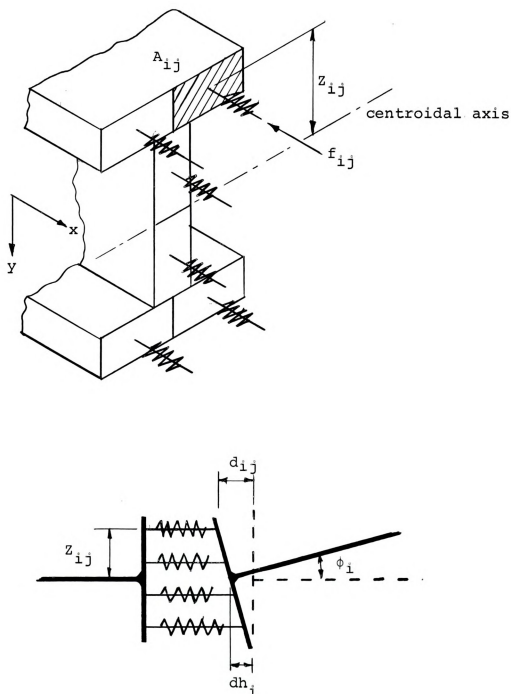
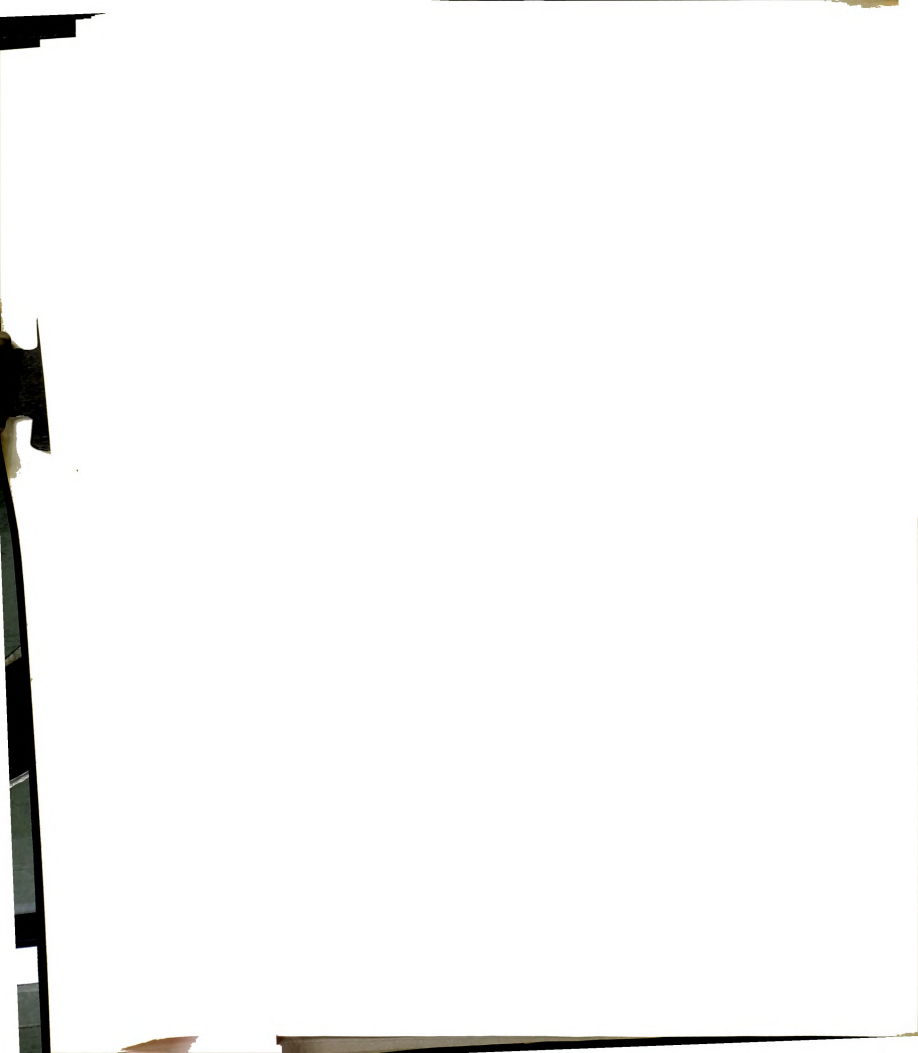


Fig. 2.1 Spring System Representation of Lumped Flexibility



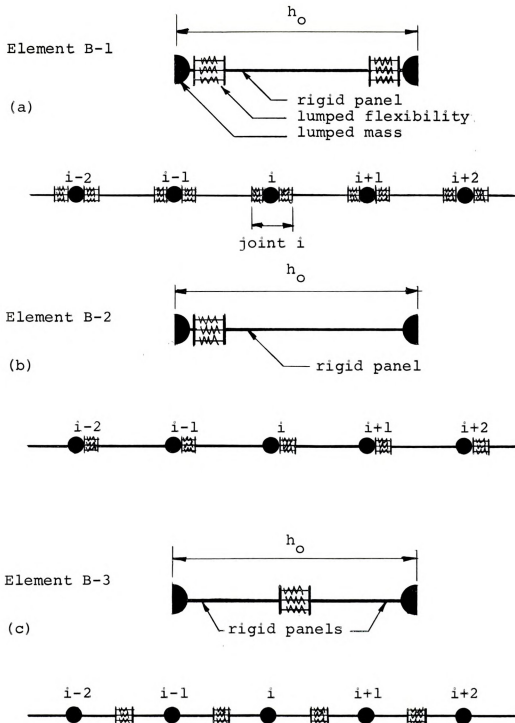
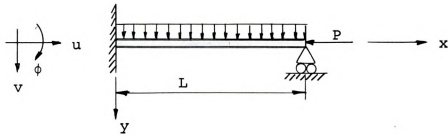
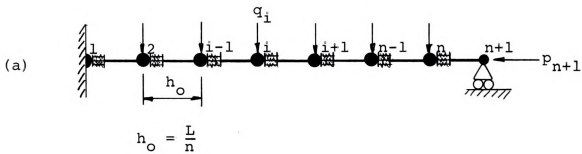


Fig. 2.2 Model Element Assemblies





Formal Model



Modified Model

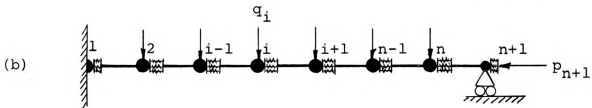
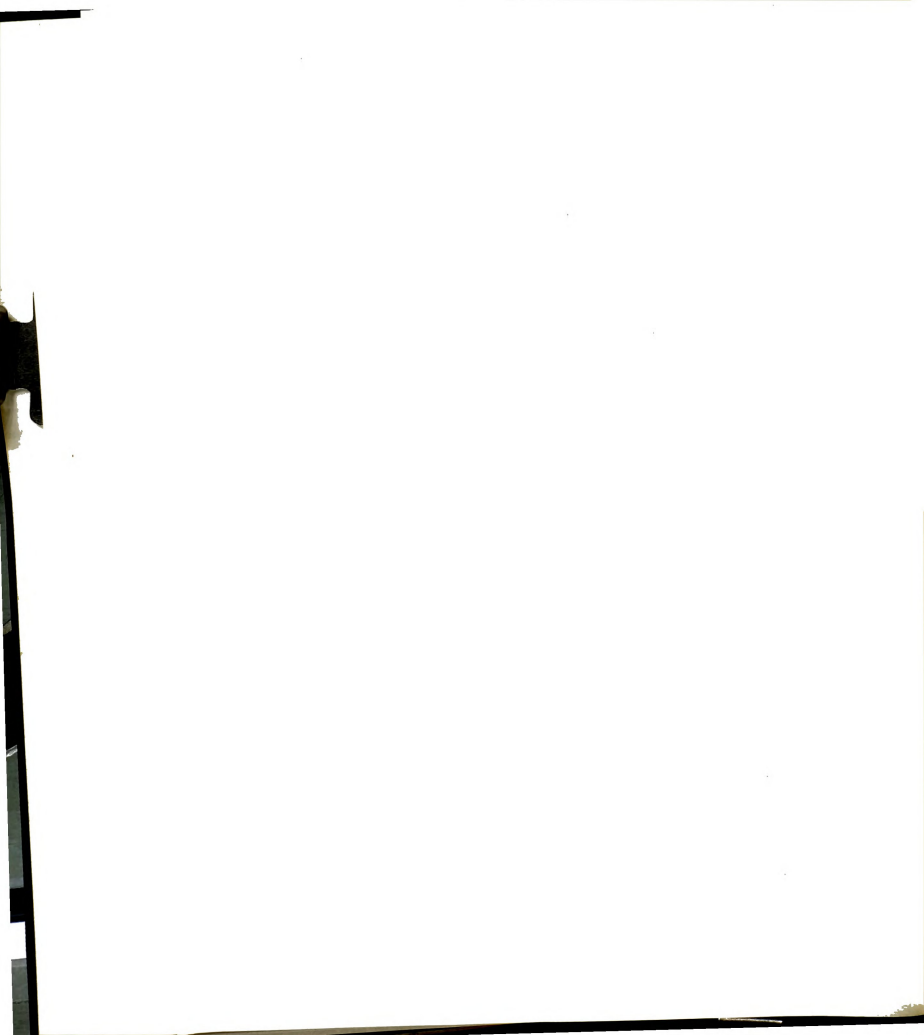


Fig. 2.3 "Formal" and "Modified" Models



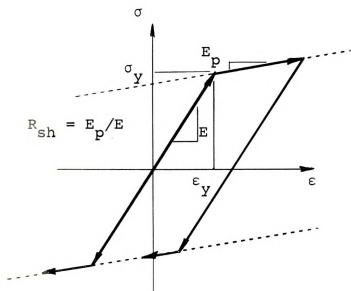


Fig. 2.4 Bilinear Stress-Strain Relation

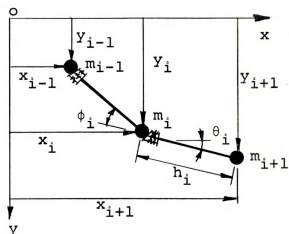


Fig. 3.1 Portion of Deformed Model

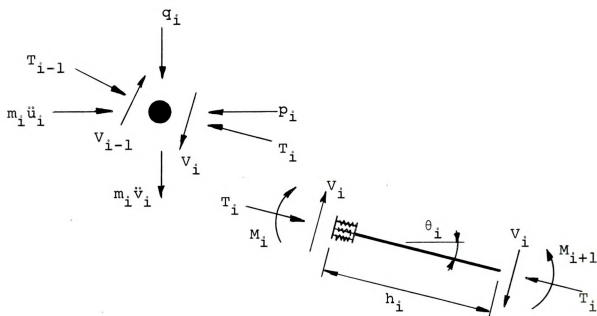
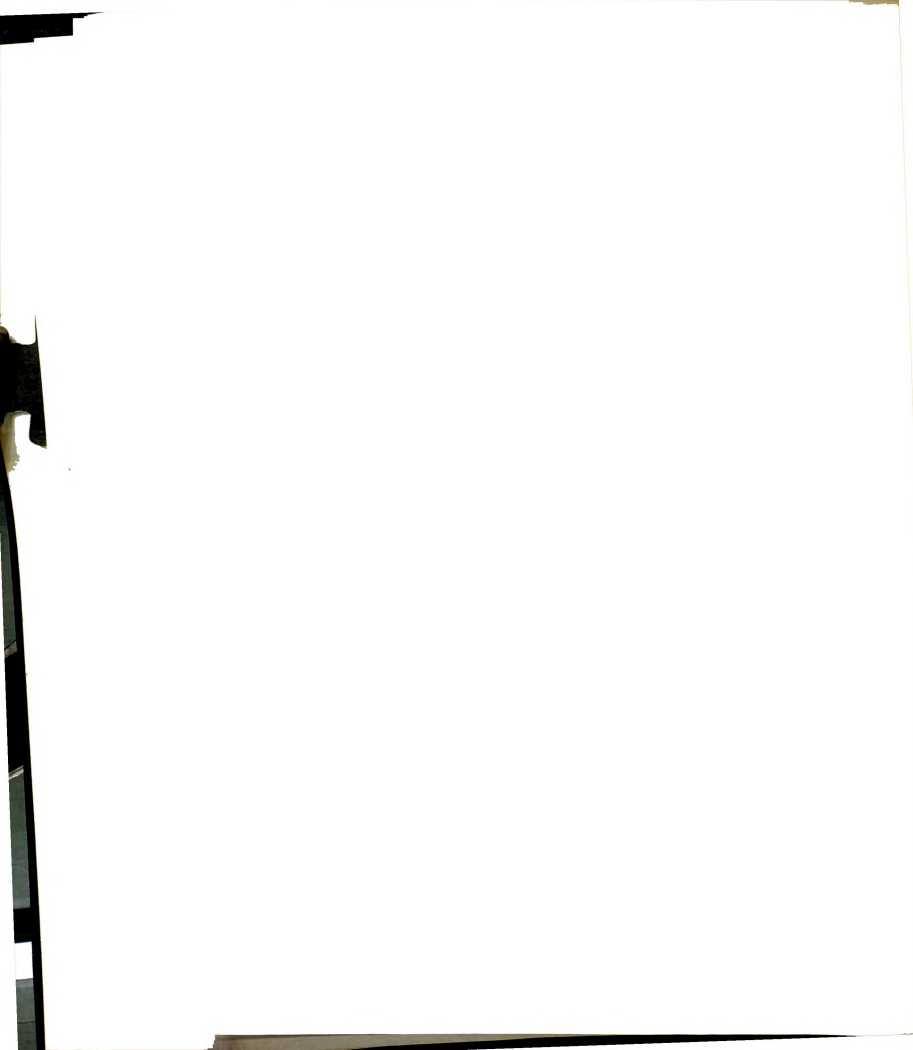
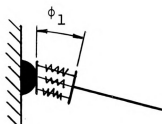


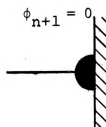
Fig. 3.2 Free-Body Diagrams of a Mass Point and a Massless Panel



Formal Model

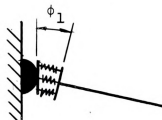


$$\text{Flex}_1 = \int_0^{h_0} \text{flex}(s) \, ds$$

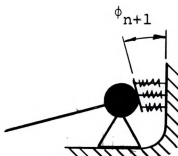


$$\text{Flex}_{n+1} = 0$$

Modified Model

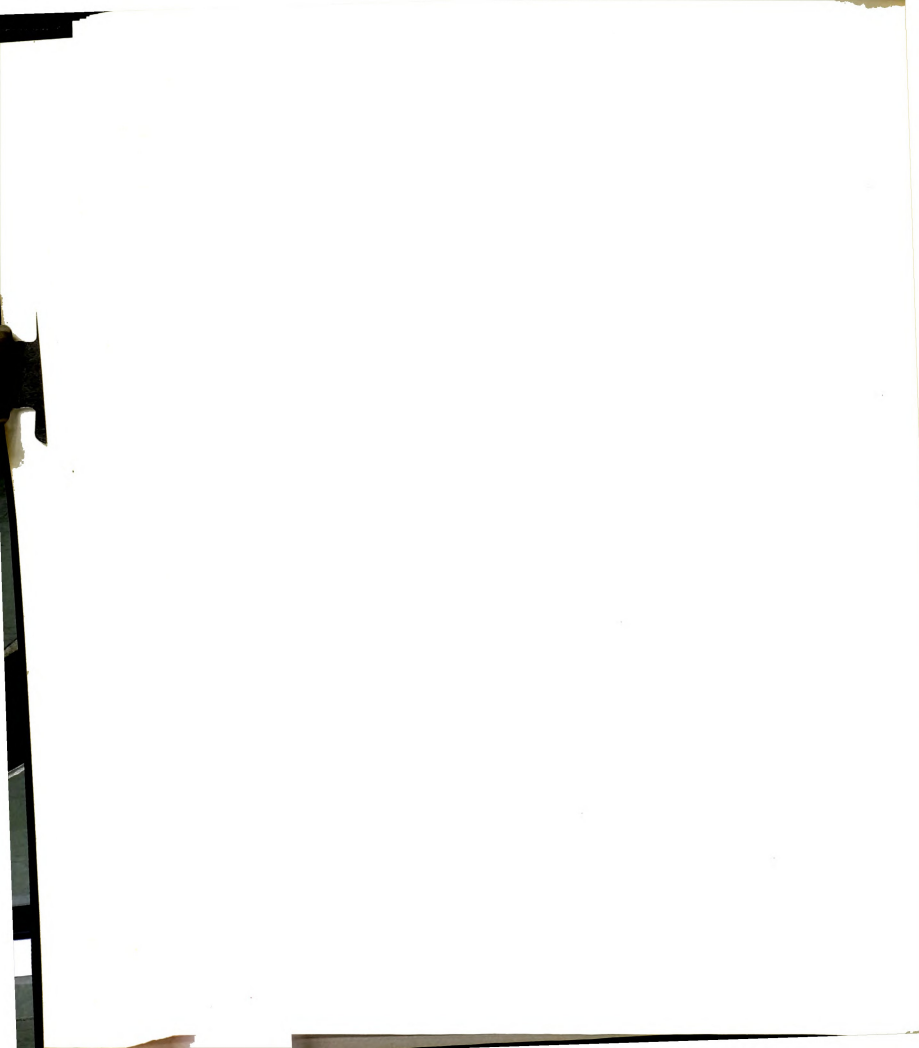


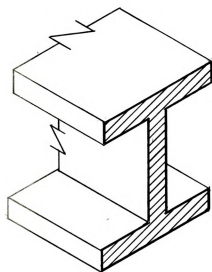
$$\text{Flex}_1 = \int_0^{h_0/2} \text{flex}(s) \, ds$$



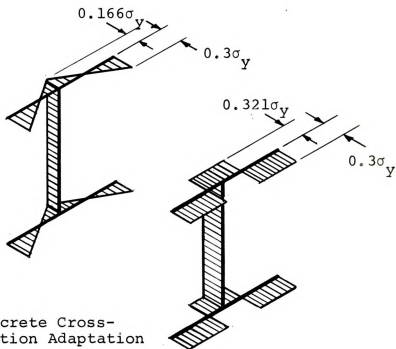
$$\text{Flex}_{n+1} = \int_{L-h_0/2}^L \text{flex}(s) \, ds$$

Fig. 3.3 Treatment of Boundary Conditions Involving Prescribed Support Rotation





8WF 31



Residual Stress Pattern
of Reference 14

Discrete Cross-
section Adaptation

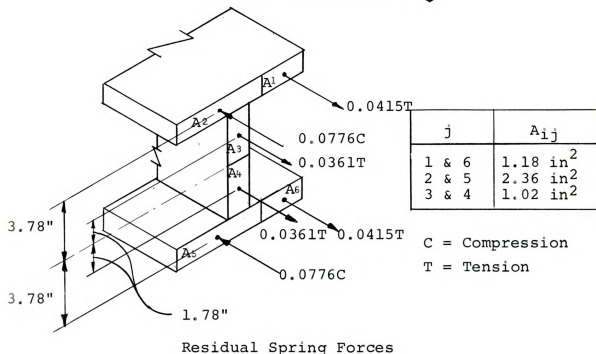


Fig. 3.4 Residual Stress Representation



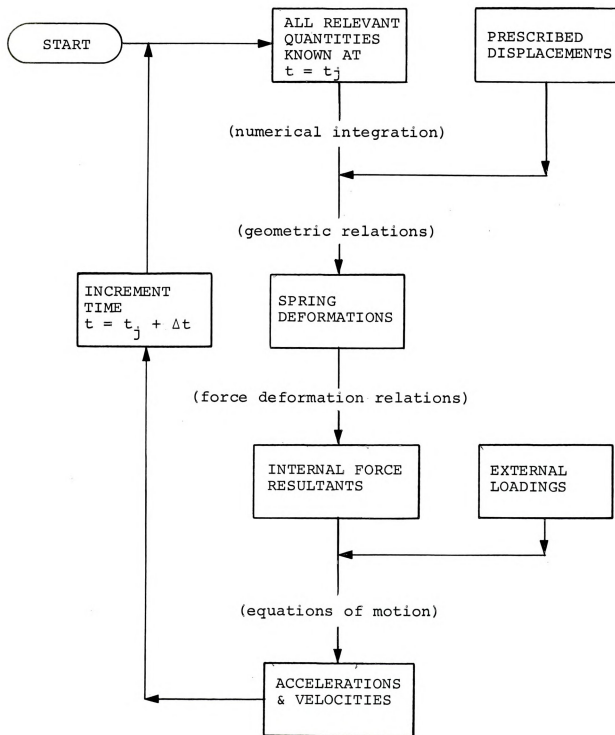


Fig. 4.1 Flow Diagram for One Step of Integration



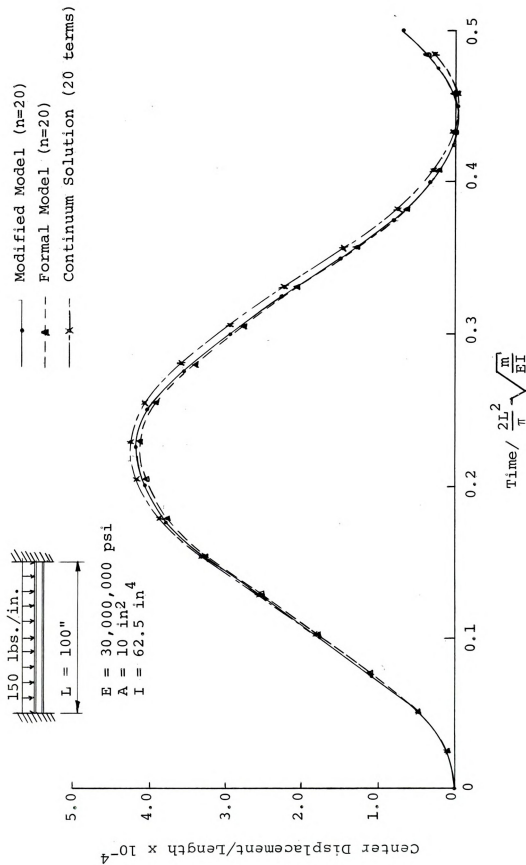


Fig. 5.1 Response History for Center Displacement



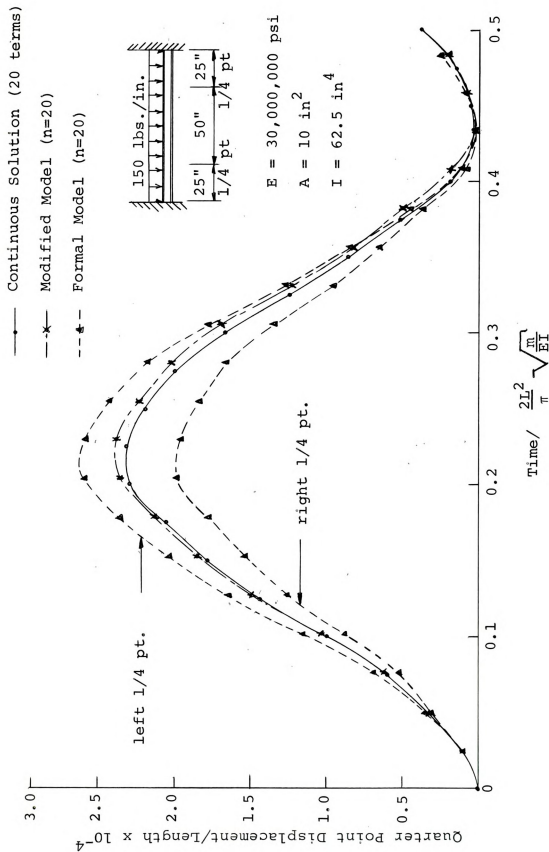
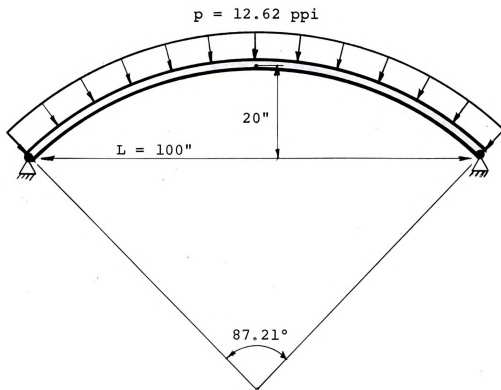


Fig. 5.2 Response History for Quarter Point Displacement





$$E = 30,000,000 \text{ psi}$$

$$A = 1 \text{ in}^2$$

$$I = 1 \text{ in}^4$$

$$R = 72.5 \text{ in}$$

$$\rho = 0.000732 \text{ lb-sec}^2/\text{in}^4$$

$$n = 12$$

Fig. 5.3 Elastic Circular Arch

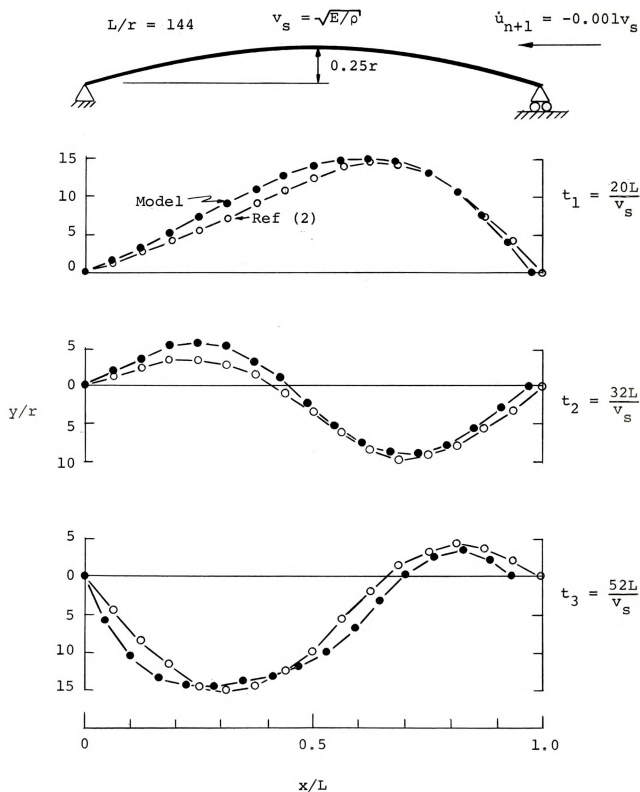


Fig. 5.4 Large Displacements of a Column

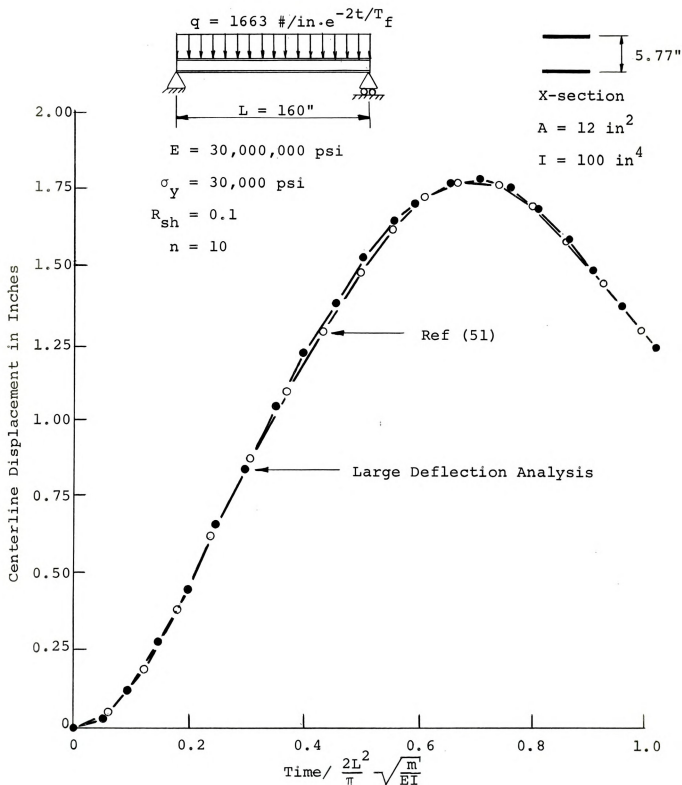
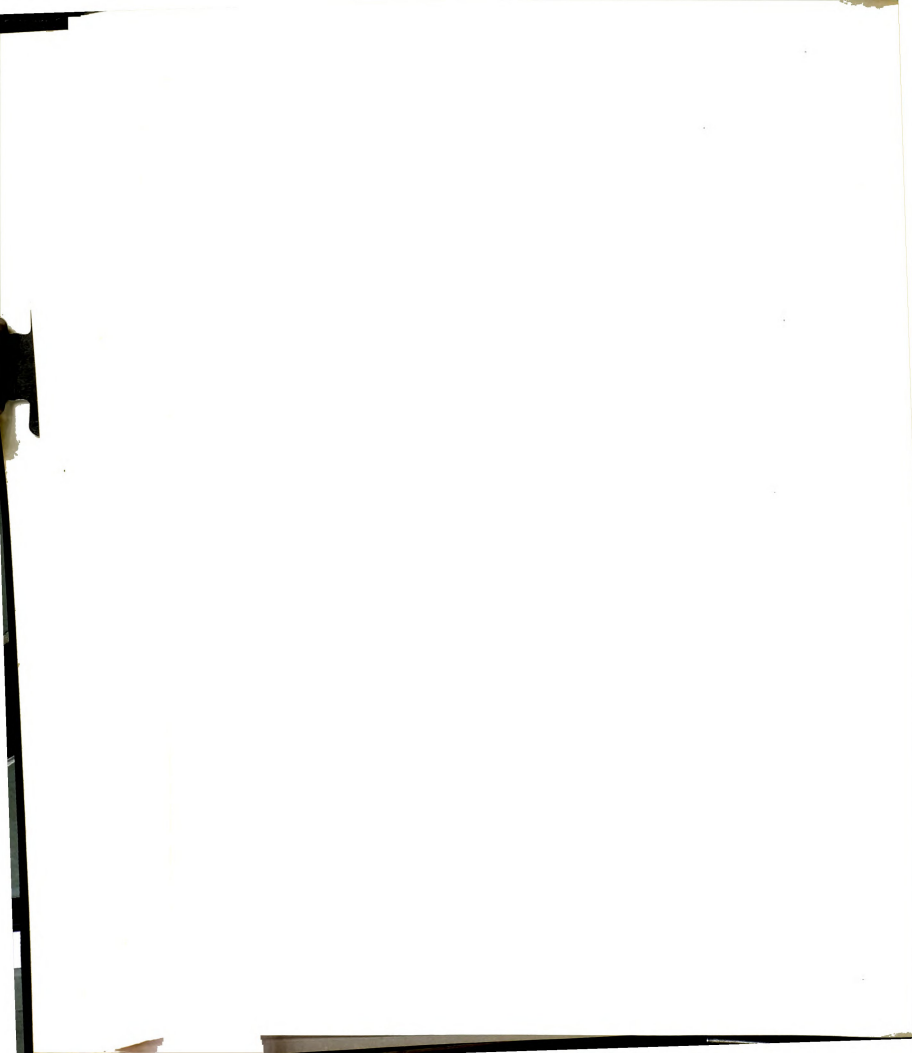


Fig. 5.5 Comparison of Large and Small Deflection Solutions for a Small Deflection Problem



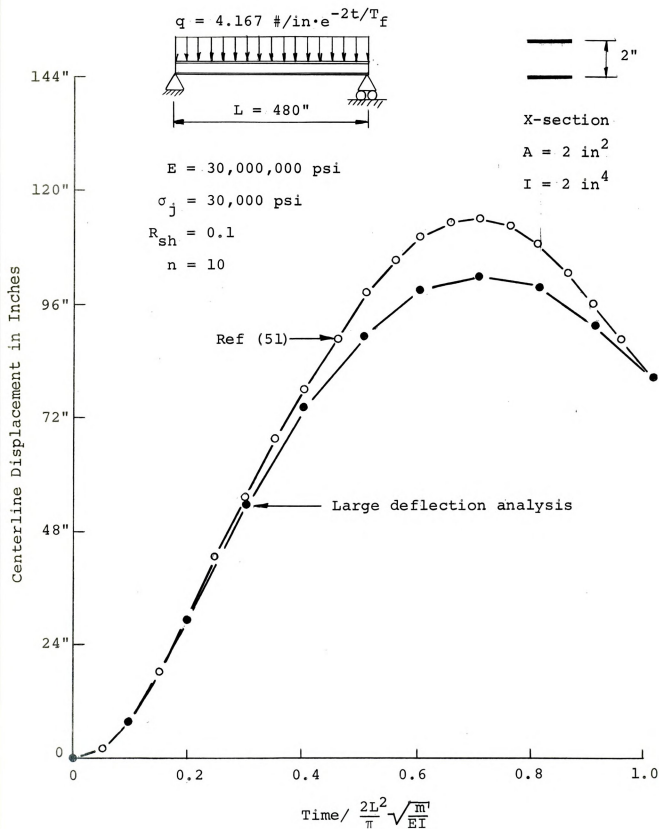


Fig. 5.6 Comparison of Large and Small Deflection Solutions for a Large Deflection Problem



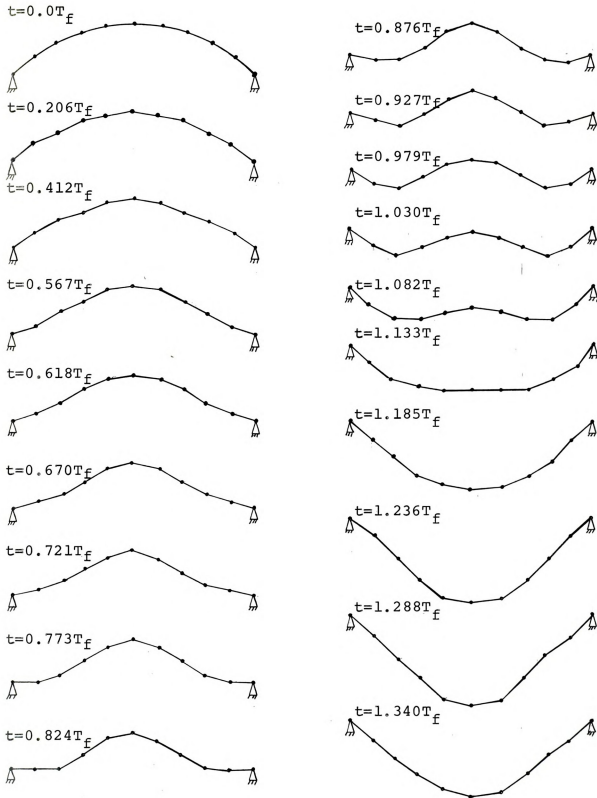
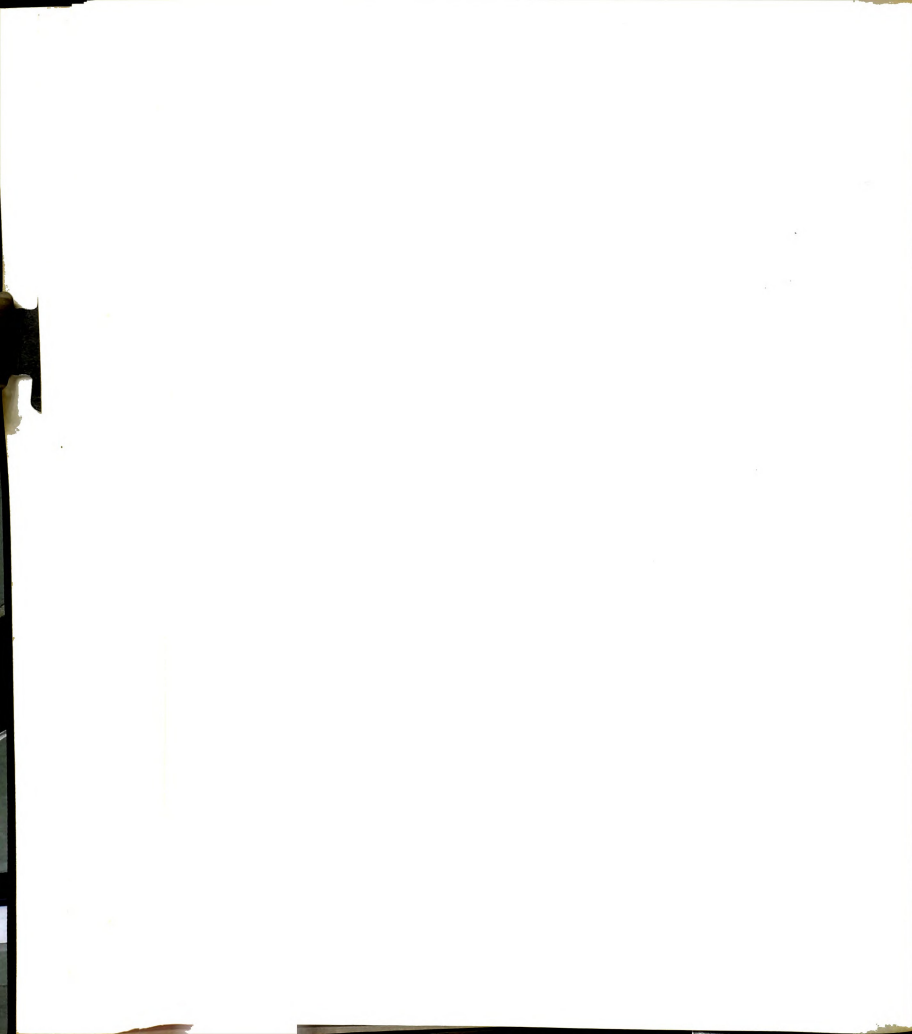


Fig. 6.1 Snap-Through of an Arch ($N = 10$)



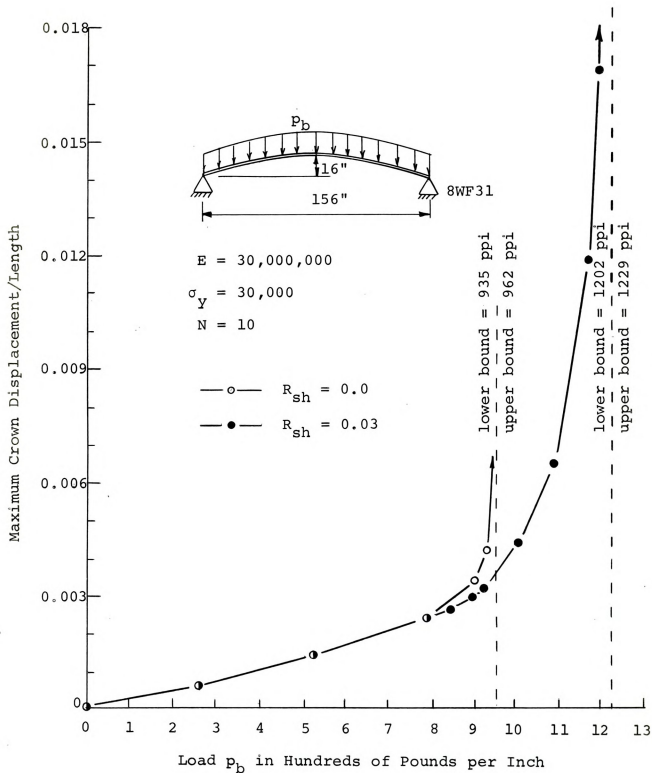


Fig. 6.2 Dynamic Snap Through Loads of a Shallow Arch



$$p_a \sin \left(\frac{2\pi s}{L} \right)$$

(a)



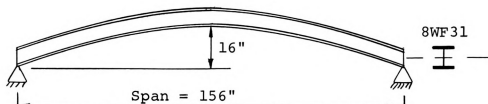
+

 p_b

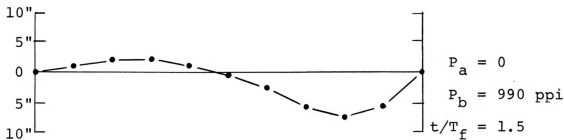
(b)



(c)



(d)



(e)

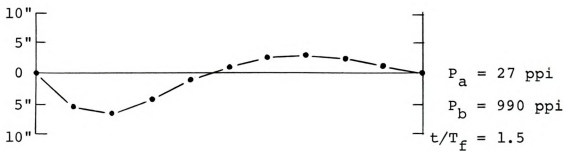


Fig. 6.3 Evaluation of Model Bias



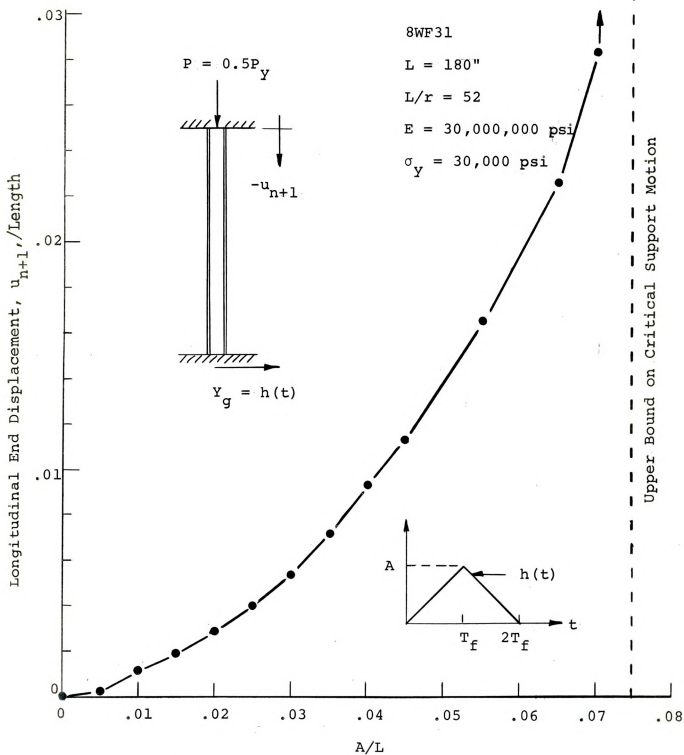


Fig. 6.4 Maximum End Displacement vs. Peak Support Motion

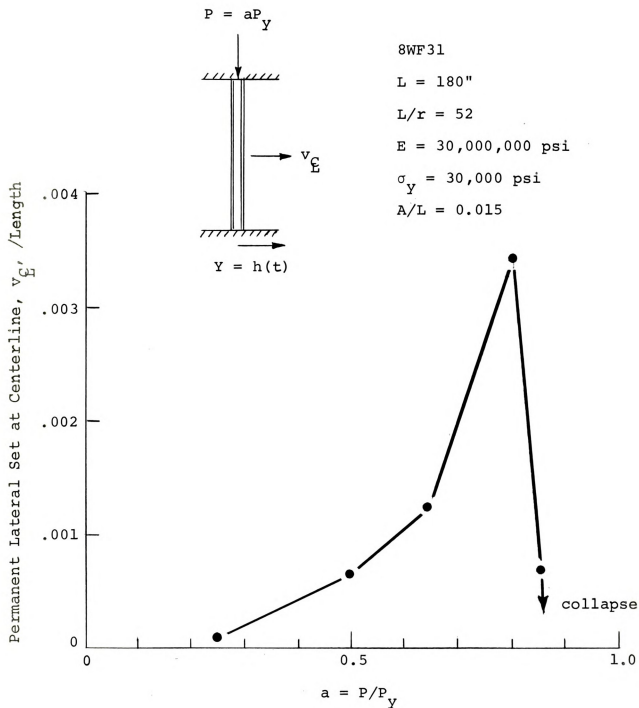


Fig 6.5 Permanent Lateral Set at \bar{L} vs. Axial Load



APPENDIX

COMPUTER PROGRAM

A.1 Introduction

For completeness the computer program written for this study is given here. The program is divided into four basic subroutines governed by the main program, "UNIAX." These subroutines represent the four advancements mentioned in section 4.3 and shown in Fig. 4.1.

The first subroutine, "BTA," is concerned with the geometry and kinematics of the member, i.e., the determination of the mass point coordinates, and the bending and compression deformations. The effect of support motion is also considered in this subroutine. Subroutine "FRC" is used to determine the internal force resultants from the deformations that are transmitted from "BTA." "FRC" also considers residual stresses, if any. In subroutine "EQM" the equations of motion, (3-7) and (3-8), are used to compute the mass point accelerations from the internal force resultants and the prescribed external loadings. The velocities of the mass points are then computed using Eq. (4-2). The last of the four basic subroutines "THK," increments the time and performs other



tasks associated with the completion of a step of integration, such as finalizing the accelerations and controlling the print-out sequencing.

The remaining subroutines and function subprograms perform certain tasks associated with the main program and the previously mentioned subroutines. Subroutine "XSEC" discretizes the cross-section of the member and computes the z_{ij} 's and the A_{ij} 's and other quantities associated with the cross-section. Subroutine "EGK" checks the energy and impulse-momentum of the system as discussed in section 4.6. Subroutine "PLT" is used to graphically display the deformed configuration of the member at periodic intervals of time and, after the problem is completed, to display a response history of the motion. Function "DPNL" computes the distance between two adjacent masses given their coordinates. "DX" computes the change in the x-coordinate between two adjacent masses given the initial y-coordinates and the initial panel length, h_0 . Finally "DEF" computes the support displacement by linear interpolation between adjacent data points for problems in which support motion is prescribed.

The program is presented in the following in three parts. The first part is a list of variable names and their meanings. Detailed flow charts of the main programs and of the subprograms are included. Finally a listing of the entire program is given. The particular program being

presented contains procedures expressly for inputting and initializing the geometry and load of circular arches subjected to normal uniform step loadings. By changing these procedures structural members other than circular arches could be considered.

A.2 List of Computer Program Variables

All variables which occur in common blocks are listed under the blocks in which they occur. Then variables which occur in the main program and in subsequent subprograms are listed where they first appear. All lists are in alphabetical order except the common blocks. All variables are defined only once. However, there may be variables with the same name but with different meanings in different subprograms. For example, T means thickness in "XSEC" while it means time in all other routines. These doubly defined variables are listed in each routine where their meaning is different from that of the main program.

Mention should be made of subscripted variables denoted by "(I,J)*." In these arrays the term "jth direction" denotes the x-direction for J=1 and y-direction for J=2.

COMMON BLOCK BC

BCX1	= boundary condition at left end in the x-direction given as either FREE, FIXED, or DEFINE;
------	---



BCYL = boundary condition at left end in the y-direction given as either FREE, FIXED or DEFINE;

BCML = rotation boundary condition at the left end given as either FREE or FIXED.

BCXN = boundary condition at right end in the x-direction given as either FREE, FIXED, or DEFINE;

BCYN = boundary condition at right end in the y-direction given as either FREE, FIXED or DEFINE;

BCMN = rotation boundary condition at the right end given as either FREE or FIXED;

FREE = BCD code representation of "FREE" used to compare with boundary conditions;

FIXED = BCD code representation of "FIXED" used to compare with boundary conditions;

DEFINE = BCD code representation of "DEFINE" used to compare with boundary conditions.

COMMON BLOCK BATEGK

X(I,J)* = coordinates of mass point I;
J = 1 gives x-coordinate,
J = 2 gives y-coordinate.

COMMON BLOCK EQMEGK

P6(I) = transverse load at the ith mass;

P(I) = longitudinal load at the ith mass.

COMMON BLOCK L

G = number of print lines in a graphical display (in PLT G is RNOFL).



COMMON BLOCK N

IN = number of elements in model;
 INP = IN + 1;
 INP2 = IN + 2;
 INP3 = IN + 3.

COMMON BLOCK P

P2 = depth, D, divided by length, L;
 P3 = length, L, divided by radius of gyration, RX;
 P4 = area, A, divided by radius of gyration squared, RX²;
 P7 = strain hardening ratio; plastic modulus E_p divided by the elastic modulus, E;
 P8 = yield stress, SY, divided by the elastic modulus, E;
 P10 = uniformly distributed load which will just cause yield in a similar simply supported span;
 PIE = π ;
 PIESQR = π^2 ;

COMMON BLOCK SEC

A(I) = ith discrete area of the cross-section divided by the total area;
 Z(I) = distance of the ith area from the neutral axis divided by the depth of the member.

COMMON BLOCK X

DISP(I,J) = response history of member; J = 1
gives time, J = 2 gives displacement;

ID = counter to keep track of subscript
I in DISP(I,J).

PROGRAM UNIAX

ALPHA = angle subtended by circular arch;

AT = total area of cross-section;

BM(I) = bending moment at joint i at $t+\Delta t$;

BS(I) = bending strain at joint i at $t+\Delta t$;

C(I) = cosine of the angle the ith panel
makes with the x-axis at $t+\Delta t$;

D = depth of the member;

DA = angle subtended by an element;

E = elastic modulus;

ES(I) = axial deformation in the ith
element at $t+\Delta t$;

H = initial element length, h_0 ;

HI(I) = deformed length of ith element;

IJKLMN = input parameter used to determine
if more data exists;

ISEC = number of discrete areas in cross-
section;

IX = moment of inertia of discrete
cross-section;

L = length of member;

LC = logical variable used to specify
convergence or nonconvergence;



LP	= logical variable used to enter print routines;
LSTART	= logical variable used to enter initialization routines;
MASS	= mass per unit length of member;
PCR	= critical elastic buckling load of a pin-ended column;
PPI	= uniformly distributed normal loading on arch;
P11	= auxiliary variable;
R	= ratio of inelastic modulus to the elastic modulus;
RAD	= radius of circular arch;
RAT	= coefficient of standard time increment used in varying the time increment;
RATIO	= ratio of the nth period of axial vibration to the nth period of bending vibration;
RX	= radius of gyration of the discrete section;
S(I)	= sine of the angle the ith panel makes with the x-axis at $t+\Delta t$;
SY	= yield stress;
T	= time;
TF	= $\frac{2L^2}{\pi} \sqrt{\frac{m}{EI}}$;
THS	= auxiliary variable;
THT	= auxiliary variable;
TI	= time increment;
TRST(I)	= axial force in the ith panel;

UDB(I,J) * = velocity of the ith mass at
 $t+\Delta t$ in the jth direction;
 UDDA(I,J) * = acceleration of the ith mass in
 the jth direction at time t ;
 Uddb(I,J) * = acceleration of the ith mass in
 the jth direction at time $t+\Delta t$;
 V(I) = shear in the ith panel at time
 $t+\Delta t$;
 ZN = number of elements in model in
 decimal form.

SUBROUTINE XSEC

B = width of flange or rectangular
 section;
 DENSITY = density of member material;
 DP = auxiliary variable;
 K = auxiliary variable;
 NF = number of discrete areas representing
 the flange;
 NW = number of discrete areas representing
 the web;
 T = thickness dimension of a discrete
 area;
 TF = thickness of the flange;
 TW = thickness of the web.

SUBROUTINE BTA

BSO(I) = initial rotation of the ith joint;
 ESO(I) = initial compression of the ith
 element;
 ICL = number of the mass point chosen for
 response history plot;



JJ = dummy index;
 MM = dummy counter;
 STB = temporary storage of BSO(I);
 STE = temporary storage of ESO(I);
 UA(I,J) * = displacement of the ith mass in the jth direction at time t;
 UB(I,J) * = displacement of the ith mass in the jth direction at time $t+\Delta t$;
 UDA(I,J) * = velocity of the ith mass in the jth direction at time t;
 XO(I,J) * = initial coordinates of the masses.

SUBROUTINE FRC

CST = program constant;
 CST2 = program constant;
 FA(I,J) = force in the jth spring at the ith section at time t;
 FB(I,J) = force in the jth spring at the ith section at time $t+\Delta t$;
 FUN1(A,B) = upper bound of the yield envelope of the force deformation relation;
 FUN2(A,B,C,) = elastic portion of the force deformation relation;
 FUN3(A,B) = lower bound of the yield envelope of the force deformation relation;
 JA(I,J) = zone factor for the jth spring at the ith section at time t
 JB(I,J) = zone factor for the jth spring at the ith section at time $t+\Delta t$;
 ST = spring deformation increment;
 STA(I,J) = deformation of the jth spring at the ith section of time t;



STB(I,J) = deformation of the jth spring at the ith section at time $t+\Delta t$;

STOA(I,J) = elastic strain axis intercept of the jth spring of the ith section at time t;

STOB(I,J) = elastic strain axis intercept of the jth spring of the ith section at time $t+\Delta t$;

STR(I,J) = stress at the jth area of the ith section;

STRAIN = temporary storage of the residual strains.

SUBROUTINE EQM

All variables have been previously defined.

SUBROUTINE EGK

APK = auxiliary variable;

BMA(I) = bending moment at the ith joint at time t;

BSA(I) = bending strain at the ith joint at time t;

CA(I) = cosine of the angle the ith panel makes with the x-axis at time t;

C1 = program constant;

C2 = program constant;

C3 = program constant;

C4 = program constant;

C5 = program constant;

C6 = program constant;

DT = time increment;

EA = energy absorbed by straining;

EAP = scaled energy absorbed by straining;
 EI = input energy;
 EIP = scaled input energy;
 EISASK = EIP-EAP-EKP;
 EK = kinetic energy;
 EKP = scaled kinetic energy;
 ESA(I) = axial deformation in the ith element at time t;
 FDH = horizontal impulse;
 FDV = vertical impulse;
 FH = FDH-VH;
 FV = FDV-VV;
 SA(I) = sine of the angle the ith panel makes with the x-axis;
 TRSTA(I) = axial force in the ith panel at time t;
 VA(I) = shear in the ith panel at time t;
 VH = horizontal momentum;
 VV = vertical momentum;
 XA(I,J) * = coordinates of the ith masspoint in the jth direction at time t;
 XAO(I,J) = unused variable.

SUBROUTINE THK

IP = print request counter;
 IRATIO = auxiliary variable;
 IRUT = auxiliary variable;
 NPR = number of print requests per fundamental period of bending vibration;



NPRT = number of steps of integration
between print request;

TMAX = length of time the solution is
to progress into the time domain.

SUBROUTINE PLT

BLANK = BCD code representation of a blank;

ICOUNT = counter;

IX(I,J) * = mass point coordinates converted
to scaled integer numbers;

K = auxiliary variable;

LINE(I) = represents 120 space print line
to be assembled;

MAX = maximum value of the scaled
integer y-coordinate;

MIN = minimum value of the scaled integer
y-coordinate;

POINT = BCD code representation of a ".";

RANGE = RMAX-RMIN;

RMAX = maximum value of the y-coordinate;

RMIN = minimum value of the y-coordinate;

SF = scale factor;

Z = BCD code representation of "x".

FUNCTION DX

DH = h_o and h_o^2 ;

DX = increment in x-coordinate between
adjacent masses;

DY = $(y_{i-1} - y_i)$ and $(y_{i-1} - y_i)^2$;

Y1 = y coordinate of the i-1 mass;

Y2 = y-coordinate of the ith mass.



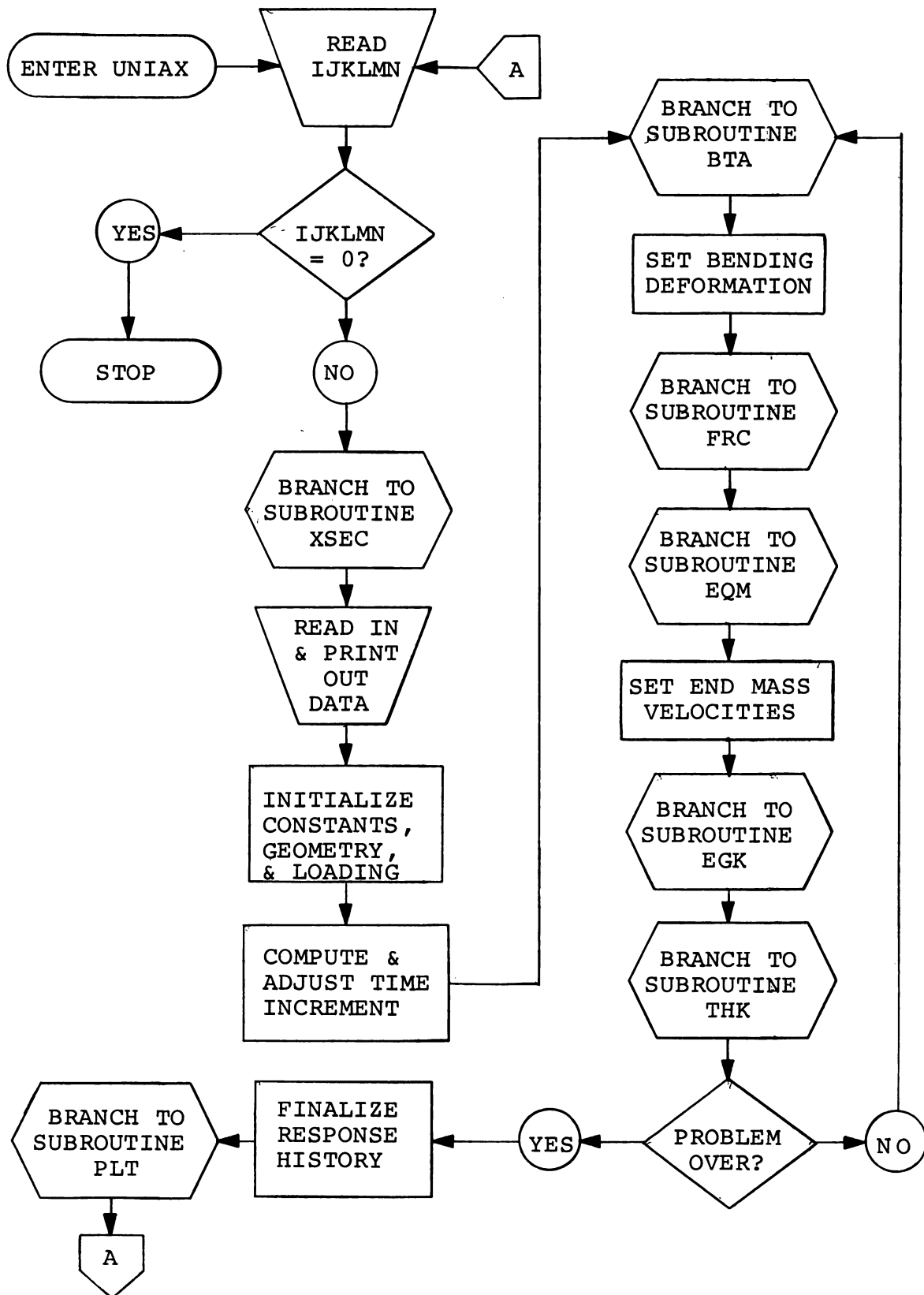
FUNCTION DPNL

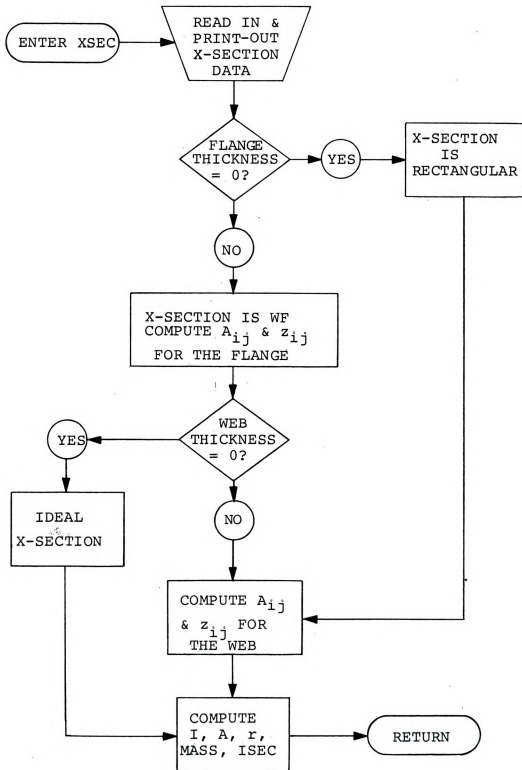
DPNL = deformed element length
 DZ = $(x_{i+1} - x_i)$ and $(x_{i+1} - x_i)^2$;
 X1 = x-coordinate of the ith mass;
 X2 = x-coordinate of i+1 mass.

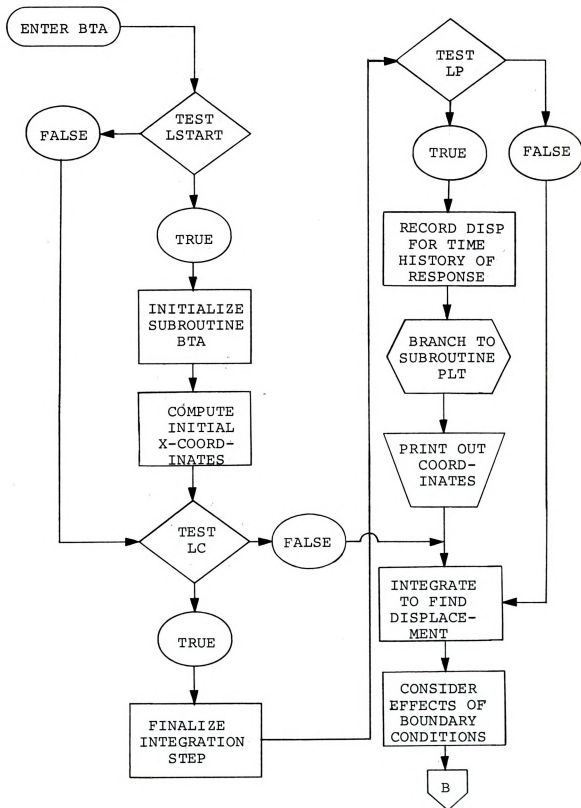
FUNCTION DEF

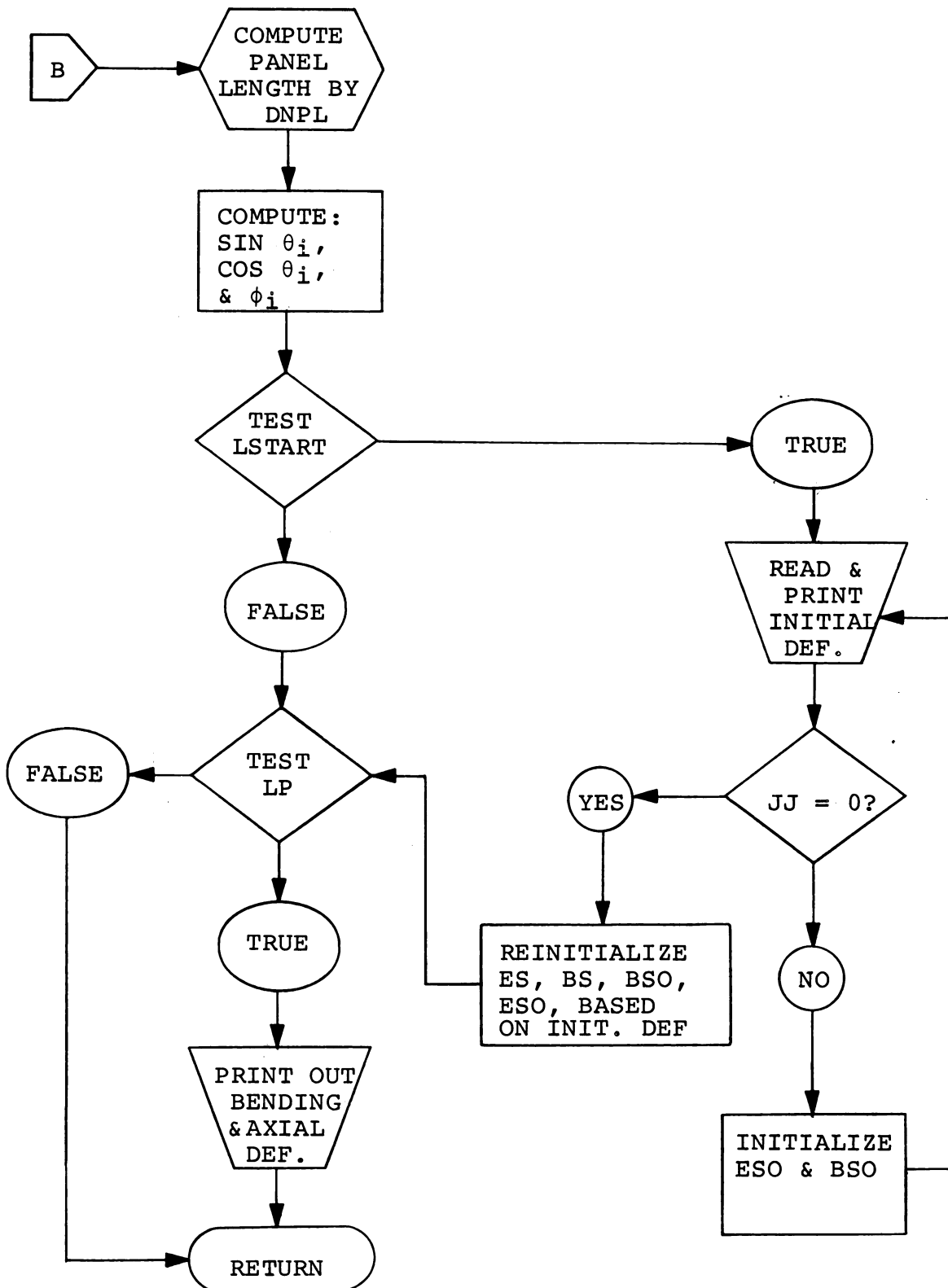
DEF = support motion at time $t+\Delta t$;
 I = number of data points to read in on input;
 N = counter;
 SLP = slope between two adjacent input points;
 TY(I,J) = ith point in prescribed support motion; J=2, ground displacement; J=1, time.

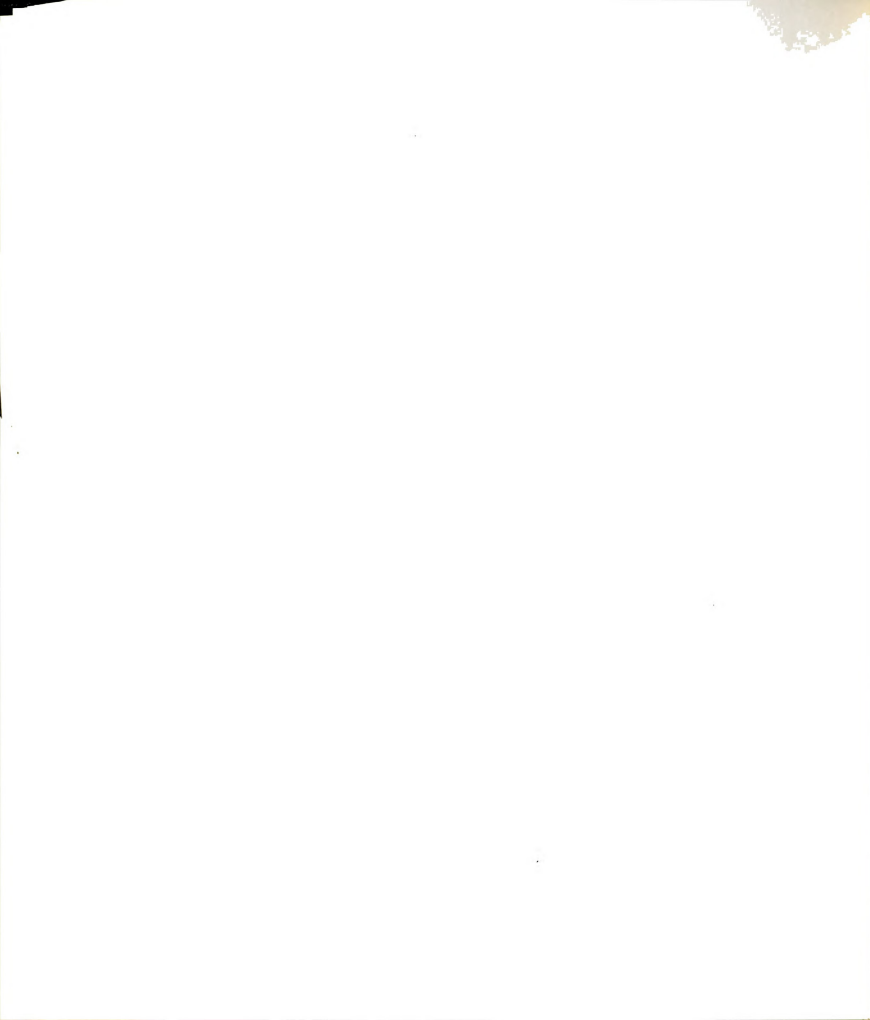


A.3 Flow DiagramsFLOW DIAGRAM FOR UNIAX

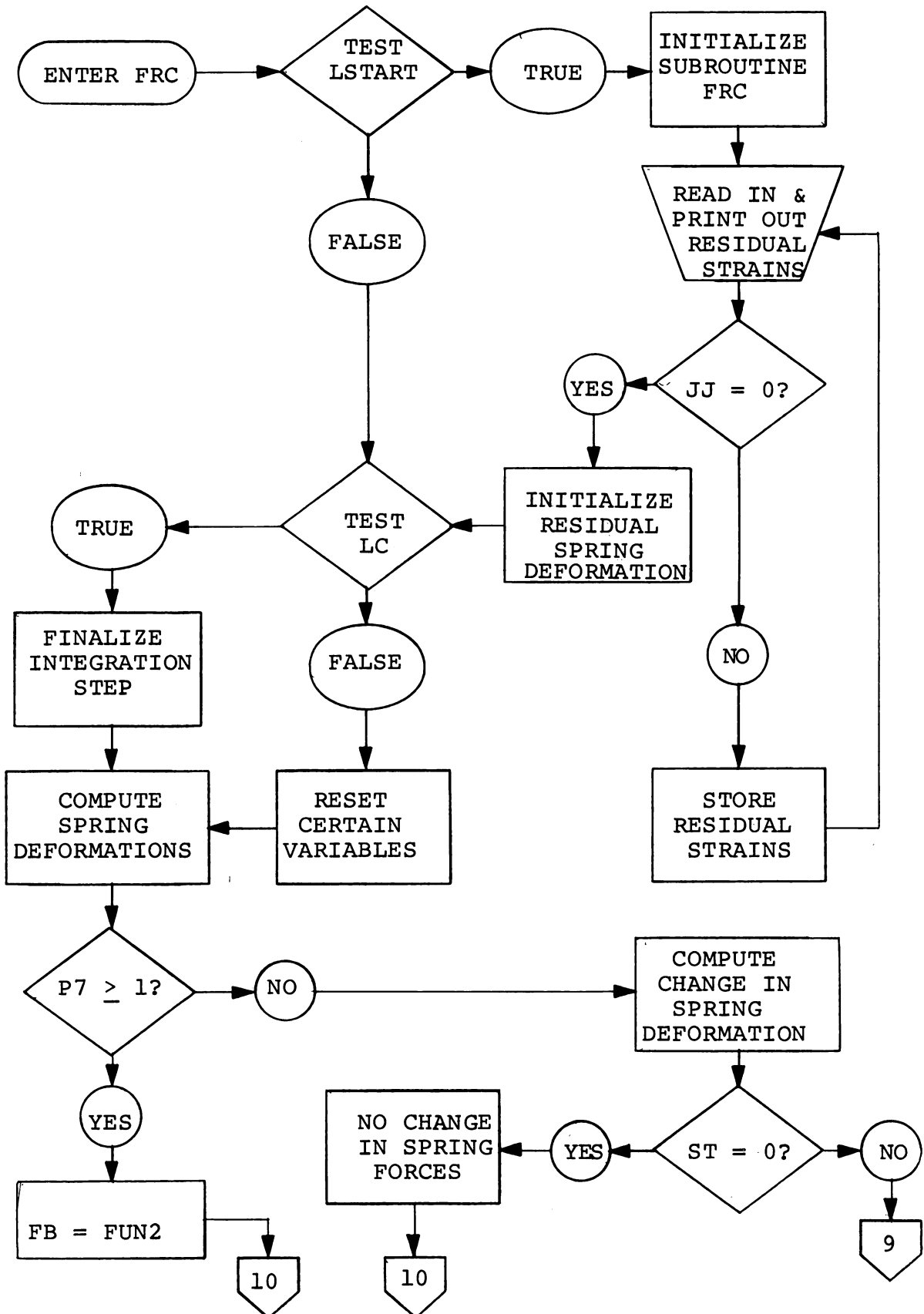
FLOW DIAGRAM FOR SUBROUTINE XSEC

FLOW DIAGRAM FOR SUBROUTINE BTA

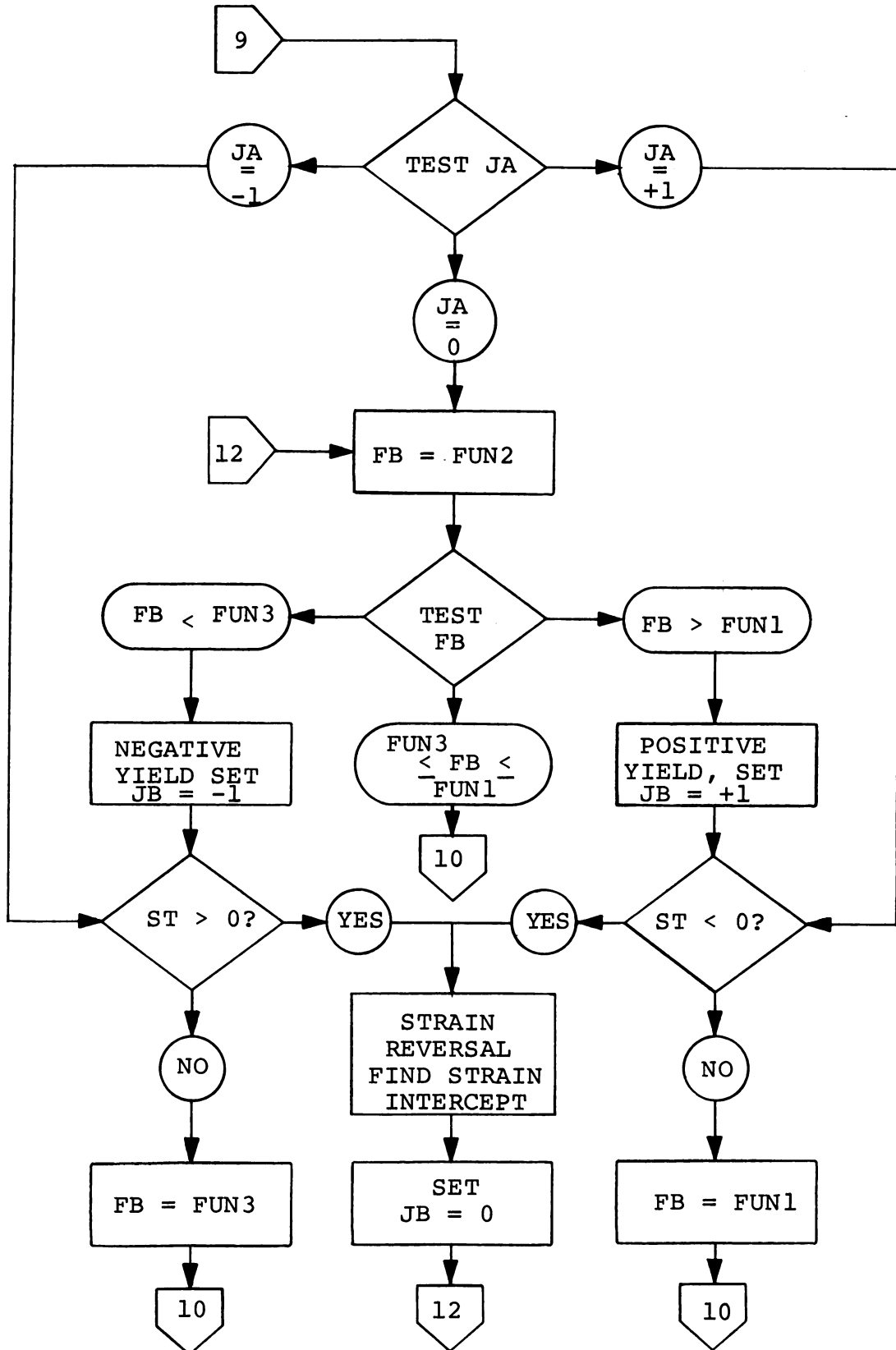
FLOW DIAGRAM FOR SUBROUTINE BTA (cont.)

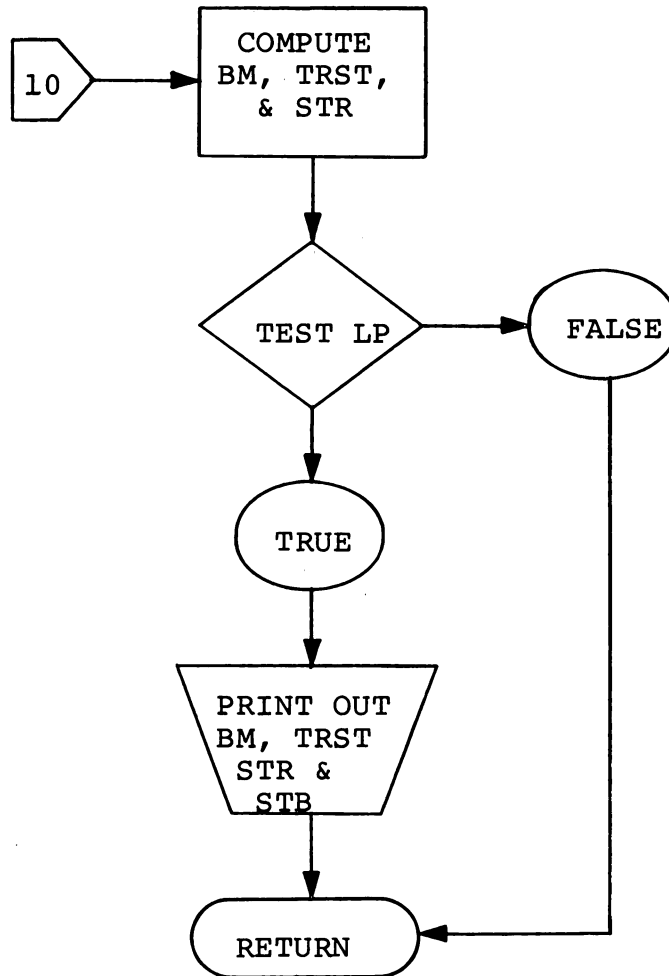


FLOW DIAGRAM FOR SUBROUTINE FRC

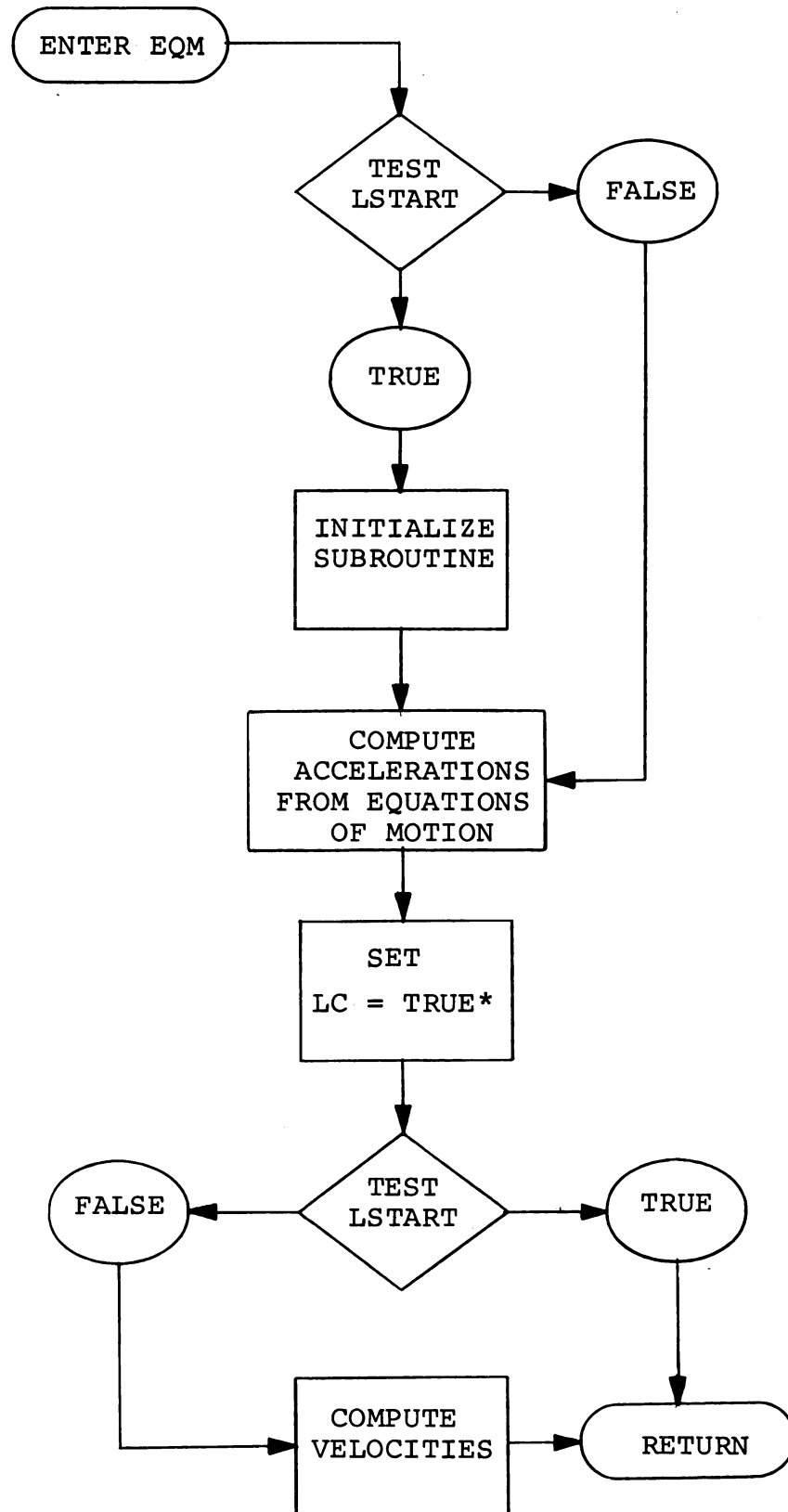


FLOW DIAGRAM FOR SUBROUTINE FRC (cont.)



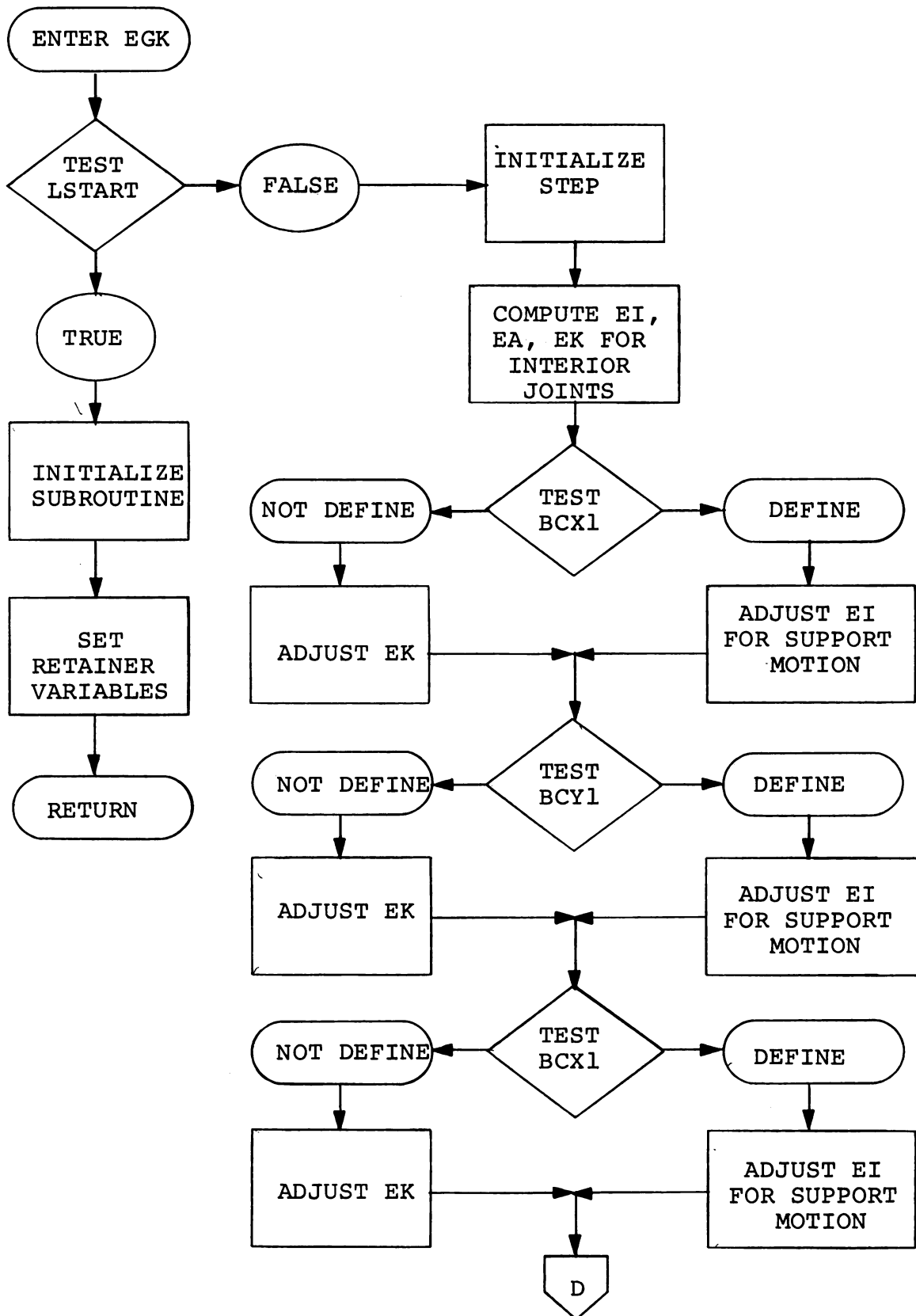
FLOW DIAGRAM FOR SUBROUTINE FRC (cont.)



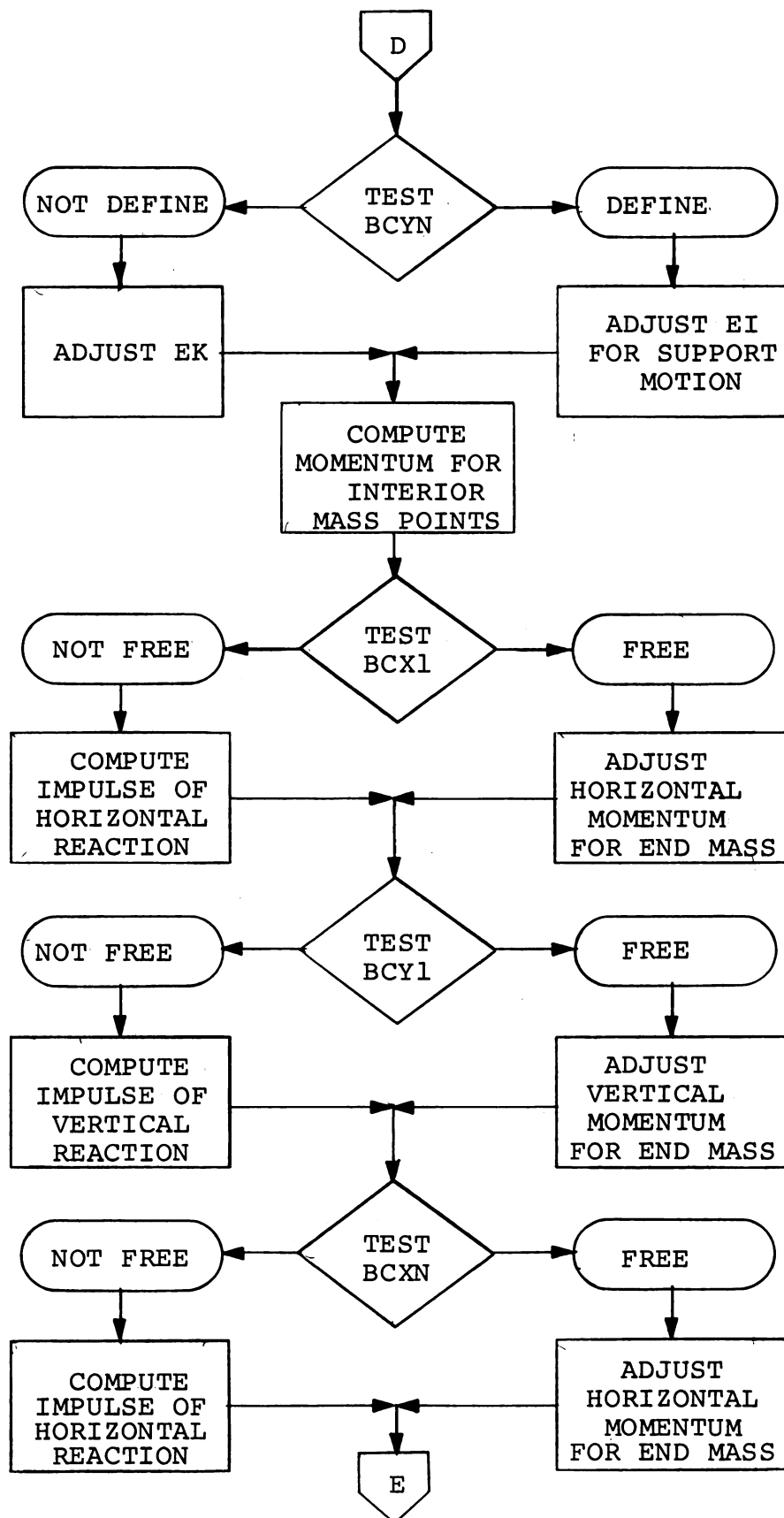
FLOW DIAGRAM FOR SUBROUTINE EQM

* $\beta = 0$ method converges automatically

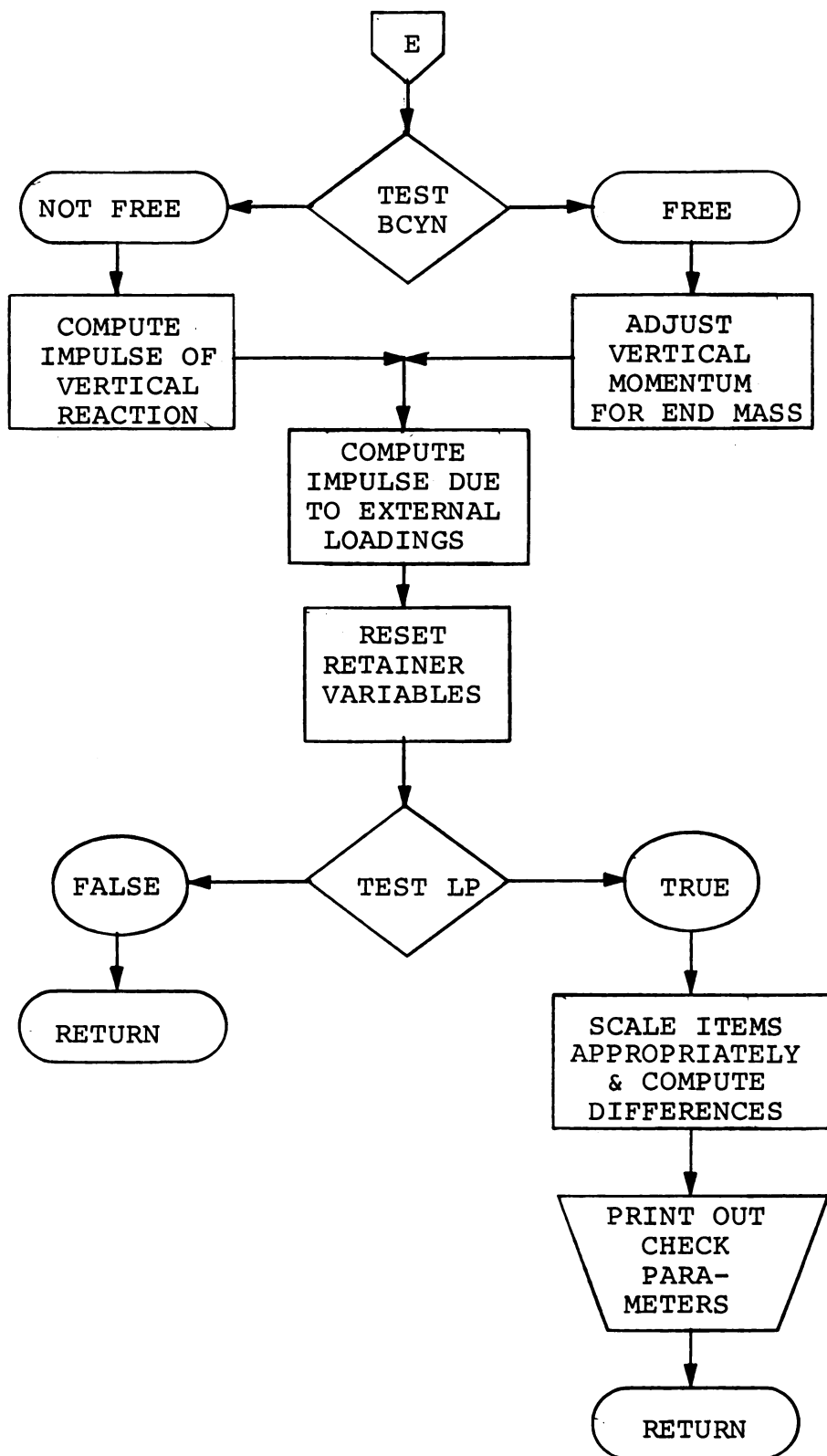
FLOW DIAGRAM FOR SUBROUTINE EGK

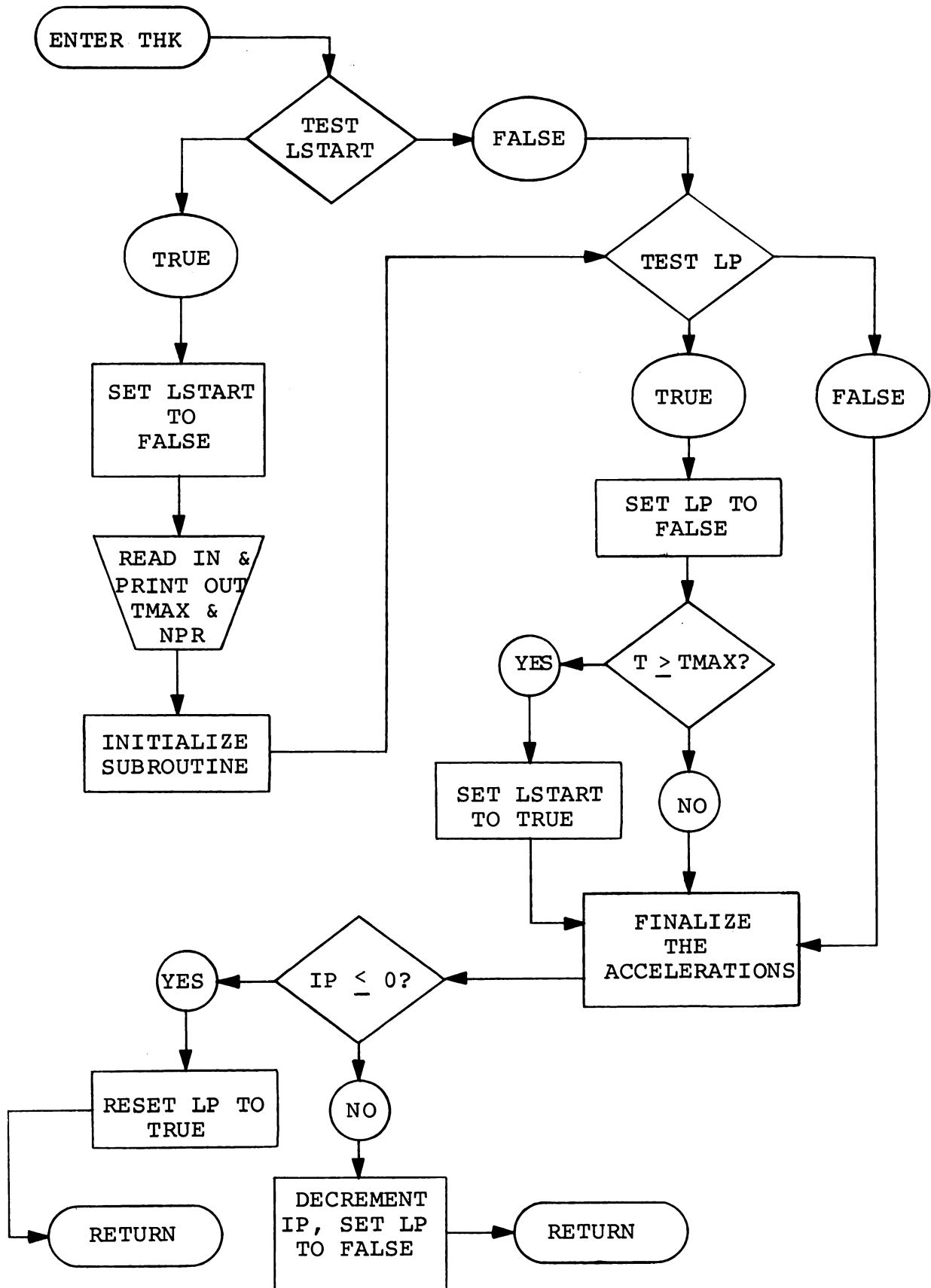


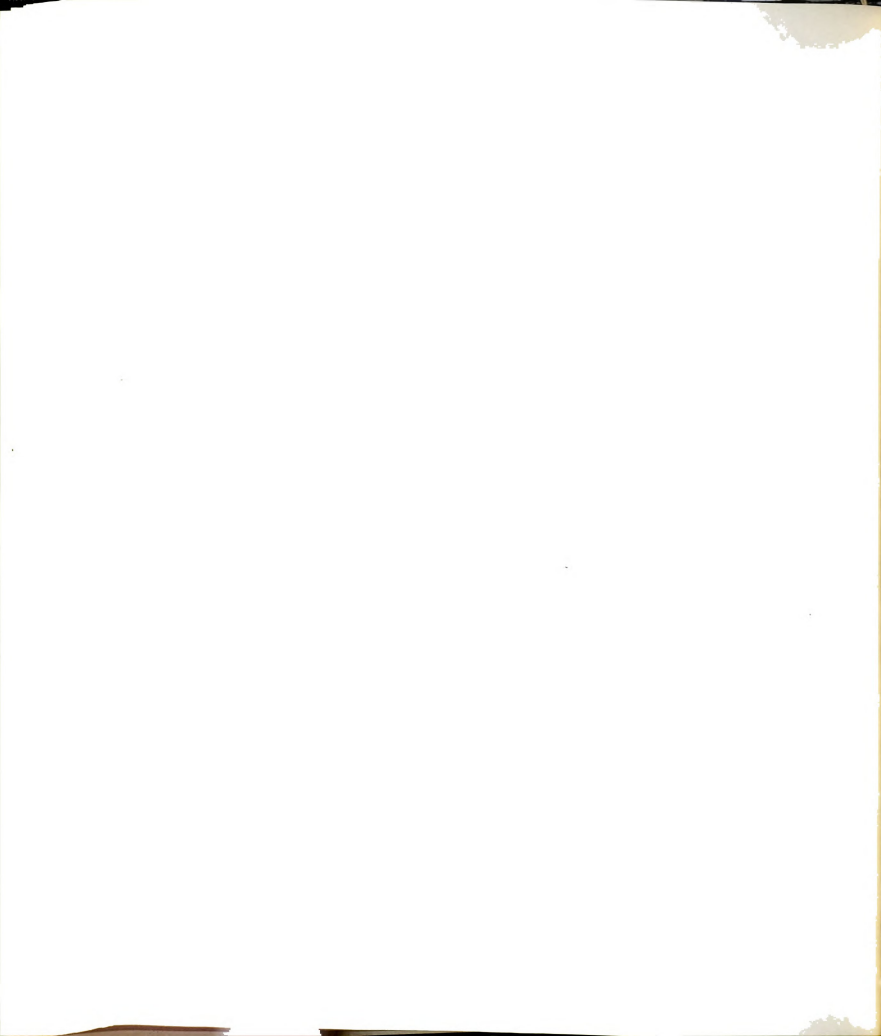
FLOW DIAGRAM FOR SUBROUTINE EGK (cont.)



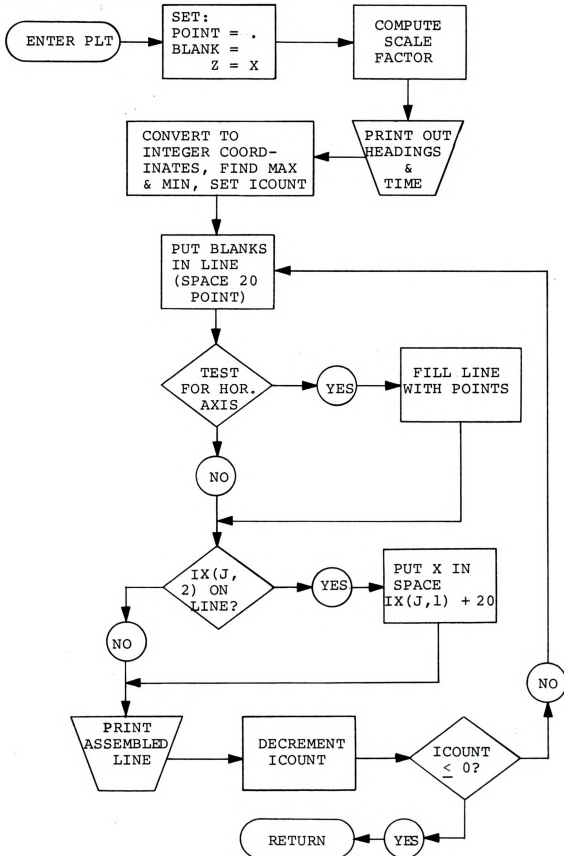


FLOW DIAGRAM FOR SUBROUTINE EGK

FLOW DIAGRAM FOR SUBROUTINE THK



FLOW DIAGRAM FOR SUBROUTINE PLT





A.4 Computer Program Listing

```

PROGRAM UNIAX
C THIS PROGRAM IS FOR CIRCULAR ARCHES.
C NONEXECUTABLE STATEMENTS
  DIMENSION UDDA(41,2),UDB(41,2),ES(41),S(41),C(41),
  1BM(41),TRST(41),UDB(41,2),V(41)
  DIMENSION A(10),Z(10),P(41),P6(41),X(41,2),HI(41)
  REAL IX,L,MASS
  INTEGER BCX1,BCY1,BCM1,BCXN,BCYN,BCMN,FREE,FIXED,DEFINE
  COMMON/SEC/A,Z
  COMMON/P/P2,P3,P4,P7,P8,P10,PIE,PIESQR
  LOGICAL LSTART,LC,LP
  COMMON/N/IN,INP,INP2,INP3
  COMMON/BC/BCX1,BCY1,BCM1,BCXN,BCYN,BCMN,FREE,FIXED,DEFINE
  COMMON/X/XDISP(41,2),ID/L/G
  COMMON/BTAEGK/X
  COMMON/EQMEGK/P6,P
C SET CONSTANTS FIXED, FREE, AND DEFINE IN ORDER TO TEST THE BOUNDARY
C CONDITIONS.
  DATA(FREE=8HFREE),(FIXED=8HFIXED),(DEFINE=8HDEFINE)
C THE FOLLOWING PORTION OF THE PROGRAM IS TO INPUT THE PARAMETERS WHICH
C DESCRIBE THE PROBLEM. ALL THE DATA SHOULD HAVE DIMENSIONS OF POUNDS,
C INCHES, OR SECONDS OR BE NONDIMENSIONAL.
C
C TEST FOR MORE DATA.
  5 READ 9,IJKLMN
  9 FORMAT(11)
  IF(IJKLMN.EQ.0)STOP
C THIS SUBROUTINE READS IN THE CROSS-SECTION DIMENSIONS AND COMPUTES THE
C NEEDED CROSS-SECTION PARAMETERS FROM THEM.
  CALL XSEC(IX,AT,RX,D,MASS,ISEC)
C READ IN OTHER NECESSARY DATA.
  READ 1,E,R,SY,RAD,ALPHA,RAT
  1 FORMAT(4(E15.6,5X))
C READ IN THE CONDITIONS OF CONSTRAINT.
  READ 2,BCX1,BCY1,BCM1,BCXN,BCYN,BCMN
  2 FORMAT(6(AB,/) )

```

```

C READ IN THE NUMBER OF PANELS.
  READ 3,IN
  3 FORMAT(I3)
C READ IN THE NORMAL LOAD IN POUNDS PER INCH.
  READ 1,PPI
C NOW PRINT OUT ALL THE DATA READ IN THAT IS OF IMPORTANCE.
  PRINT 1,E,R,SY,RAD,ALPHA,RAT,IX,AT,RX,MASS
  PRINT 2,BCX1,BCY1,BCM1,BCXN,BCYN,BCMN
  PRINT 3,IN
  PRINT 1,PPI
C THE NEXT PORTION OF THE PROGRAM COMPUTES CERTAIN CONSTANTS THAT ARE USED IN
C THE PROGRAM.
  G=10.
  ZN=IN
  PIE=3.141592654
  PIESQR=PIE*PIE
  LSTART=LC=LP=,TRUE.
  INP=IN+1
  INP2=IN+2
  INP3=IN+3
  ALPHA=ALPHA*PIE/180.
  DO 4 J=1,INP3
    P(J)=P6(J)=0.0
    DO 4 K=1,2
      X(J,K)=0.0
      4 UDDA(J,K)=UDDB(J,K)=0.0
C FROM THE GEOMETRY OF THE PROBLEM COMPUTE THE Y-COORDINATES OF THE MASS POINTS
C FOR A CIRCULAR ARCH. THE X-COORDINATES WILL BE COMPUTED IN SUBROUTINE BTA.
  DA=ALPHA/ZN
  L=2.*ZN*RAD*SIN(0.5*DA)
  P11=RAD/L
  DO 20 I=3,INP
    THT=(I-2)*0.5*DA
    THS=0.5*ALPHA-THT
    20 X(I,2)=-P11*2.0*SIN(THT)*SIN(THS)
    TF=2.*L*MSQR(MASS/(E*IX))/PIE

```



```

H=1.0/ZN
P2=D/L
P3=RX/L
P4=IX/RX**4
P7=R
P8=SY/E
PCR=E*IX*(PIE/L)**2
P10=16.*SY*IX/(L*L*D)
DO 21 I=3,INP
  THT=((1-2)*DA-0.5*ALPHA
  P6(I)=PPI* $\cos$ (THT)/P10
  21 P(I)=PPI*L* $\sin$ (THT)/(PCR*ZN)
C THE NEXT PORTION OF THE PROGRAM CHOOSES A TIME INCREMENT FOR THE SOLUTION.
C THE CONSTANT RATIO IS THE RATIO BETWEEN THE SMALLEST AXIAL PERIOD AND THE
C SMALLEST BENDING PERIOD. IT IS EQUAL TO  $\pi^2 E R / L$ .
C THE TIME INCREMENT IS FIRST BASED UPON THE BENDING PERIOD. IF THE AXIAL
C PERIOD ACTUALLY GOVERNS THE SELECTION OF THE TIME INCREMENT THE TIME INCREMENT
C IS LATER ADJUSTED.
  RATIO=PIE*ZN*P3
  TI=.1/(ZN*ZN)*RAT
  T=0.0
C CHECK TO SEE IF THE TIME INCREMENT NEEDS ADJUSTING.
  IF(RATIO.LT.1.)TI=RATIO*TI
C PRINT OUT THE TIME INCREMENT.
  PRINT 10,TI
  10 FORMAT(1H ,*TI = ,E15.7)
C
C
C THE NUMERICAL PROCEDURE IS ENTERED BY CALLING SUBROUTINE BTA. THIS SUBROUTINE
C USES THE BETA EQUAL ZERO METHOD TO COMPUTE THE DISPLACEMENTS OF THE
C MASSPOINTS, THE COORDINATES, THE DEFORMATION PARAMETERS, AND THE SINES AND
C COSINES OF THE PANELS.
  6 CALL BTA(UPDA,UDBB,H1LG,LP,LP,START,BS,ES,S,C,T,TI,UDB,H1)
C THE CONDITIONS OF CONSTRAINT ARE CHECKED FOR THE ROTATIONAL DEGREES OF FREEDOM
C AT BOTH ENDS OF THE SPAN.
  IF(BCM1.EQ.FIXED)BS(2)=2.*BS(2)

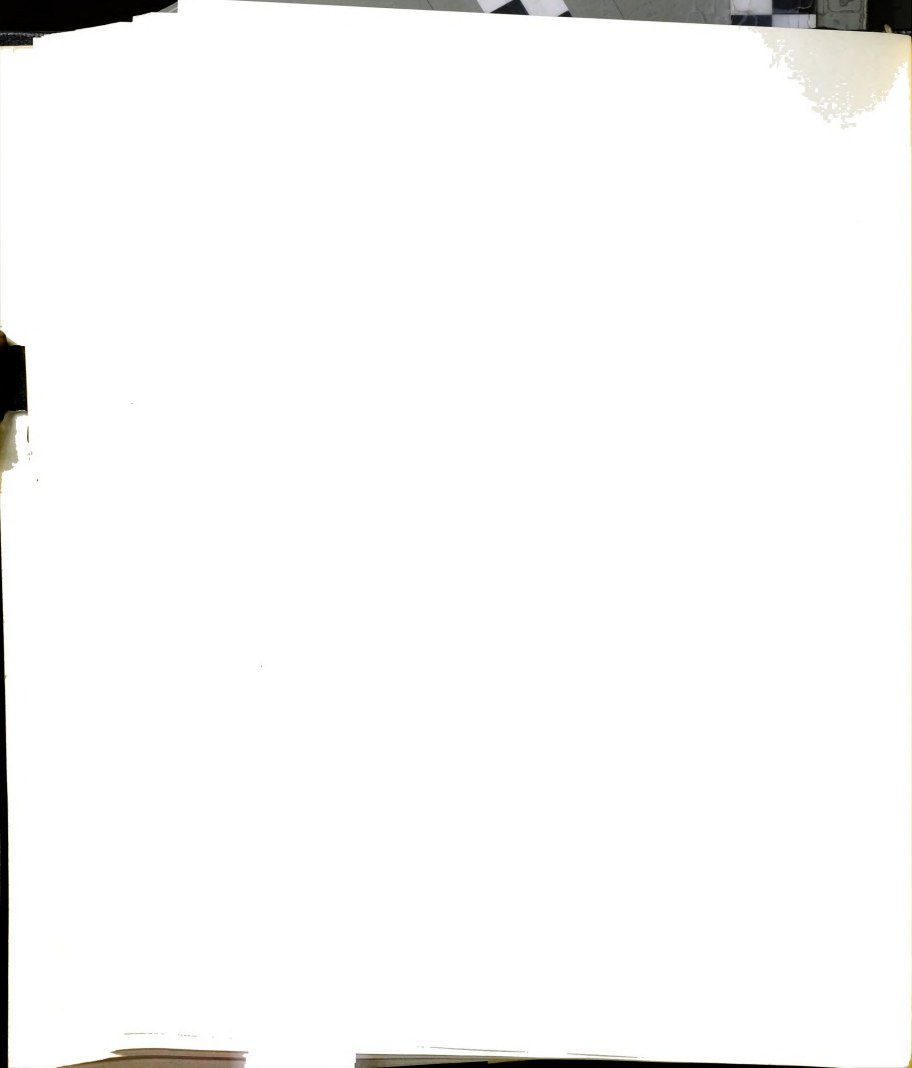
```




```

IF(BCM1.EQ.FREE)BS(2)=0.
IF(BCMN.EQ.FIXED)BS(1NP2)=2.*BS(1NP2)
IF(BCMN.EQ.FREE)BS(1NP2)=0.
C THE MOMENTS AND THRUSTS ARE CALCULATED IN SUBROUTINE FRC.
CALL FRC(BS,ES,LSTART,LC,H,BM,TRST,LP,ISEC)
C THE ACCELERATIONS OF THE MASSPOINTS ARE CALCULATED IN SUBROUTINE EGM. THE
C VELOCITIES ARE ALSO COMPUTED IN THIS ROUTINE.
CALL EGM(UDDA,UODB,UDB,TRST,BM,LC,LSTART,S,C,HI,TI,H,V)
C IN ORDER FOR THE ENERGY CHECK SUBROUTINE TO GIVE CORRECT RESULTS THE
C VELOCITIES OF THE END MASSPOINTS MUST BE ZEROED FOR CERTAIN CONDITIONS OF
C CONSTRAINT.
IF(BCX1.NE.FREE)UDB(2,1)=0.0
IF(BCY1.NE.FREE)UDB(2,2)=0.0
IF(BCXN.NE.FREE)UDB(1NP2,1)=0.0
IF(BCYN.NE.FREE)UDB(1NP2,2)=0.0
C THE NEXT SUBROUTINE CHECKS THE ENERGY AND THE IMPULSE AND MOMENTUM.
CALL ECK(TI,UDB,BM,S,C,TRST,LP,LSTART,ES,BS,V)
C SUBROUTINE THK IS A LOGICAL ROUTINE THAT DETERMINES IF IT IS TIME TO PRINT,
C INCREMENTS THE TIME AND DETERMINES IF THE PROBLEM IS COMPLETED.
CALL THK(LC,LP,LSTART,UDDA,UODB,T,TI,RATIO,RAT)
C IF THE PROBLEM HAS BEEN COMPLETED THEN LSTART IS TRUE.
IF(LSTART)GO TO 7
GO TO 6
C IF THE PROBLEM IS COMPLETED THE NEXT PORTION OF THE PROGRAM PRINTS OUT A TIME
C HISTORY OF THE CENTERLINE OR END DISPLACEMENT OF THE MEMBER DEPENDING ON
C THE BOUNDARY CONDITIONS OF THE PROBLEM.
C THIS DO LOOP UNITIZES THE TIME RANGE.
7 DO 8 J=1,1D
8 DISP(J,1)=DISP(J,1)/DISP(1D,1)
C SETTING G EQUAL TO 40 CAUSES THE GRAPH TO BE DRAWN ON 40 LINES OF PRINT.
G=40.
CALL PLT(DISP,1D,T)
C THIS PROBLEM IS NOW COMPLETE. GO TO THE BEGINNING AND CHECK FOR MORE DATA.
GO TO 5
END

```



```

SUBROUTINE XSEC(IX,AT,RX,D,MASS,ISEC)
C THIS SUBROUTINE IS TO COMPUTE THE CROSS-SECTION PARAMETERS FROM THE DIMENSIONS
C OF THE CROSS-SECTION.
C NONEXECUTABLE STATEMENTS
DIMENSION A(10),Z(10)
REAL IX,MASS
COMMON/SEC/A,Z
C READ IN AND PRINT OUT THE DIMENSIONS OF THE CROSS-SECTION. ISEC IS THE NUMBER
C OF DISCRETE AREAS THAT ONE-HALF OF THE CROSS-SECTION IS DIVIDED INTO.
READ 1,ISEC,DENSITY,B,D,TF,TW
PRINT 1,ISEC,DENSITY,B,D,TF,TW
1 FORMAT(12,8X,5E10.3)
C IF THE THICKNESS OF THE FLANGE IS GIVEN AS ZERO THEN THE CROSS-SECTION IS
C TREATED AS A RECTANGLE.
IF(TF)3,3,2
3 NF=1
NW=ISEC
TW=B
GO TO 7
C NF IS THE NUMBER OF DISCRETE SECTIONS ASSIGNED TO EACH FLANGE.
C NW IS THE NUMBER OF DISCRETE SECTIONS ASSIGNED TO EACH WEB.
2 NW=ISEC/2
NF=ISEC-NW
C THE REMAINING PORTIONS OF THIS PROGRAM COMPUTE THE AREAS AND Z DISTANCES OF
C THE DISCRETE SECTIONS. THE MOMENT OF INERTIA, TOTAL AREA, AND RADIUS OF
C GYRATION ARE ALSO COMPUTED.
C THE MASS PER UNIT LENGTH OF THE CROSS-SECTION IS ALSO COMPUTED.
T=TF/NF
DP=(D+T)/2.
DO 4 I=1,NF
A(I)=B*T
4 Z(I)=DP-I*T
NF=NF+1
7 IF(NW)6,6,8
8 T=(D/2.-TF)/NW
DP=(D+T)/2.-TF

```



```

DO 5 I=NF,ISEC
  A(I)=TW*T
  5 Z(I)=DP-(I+1-NF)*T
  AT=IX=0.
  6 DO 9 I=1,ISEC
    IX=2.*Z(I)*Z(I)*A(I)+IX
    9 AT=AT+2.*A(I)
    RX=SQRT(IX/AT)
    K=2*ISEC+1
    DO 10 I=1,ISEC
      A(I)=A(I)/AT
      Z(I)=Z(I)/D
      A(K-I)=A(I)
    10 Z(K-I)=-Z(I)
    MASS=DENSITY*AT
  C IN ORDER FOR THE VARIABLE ISEC TO BE USED ELSEWHERE IT MUST BE DOUBLED SO THAT
  C IT REPRESENTS THE TOTAL NUMBER OF DISCRETE AREAS IN THE CROSS-SECTION.
  ISEC=2*ISEC
  RETURN
END

C
C
SUBROUTINE BTA(UDDA,Uddb,H,LC,LP,LSTART,BS,ES,S,C,TI,UDB,HI)
C THIS ROUTINE COMPUTES THE DISPLACEMENTS OF THE MASS POINTS BY THE BETA
C EQUAL ZERO METHOD. MOST OF THE GEOMETRY CONSIDERATIONS ARE INCLUDED IN THIS
C SUBROUTINE. THE RESULTS OBTAINED FROM IT ARE USED TO COMPUTE THE INTERNAL
C RESULTANTS IN THE FRC SUBROUTINE.
  INTEGER BCX1,BCY1,BCM1,BCXN,BCYN,BCMN,BCMN,FREE,FIXED,DEFINE
  LOGICAL LP,LC,LSTART
  DIMENSION UA(41,2),UB(41,2),UDA(41,2),UDB(41,2),UDDA(41,2)
  1,UDB(41,2),BS(41),ES(41),S(41),C(41),X(41,2),XO(41,2),HI(41),
  2BSO(41),ESO(41)
  COMMON/P/P2,P3,P4,P7,P8,P10,PIE,PIESQR
  COMMON/BTAEKG/X
  COMMON/N/IN,INP,INP2,INP3
  COMMON/BC/BCX1,BCY1,BCM1,BCXN,BCYN,BCMN,BCMN,FREE,FIXED,DEFINE

```

BTA	4
BTA	6
BTA	7

```

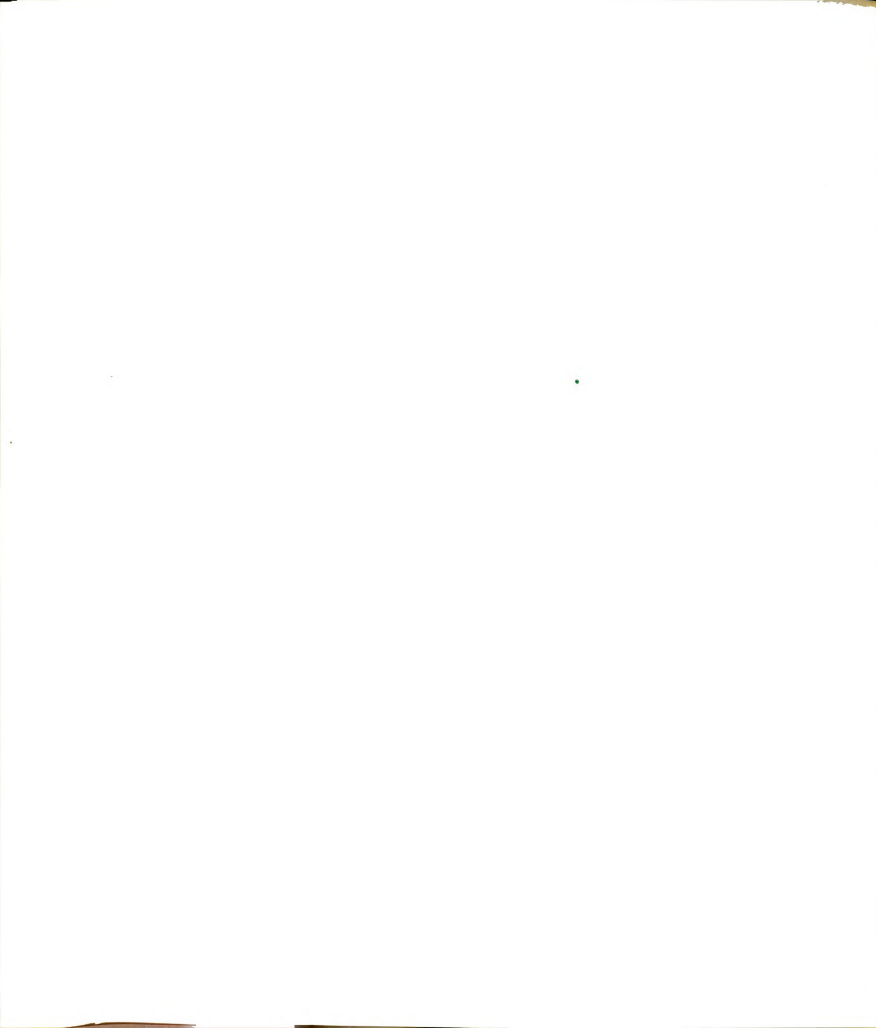
COMMON/X/ DISP(41,2),ID
C INITIALIZATION OF THE STEP.
C CHECK LSTART. IF LSTART EQUAL TRUE, THEN EVERY THING MUST BE
C INITIALIZED SINCE IT INDICATES THE BEGINING OF A PROBLEM
IF(.NOT..LSTART)GO TO 1
HI(1)=HI(INP2)=HI(INP3)=H
MM=0
ID=1
C ICL DETERMINES WHICH MASSPOINT WILL BE CHOSEN FOR THE TIME HISTORY.
C IF BCYN IS EITHER FIXED OR DEFINED THEN ICL = INP3/2+1
C IF BCYN = FREE THEN ICL = INP2
ICL=INP3/2+1
IF(BCYN.EQ.FREE)ICL=INP2
C ZERO CERTAIN VARIABLES.
ES(1)=0.
ES(INP2)=0.
DO 2 J=1,INP3
BSO(J)=ESO(J)=0.$ DO 2 K=1,2
2 XO(J,K)=UB(J,K)=UDB(J,K)=0.0
DO 1313 J=3,INP
1313 XO(J,2)=X(J,2)
C ESTABLISH THE X-COORDINATES SUCH THAT THE DISTANCE BETWEEN ADJACENT
C PANELS IS EQUAL TO H.
DO 4 J=3,INP2
4 XO(J,1)=XO(J-1,1)+DX(H,XO(J,2),XO(J-1,2))
C COMPUTE IMAGINARY JOINT LOCATIONS SUCH THAT ES AND BS EQ 0
DO 17 K=1,2
XO(1,K)=-XO(3,K)
17 XO(INP3,K)=2.*XO(INP2,K)-XO(INP,K)
C AT START DEFLECTIONS AND INITIAL DEFLECTIONS ARE EQUAL
DO 7 J=1,INP3
DO 7 K=1,2
7 X(J,K)=XO(J,K)
C COMPUTE THE SINES AND COSINES OF THE IMAGINARY PANELS.
S(1)=(X(2,2)-X(1,2))/H
C(1)=(X(2,1)-X(1,1))/H

```

BTA 10
BTA 11
BTA 12

BTA 26
BTA 28

BTA 29
BTA 31
BTA 32




```

S(INP2)=X(INP3,2)-X(INP2,2))/H
C(INP2)=(X(INP3,1)-X(INP2,1))/H
C INITIALIZATION FOR START OF PROBLEM IS COMPLETED
C NOW CHECK TO SEE IF INTEGRATION HAS CONVERGED IE. LC = TRUE
1 IF(.NOT.LC)GO TO 5
C IF THE INTEGRATION HAS CONVERGED THIS WILL FINALIZE STEP
DO 6 K=1,2
DO 6 J=1,INP3
  UA(J,K)=UB(J,K)
  6 UDA(J,K)=UDB(J,K)
C CHECK TO SEE IF IT IS TIME TO PRINT IE LP = TRUE
  IF(.NOT.LP)GO TO 5
C RECORD THE DEFLECTION OF MASS POINT ICL AND THE TIME TO BE PLOTTED
C LATER
  ID=ID+1
  IF(ID.GT.41)GO TO 18
  DISP(ID,2)=X(ICL,2)
  DISP(ID,1)=T
  18 CALL PLOT(X,INP2,T)
  PRINT 14
  14 FORMAT(1H0,11HCOORDINATES)
  PRINT 15,((X(J,K),K=1,2),J=1,INP3)
  15 FORMAT((BE15.7))
C COMPUTE THE DISPLACEMENTS BY THE BETA EQUAL ZERO METHOD.
  5 DO 8 J=2,INP2
  DO 8 K=1,2
    UB(J,K)=UA(J,K)+TI*UDA(J,K)+.5*TI*TI*UDDA(J,K)
C COMPUTE COORDINATES FROM DEFLECTIONS
    8 X(J,K)=X0(J,K)+UB(J,K)
    MM=MM+1
C SET THE DISPLACEMENT BOUNDARY CONDITIONS
    IF(BCX1.EQ.FIXED)X(2,1)=X0(2,1)
    IF(BCY1.EQ.FIXED)X(2,2)=X0(2,2)
    IF(BCXN.EQ.FIXED)X(INP2,1)=X0(INP2,1)
    IF(BCYN.EQ.FIXED)X(INP2,2)=X0(INP2,2)
    IF(BCX1.EQ.DEFINE)X(2,1)=DEF(T,LSTART)+X0(2,1)

```

BTA 33

BTA 35

BTA 37

BTA 39

BTA 40

BTA 41

BTA 45

BTA 48

BTA 49



```

      IF (BCY1.EQ.DEF)X(2,2)=DEF(T,LSTART)+XO(2,2)
      IF (BCXN.EQ.DEF)X(INP2,1)=DEF(T,LSTART)+XO(INP2,1)
      IF (BCYN.EQ.DEF)X(INP2,2)=DEF(T,LSTART)+XO(INP2,2)
      C COMPUTE THE DEFORMED PANEL LENGTH
      DO 9 J=2,INP
      HI(J)=DPNL(X(J,1),X(J+1,1),X(J,2),X(J+1,2))
      C COMPUTE SINES AND COSINES
      SJ(J)=(X(J+1,2)-X(J,2))/HI(J)
      CJ(J)=(X(J+1,1)-X(J,1))/HI(J)
      C COMPUTE THE AXIAL DEFORMATION
      9 ES(J)=H-HI(J)+ESO(J)
      C COMPUTE BENDING DEFORMATION
      DO 10 J=2,INP2
      10 BS(J)=ASIN(-S(J)*C(J-1)+S(J-1)*C(J))+BSO(J)
      IF(LSTART)GO TO 11
      21 IF(.NOT.LP)GO TO 13
      C IF LP = TRUE, PRINT OUT THE MATERIAL AS DEFINED BELOW.
      PRINT 19
      19 FORMAT(16HOB5(J) AND ES(J))
      PRINT 20,(BS(J),J=1,INP3),(ES(J),J=1,INP3)
      20 FORMAT(/,16E20,10)
      13 RETURN
      C READ IN THE INITIAL DEFORMATIONS FOR THE STATIC LOADINGS.
      11 READ 30,JJ,STE,STB
      PRINT 30,JJ,STE,STB
      30 FORMAT(12,8X,2E15,6)
      IF(JJ.EQ.0)GO TO 31
      ESO(JJ)=STE*(P8*H)
      BSO(JJ)=STB
      GO TO 11
      31 DO 12 J=1,INP3
      ESO(J)=ESO(J)-ES(J)
      BSO(J)=BSO(J)-BS(J)
      BS(J)=BSO(J)+BS(J)
      12 ES(J)=ESO(J)+ES(J)
      GO TO 21
      END

```

BTA 56

BTA 58

BTA 59

BTA 60

BTA 61

BTA 64

BTA 67

BTA 68

BTA 72



```

SUBROUTINE FRC(BS,ES,LSTART,LC,H,BM,TRST,LP,ISEC)
C THIS ROUTINE CALCULATES THE INTERNAL RESULTANTS, MOMENT AND THRUST
  DIMENSION BS(41),ES(41),JA(41,10),JB(41,10),STA(41,10),STB(41,10),
  1STOA(41,10),STOB(41,10),FA(41,10),FB(41,10),Z(10),A(10),BM(41),
  2TRST(41),STR(41,10)
  LOGICAL LSTART,LC
  COMMON/SEC/A,Z
  COMMON/P/P2,P3,P4,P7,P8,P10,PIE,PIESQR
  COMMON/N/IN,INP,INP2,INP3
C THE STATEMENT FUNCTIONS IN THIS ROUTINE ARE USED TO COMPUTE SPRING FORCES.
  FUN2(A,B,C)=CST*C*(A-B)
  FUN1(A,B)=CST*B*(P7*(A-1.))+1.)
  FUN3(A,B)=CST*B*(P7*(A+1.))-1.)
C CHECK TO SEE IF IT IS THE BEGINNING OF THE PROBLEM.
  IF(.NOT.LSTART)GO TO 1
  MM=0
C INITIALIZE THE ROUTINE
  2 FORMAT(12/(8F10.7))
  PRINT 2,ISEC,(Z(J),A(J),J=1,ISEC)
C SET CERTAIN PARAMETERS TO THEIR INITIAL VALUES
  CST=PB/(PIE*P3)**2
  CST2=PIE**2*P2/(2.*P8)
  TRST(1)=0.
  TRST(INP2)=0.
  DO 3 K=1,ISEC
    STOB(1,K)=0.0
    DO 3 J=2,INP2
      JA(J,K)=JB(J,K)=0
    3 STB(J,K)=0.0
C READ IN THE INITIAL RESIDUAL STRAINS.
  22 READ 24,JJ,STRAIN
  PRINT 24,JJ,STRAIN
  IF(JJ.EQ.0)GO TO 21
  STOB(1,JJ)=STRAIN
  GO TO 22
  21 DO 23 J=2,INP2

```



```

DO 23 K=1,ISEC
  STOB(J,K)=STOB(1,K)
  23 FB(J,K)=FUN2(0.0,STOB(J,K),A(K))
  24 FORMAT(12,BX,E15.6)
C CHECK TO SEE IF PREVIOUS STEP HAS CONVERGED
  1 IF(.NOT.LC)GO TO 4
C IF STEP HAS CONVERGED THIS WILL FINALIZE IT BY SETTING THE FINAL
C VALUES EQUAL TO THE TRIAL VALUES
DO 5 J=2,INP2
DO 5 K=1,ISEC
  JA(J,K)=JB(J,K)
  STA(J,K)=STB(J,K)
  STOA(J,K)=STOB(J,K)
  5 FA(J,K)=FB(J,K)
  GO TO 6
C IF THE STEP HAS NOT CONVERGED RESET THE PERMANENT STRAIN TO THE
C LAST CONVERGED VALUE
  4 DO 7 J=2,INP2
    DO 7 K=1,ISEC
      JB(J,K)=JA(J,K)
      7 STOB(J,K)=STOA(J,K)
    DO 8 J=2,INP2
      BM(J)=0.
      TRST(J)=0.
    DO 8 K=1,ISEC
C NOW FIND THE STRAIN IN EACH SPRING
      STB(J,K)=(ES(J)+P2*Z(K)*BS(J))/(P8*H)
      IF(P7.LT.1.0)GO TO 16
      FB(J,K)=FUN2(STB(J,K),0.0,A(K))
      GO TO 10
    16 ST=STB(J,K)-STA(J,K)
C IF ST IS EQUAL TO ZERO NO ADDITIONAL STRAINING HAS TAKEN PLACE
C AND HENCE THE FORCE IN THE SPRING IS UNCHANGED
      IF(ST.NE.0.)GO TO 9
      FB(J,K)=FA(J,K)

```




```

GO TO 10
C TEST JA TO SEE WHAT ZONE OF THE STRESS STRAIN DIAGRAM THE SPRING IS IN
C JA = +1 IMPLIES POSITIVE YIELDING, JA = -1 IMPLIES NEGATIVE YIELDING
C AND JA = 0 IMPLIES ELASTIC ZONE      GO TO THE APPROPRIATE ZONE.
  9 IF(JA(J,K))11,12,13
 14 JB(J,K)=-1
C CHECK TO SEE IF A REVERSAL IN STRAINING HAS OCCURRED
 11 IF(ST)17,17,18
 15 JB(J,K)=+1
C CHECK TO SEE IF A REVERSAL IN STRAINING HAS OCCURRED.
 13 IF(ST)18,19,19
C IF A REVERSAL OF STRAINING HAS OCCURRED, COMPUTE THE PERMANENT SET AND
C CHANGE THE ZONE FACTOR JB
 18 STOB(J,K)=STA(J,K)-FA(J,K)/(CST*A(K))
  JB(J,K)=0
C COMPUTE THE FORCE IN THE SPRING
 12 FB(J,K)=FUN2(STB(J,K),STOB(J,K),A(K))
C CHECK TO SEE IF YIELDING HAS OCCURRED.
  IF (FB(J,K).LT.FUN3(STB(J,K),A(K)))GO TO 14
  IF(FB(J,K).GT.FUN1(STB(J,K),A(K)))GO TO 15
  GO TO 10
C COMPUTE THE FORCE IN THE SPRING
 17 FB(J,K)=FUN3(STB(J,K),A(K))
  GO TO 10
C COMPUTE THE FORCE IN THE SPRING
 19 FB(J,K)=FUN1(STB(J,K),A(K))
C COMPUTE THE MOMENTS AND THRUSTS
 10 BM(J)=BM(J)+Z(K)*FB(J,K)*P2*CST2
  ST(J,K)=FB(J,K)/(CST*A(K))
  8 TRST(J)=TRST(J)+FB(J,K)
  MM=MM+1
  IF(.NOT.LP)GO TO 20
C IF LP EQUAL TRUE, PRINT OUT THE BELOW VALUES.
  PRINT 101
 101 FORMAT(9H0STR(J,K))
  PRINT 100,((STR(J,K),K=1,ISEC),J=1,INP3)

```

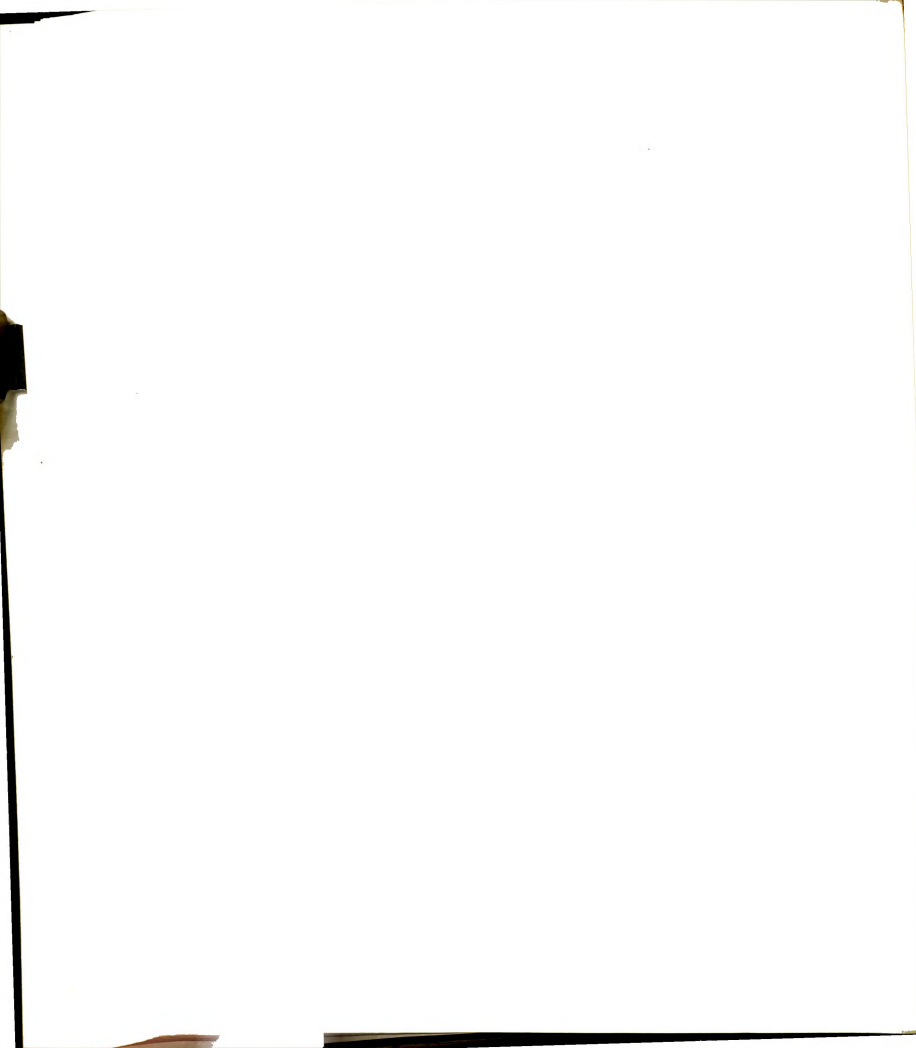


```

PRINT 102
102 FORMAT(9H0STB(J,K))
PRINT 100,((STB(J,K),K=1,ISEC),J=1,INP3)
PRINT 103
103 FORMAT(18H0BM(J) AND TRST(J))
PRINT 100,(BM(J),J=1,INP3),(TRST(J),J=1,INP3)
100 FORMAT(/,(6E20,10))
20 RETURN
END

C
C
SUBROUTINE EQM(UDDA,Uddb,UDb,TRST,BM,LC,LSTART,S,C,HI,TI,H,V)
C EQUATION OF MOTION SUBROUTINE
C THIS ROUTINE COMPUTES THE ACCELERATION OF THE MASS POINTS.
DIMENSION UDDA(41,2),Uddb(41,2),UDb(41,2),V(41), TRST(41),
1BM(41),S(41),C(41),P(41),P6(41),HI(41)
COMMON/EQMEGK/P6,P
COMMON/P/P2,P3,P4,P7,P8,P10,PIE,PIESQR
COMMON/N/IN,INP,INP2,INP3
LOGICAL LSTART,LC
IF(.NOT.LSTART)GO TO 1
ZN=IN
C THE SHEARS ARE DETERMINED FROM THE MOMENTS FOR USE IN THE EQUATIONS OF MOTION.
1 DO 9 I=1,INP2
9 V(I)=(BM(I+1)-BM(I))/HI(I)
V(INP2)=0.0
C COMPUTE THE ACCELERATIONS
C THERE ARE SIX TYPES OF EQUATIONS ALL BASICALLY THE SAME. TWO FOR THE
C INTERIOR MASSES, TWO FOR THE RIGHT END, AND TWO FOR THE LEFT END.
C IN EACH PAIR ONE EQUATION IS FOR THE HORIZONTAL DIRECTION AND THE OTHER IS
C FOR THE VERTICAL DIRECTION.
DO 7 J=3,INP
UDDB(J,2)=4.*ZN*(TRST(J-1)*S(J-1)+P6(J)*P8*16./(ZN*P2*PIESQR))-
1TRST(J)*S(J)+P8*2./(P2*PIESQR)*(V(J)*C(J)-V(J-1)*C(J-1))
UDDB(J,1)=4.*ZN*(TRST(J-1)*C(J-1)-TRST(J)*C(J)+P8*2./(P2*PIESQR)*
1(V(J-1)*S(J-1)-V(J)*S(J))-P(J))

```



```

7 CONTINUE
J=2
UDB(J,2)=8.*ZN*(TRST(J-1)*S(J-1)+P6(J)*P8*16./(ZN*P2*PIESQR)-
1TRST(J)*S(J)+P8*2./(P2*PIESQR)*(V(J)*C(J)-V(J-1)*C(J-1)))
UDB(J,1)=8.*ZN*(TRST(J-1)*C(J-1)-TRST(J)*C(J)+P8*2./(P2*PIESQR)*
1(V(J-1)*S(J-1)-V(J)*S(J))-P(J))
J=INP2
UDB(J,2)=8.*ZN*(TRST(J-1)*S(J-1)+P6(J)*P8*16./(ZN*P2*PIESQR)-
1TRST(J)*S(J)+P8*2./(P2*PIESQR)*(V(J)*C(J)-V(J-1)*C(J-1)))
UDB(J,1)=8.*ZN*(TRST(J-1)*C(J-1)-TRST(J)*C(J)+P8*2./(P2*PIESQR)*
1(V(J-1)*S(J-1)-V(J)*S(J))-P(J))
LC=.TRUE.
C COMPUTE THE VELOCITIES NOW THAT THE ACCELERATIONS ARE KNOWN. THIS STEP IS
C SKIPPED THE FIRST TIME THROUGH THE PROCEDURE.
IF(LSTART)RETURN
DO 5 J=2,INP2
DO 5 K=1,2
5 UDB(J,K)=UDB(J,K)+.5*TI*(UDDA(J,K)+UDB(J,K))
RETURN
END

C
C
SUBROUTINE EGK(DT,UDB,BM,S,C,TRST,LP,LSTART,ES,BS,V)
C THIS SUBROUTINE CHECKS THE INPUT ENERGY OF THE SYSTEM AGAINST THE ABSORBED
C ENERGY AS A PROGRAM CHECK. THESE TWO ENERGIES SHOULD REASONABLY AGREE.
C THE SUBROUTINE ALSO CHECKS THE IMPULSE AGAINST THE MOMENTUM AS ANOTHER
C PROGRAM CHECK.
C NONEXECUTABLE STATEMENTS
DIMENSION UDB(41,2),BM(41),S(41),C(41),TRST(41),BMA(41),TRSTA(41),
1XA(41,2),XAO(41,2),SA(41),CA(41),ES(41),BS(41),V(41),X(41,2),
2P(41),ESA(41),BSA(41),VA(41),P6(41)
LOGICAL LP,LSTART
INTEGER BCX1,BCY1,BCM1,BCXN,BCYN,BCMN,FREE,FIXED,DEFINE
COMMON/P2,P4,P7,P8,P10,PIE,PIESQR
COMMON/N/IN,INP,INP2,INP3
COMMON/BC/BCX1,BCY1,BCM1,BCXN,BCYN,BCMN,FREE,FIXED,DEFINE

```



```

COMMON/EQMEGK/P6,P
COMMON/BTAEGK/X
C THIS PORTION OF THE SUBROUTINE COMPUTES CERTAIN CONSTANTS AND INITIALIZES THE
C ROUTINE.
  IF(.NOT.LSTART)GO TO 1
  ZN=IN
  C1=2.*P8/(P2*PIESQR)
  C2=1.0/(8.*ZN)
  C3=2.*P8 /(P2*PIESQR)
  C4=16.*P8/(PIESQR*ZN*P2)
  C5=2.*C2
  C6=0.5*P2*P2*PIESQR/(P8*P8)

C
  BS(2)=0.5*BS(2)
  BS(INP2)=0.5*BS(INP2)
  DO 2 I=1,INP3
    VA(I)=V(I)
    BSA(I)=BS(I)
    ESA(I)=ES(I)
    BMA(I)=BM(I)
    TRSTA(I)=TRST(I)
    XA(I,1)=XAO(I,1)=X(I,1)
    XA(I,2)=XAO(I,2)=X(I,2)
    SA(I)=S(I)
    2 CA(I)=C(I)

C
  EI=EA=FDH=FDV=0.0
  RETURN

C
C INITIALIZE OR SET EQUAL TO ZERO THE KINETIC ENERGY AND THE MOMENTAS.
  1 EK=VH=VV=0.0
C SINCE THE BENDING STRAINS WERE DOUBLED TO FIND THE INTERNAL RESULTANTS IT IS
C NOW NECESSARY TO HALVE THEM IN ORDER TO COMPUTE THE ABSORBED ENERGY.
  BS(INP2)=0.5*BS(INP2)
  BS(2)=0.5*BS(2)
C THIS COMPUTES THE KINETIC ENERGY OF THE INTERIOR MASS POINTS.

```




```

DO 3 I=3, INP
3 EK=EK+C2*(UDB(I,1)*UDB(I,1)+UDB(I,2)*UDB(I,2))
C THIS COMPUTES THE STRAIN ENERGY OF ALL THE SPRING SYSTEMS IN THE MODEL.
DO 4 I=2, INP2
EA=EA+0.5*C1*((BMA(I)+BM(I))*(BS(I)-BSA(I)))
4 EA=EA+0.5*((TRSTA(I)+TRST(I))*(ES(I)-ESA(I)))
C THIS STEP COMPUTES THE INPUT ENERGY DUE TO EXTERIOR LOADS ACTING ON THE
C INTERIOR MASS POINTS.
DO 5 I=3, INP
5 EI=EI+C4*P6(I)*(X(I,2)-XA(I,2))-P(I)*(X(I,1)-XA(I,1))
C THE FOLLOWING STEPS COMPUTE THE INPUT ENERGY AND ADJUST THE KINETIC ENERGY
C ACCORDING TO THE SUPPORT CONDITIONS OF THE PROBLEM.
IF(BCX1-DEFINE)7,8,7
8 EI=EI+0.5*(( V(2) *S(2)+ VA(2) *SA(2))*C3+(TRST(2)*
1C(2)+TRSTA(2)*CA(2)))*(X(2,1)-XA(2,1))
GO TO 9
7 EK=EK+C2*UDB(2,1)*UDB(2,1)*0.5
EI=EI-P(2)*(X(2,1)-XA(2,1))
9 IF(BCY1-DEFINE)10,11,10
11 EI=EI+0.5*((TRST(2)*S(2)+TRSTA(2)*SA(2))-C3*( V(2) *C(2)+
1 VA(2) *CA(2)))*(X(2,2)-XA(2,2))
GO TO 12
10 EK=EK+C2*UDB(2,2)*UDB(2,2)*0.5
EI=EI+P6(2)*(X(2,2)-XA(2,2))*C4
12 IF(BCXN-DEFINE)13,14,13
14 EI=EI-0.5*((TRST(INP)*C(INP)+TRSTA(INP)*CA(INP))+C3*( V(INP)
1 *S(INP)+ VA(INP) *SA(INP)))*(X(INP2,1)-
2XA(INP2,1))
GO TO 15
13 EK=EK+C2*UDB(INP2,1)*UDB(INP2,1)*0.5
EI=EI-P(INP2)*(X(INP2,1)-XA(INP2,1))
15 IF(BCYN-DEFINE)16,17,16
17 EI=EI-0.5*((TRST(INP)*S(INP)+TRSTA(INP)*SA(INP))-C3*( V(INP)
1 *C(INP)+ VA(INP) *CA(INP)))*(X(INP2,2)-
2XA(INP2,2))
GO TO 18

```



```

16 EK=EK+C2*UDB(INP2,2)*UDB(INP2,2)*0.5
   EI=E1+P6(INP2)*(X(INP2,2)-XA(INP2,2))*C4
C
C THE NEXT PORTION OF THE SUBROUTINE IS CONCERNED WITH THE IMPULSE MOMENTUM
C CHECK.
C THE VERTICAL AND HORIZONTAL MOMENTUMS ARE COMPUTED FOR THE INTERIOR MASS
C POINTS.
18 DO 19 I=3,INP
   VH=VH+C5*UDB(I,1)
19 VV=VV+C5*UDB(I,2)
C THE FOLLOWING STEPS ADJUST THE MOMENTUMS DEPENDING UPON THE SUPPORT CONDITIONS
C AND COMPUTE THE IMPULSE ON THE MEMBER.
   IF(BCX1-FREE)20,21,20
21 VH=VH+C2*UDB(2,1)
   FDH=FDH-P(2)*DT
   GO TO 22
20 FDH=FDH+DT*(TRST(2)*C(2)+TRSTA(2)*CA(2)+C3*( V(2) *S(2)
1+ VA(2) *SA(2)))*0.5
22 IF(BCY1-FREE)23,24,23
24 VV=VV+C2*UDB(2,2)
   FDV=FDV+P6(2)*DT*C4
   GO TO 25
23 FDV=FDV+DT*(TRST(2)*S(2)+TRSTA(2)*SA(2)-C3*( V(2) *C(2)
1+ VA(2) *CA(2)))*0.5
25 IF(BCXN-FREE)26,27,26
27 VH=VH+C2*UDB(INP2,1)
   FDH=FDH-P(INP2)*DT
   GO TO 28
26 FDH=FDH-DT*(TRST(INP)*C(INP)+TRSTA(INP)*CA(INP) +C3*( V(INP)
1 *S(INP) + VA(INP) *SA(INP)))*0.5
28 IF(BCYN-FREE)29,30,29
30 VV=VV+C2*UDB(INP2,2)
   FDV=FDV+P6(INP2)*DT*C4
   GO TO 31
29 FDV=FDV-DT*(TRST(INP)*S(INP)+TRSTA(INP)*SA(INP)-C3*( V(INP)
1 *C(INP) + VA(INP) *CA(INP)))*0.5

```



```

C THIS STEP COMPUTES THE IMPULSE DUE TO THE EXTERNAL LOADS ACTING UPON THE
C MEMBER.
  31 DO 32 I=3,INP
    FDH=FDH-DT*P(I)
  32 FDV=FDV+DT*P6(I)*C4
C THE FOLLOWING STEPS FINALIZE THE PROCEDURE.
  DO 33 I=2,INP2
    VA(I)=V(I)
    BSA(I)=BS(I)
    ESA(I)=ES(I)
    BMA(I)=BM(I)
    TRSTA(I)=TRST(I)
    XA(I,1)=X(I,1)
    XA(I,2)=X(I,1,2)
    SA(I)=S(I)
  33 CA(I)=C(I)
C IF IT IS TIME TO PRINT, THE ENERGIES AND THE IMPULSE AND MOMENTUM ARE
C SCALED IN AN APPROPRIATE MANNER AND PRINTED OUT.
  IF(.NOT.LP)RETURN
  EIP=E1*C6
  EAP=EA*C6
  EKP=EK*C6
  APK=EAP+EK
  EISASK=EIP-EAP-EKP
  FV=FDV-VV
  FH=FDH-VH
  PRINT 49
  PRINT 50,EIP,EKP,EAP,EISASK,FDH,VH,FH,FDV,VV,FV
  50 FORMAT(1H ,10E13,4)
  49 FORMAT(1H-,7X,*E1*,11X,*EK*,11X,*EA*,6X,*E1- (EA+EK)*,8X,*FDH*,
    110X,*VH*,8X,*FDH-VH*,10X,*FDV*,10X,*VV*,8X,*FDV-VV*)
  RETURN
END

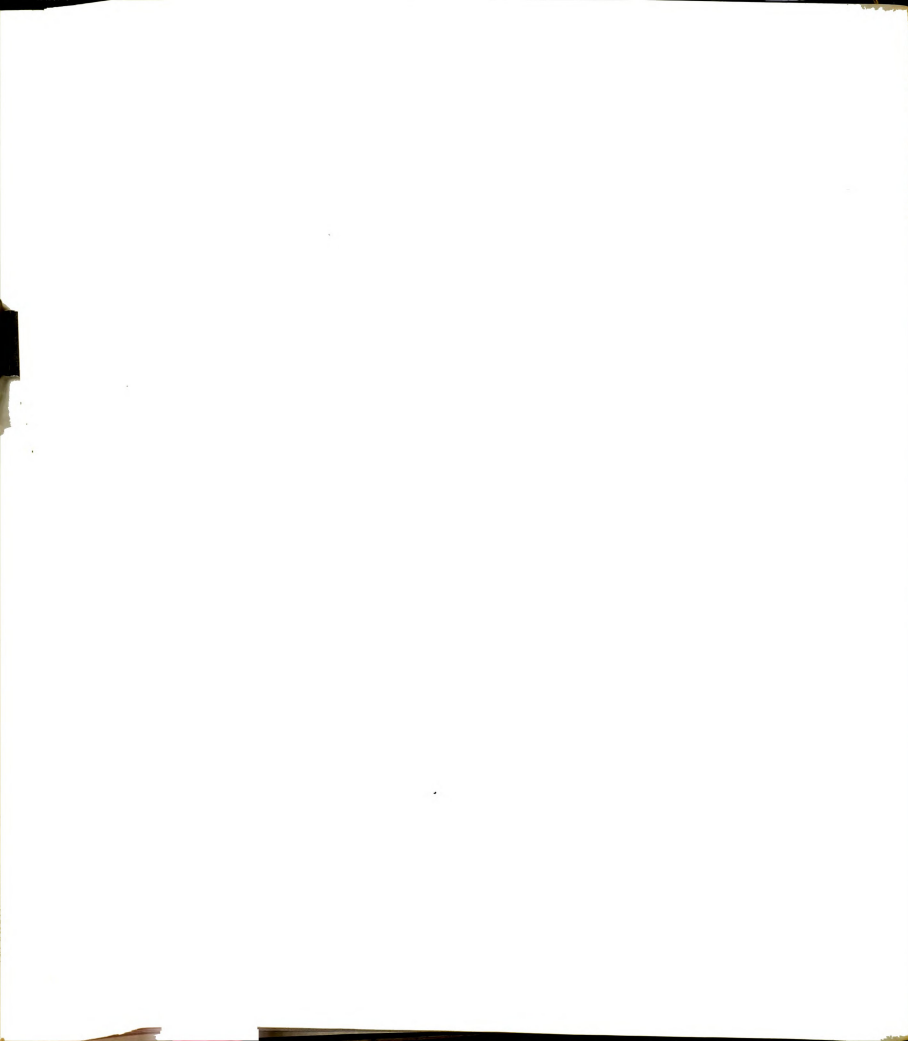
```



```

SUBROUTINE THK(LC,LP,LSTART,UDDA,Uddb,T,TI,RATIO,RAT)
C THIS ROUTINE DOES MISCELLANEOUS CHECKING AND FINALIZING.
  DIMENSION UDDA(41,2),Uddb(41,2)
  COMMON/N/IN,INP,INP2,INP3
  LOGICAL LSTART,LC,LP
  IF(.NOT.LSTART)GO TO 1
  LSTART=.FALSE.
C THE NUMBER OF STEPS BETWEEN PRINT OUTS IS NPRT + 1.
C TMAX IS THE TIME INTERVAL OF THE PROBLEM
C NPR IS THE NUMBER OF PRINTOUTS PER PERIOD OF VIBRATION
  READ 3,TMAX,NPR
  3 FORMAT(6X,F6.2,10X,I3)
  PRINT 3,TMAX,NPR
  IRUT=100.*RAT*NPR
  NPRT=1000*IN*IN/IRUT
  IRATIO=100.*RATIO
  IF(IRATIO.LT.100)NPRT=100*NPRT/IRATIO
  LP=.FALSE.
  IP=NPRT
  1 IF(.NOT.LP)GO TO 11
  LP=.FALSE.
  IF(T.GT.TMAX)LSTART=.TRUE.
C IF THE STEP HAS CONVERGED
  11 DO 9 J=2,INP2
  DO 9 K=1,2
  9 UDDA(J,K)=Uddb(J,K)
C INCREMENT THE TIME.
  5 T=T+TI
C CHECK TO SEE IF IT IS TIME TO PRINT
  IF(IP.LE.0)GO TO 10
C DECREMENT THE PRINT COUNTER, IP.
  IP=IP-1
  LP=.FALSE.
  RETURN
  10 LP=.TRUE.
  IP=NPRT
  RETURN
  END

```

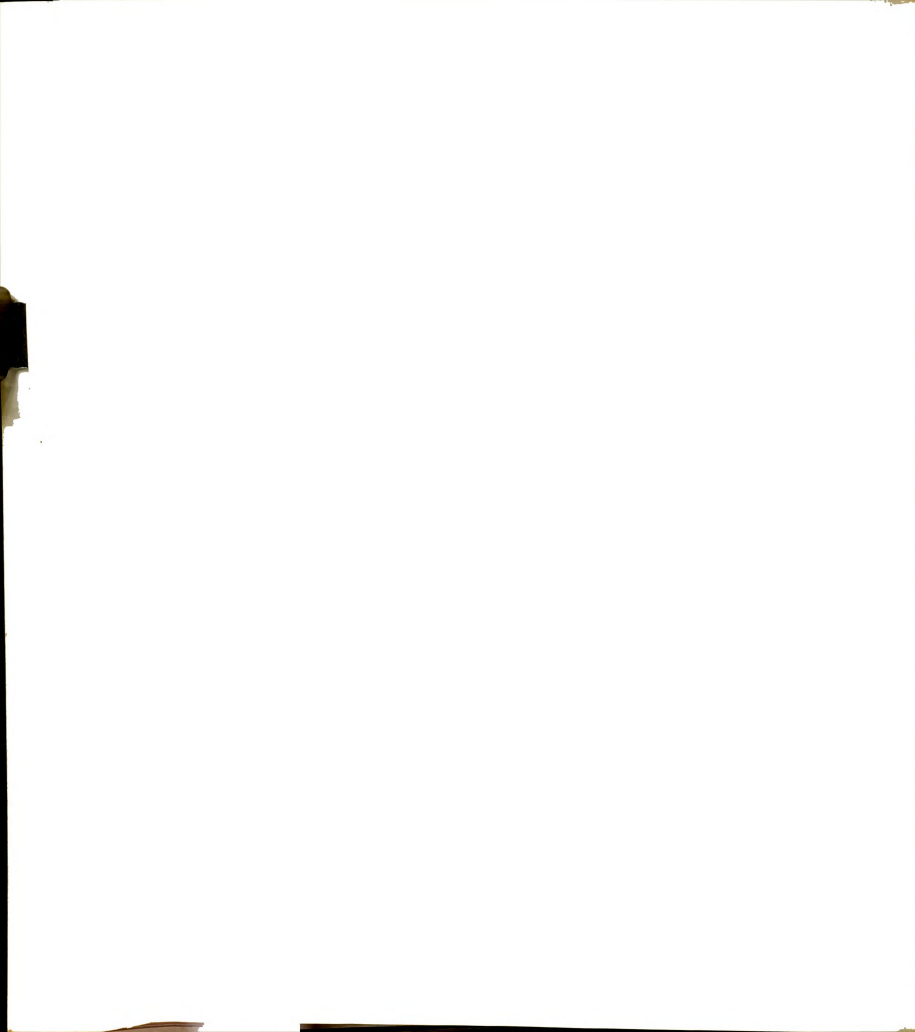



```

SUBROUTINE PLT(X,INP2,T)
C THIS ROUTINE PLOTS THE X AND Y COORDINATES OF THE JOINTS
  DIMENSION X(41,2),LINE(120),IX(41,2)
  COMMON/LRNOFL
C THE NEXT STATEMENT ASSIGNS POINT = **, BLANK = , AND Z= X.
  INTEGER POINT, BLANK, Z
  DATA (POINT=1H,), (BLANK=1H ), (Z=1HX)
C RNOFL = NUMBER OF LINES PER GRAPH
C FIND THE MAXIMUM AND MINIMUM Y COORD
  RMAX=0.
  RMIN=0.
  DO 2 J=2,INP2
    IF(RMAX.LT.X(J,2))RMAX=X(J,2)
    IF(RMIN.GT.X(J,2))RMIN=X(J,2)
  2 CONTINUE
  RANGE=RMAX-RMIN
  IF(RANGE.EQ.0.)SF=60.
  IF(RANGE.NE.0.)GO TO 13
C COMPUTE THE SCALE FACTOR IN THE VERTICAL OR Y DIRECTION
  SF=RNOFL/RANGE
C IF THE MAXIMUM ABSOLUTE DEFLECTION IS GREATER THAN 0.25 SET THE
C SCALE FACTOR SF EQUAL TO 60. THIS WILL PLOT THE X AND Y AXIS TO
C THE SAME SCALE 10 INCHES EQUAL TO ONE UNIT
  IF(RMAX.GT.0.25.OR.-RMIN.GT.0.25)SF=60.
C PRINT OUT THE TIME AND THE VERTICAL SCALE FACTOR
  13 IF(RANGE.GT.1.5)SF=RNOFL/RANGE $ PRINT 10,T
  10 FORMAT(1H1,6HTIME =,E15.7)
  PRINT 11,SF
  11 FORMAT(1H ,16HVERTICAL SCALE =,F6.2,15H LINES PER UNIT,39H HORIZONTAL
  1AL SCALE = 100 SPACES PER UNIT)
  PRINT 12
  12 FORMAT(1H ,42H100 SPACES = 10 INCHES, 60 LINES = 10 INCHES,/)
C CONVERTS FLOATING COORD TO FIXED COORD AND SCALES THEM
  DO 1 J=2,INP2
    IX(J,2)=-(SF*X(J,2)+SIGN(.5,X(J,2)))
    1 IX(J,1)= 100.*X(J,1)+SIGN(.5,X(J,1))

```

2 PLT
 3 PLT
 4 PLT
 5 PLT
 6 PLT
 7 PLT
 10 PLT
 11 PLT
 13 PLT
 14 PLT
 15 PLT
 16 PLT
 18 PLT
 20 PLT
 21 PLT
 22 PLT
 23 PLT
 24 PLT
 25 PLT
 26 PLT
 27 PLT
 28 PLT
 29 PLT
 30 PLT
 31 PLT



```

C FIND MAX AND MIN FOR VERTICAL DIMENSIONS
MAX=0
MIN=0
DO 3 J=2,INP2
  IF(MAX.LT.IX(J,2))MAX=IX(J,2)
  IF(MIN.GT.IX(J,2))MIN=IX(J,2)
3 CONTINUE
C SET THE COUNTER TO THE NUMBER OF LINES TO BE PRINTED.
ICOUNT=MAX-MIN+1
C PUT BLANKS INTO EVERY SPACE EXCEPT SPACE NO. 20
DO 5 J=1,120
  5 LINE(J)=BLANK
  LINE(20)=POINT
C CHECK TO SEE IF LINE IS X AXIS. IF YES PUT DOT IN EVERY SPACE
  IF(ICOUNT.NE.1-MIN)GO TO 6
  DO 7 J=1,120
    7 LINE(J)=POINT
C NOW, PUT APPROPRIATE POINTS ON THE LINE
DO 8 J=2,INP2
  IF(IX(J,2).NE.ICOUNT+MIN-1)GO TO 8
  K=1X(J,1)
  LINE(K+20)=Z
8 CONTINUE
C PRINT THE ASSEMBLED LINE
PRINT 9,LINE
9 FORMAT(1H ,120A1)
C DECREMENT THE COUNTER BY SUBTRACTING ONE
ICOUNT=ICOUNT-1
C CHECK TO SEE IF ALL THE DATA HAS BEEN PLOTTED
  IF(ICOUNT.GT.0)GO TO 4
  RETURN
END

```

PLT 35
 PLT 36
 PLT 37

 PLT 39
 PLT 40
 PLT 41

 PLT 43
 PLT 44
 PLT 45
 PLT 46
 PLT 47

 PLT 49
 PLT 50
 PLT 51

 PLT 54
 PLT 55
 PLT 56
 PLT 57
 PLT 58
 PLT 59
 PLT 60

 PLT 62
 PLT 63
 PLT 64
 PLT 65
 PLT 66



```

DOUBLE PRECISION FUNCTION DX(H,Y1,Y2)
C THIS FUNCTION COMPUTES THE CHANGE IN THE X COORDINATE FROM ONE MASS POINT TO
C ANOTHER GIVEN THE INITIAL Y COORDINATES.
C AND UNDEFORMED PANEL LENGTHS
  DH=H $ DY=Y2-Y1 $ DH=DH*DH $ DY=DY*DY
  DX=DSQRT(DH-DY)
  RETURN
END
C
C
DOUBLE PRECISION FUNCTION DPNL(X1,X2,Y1,Y2)
C THIS FUNCTION COMPUTES THE STRAINED PANEL LENGTH
C DPNL STANDS FOR DEFORMED PANEL LENGTH
  DZ=X2-X1 $ DY=Y2-Y1 $ DZ=DZ*DZ $ DY=DY*DY
C FINALLY COMPUTING DEFORMED LENGTH
  DPNL=DSQRT(DZ+DY)
  RETURN
END
C
C
FUNCTION DEF(T,LSTART)
C THIS FUNCTION DEFINES THE MOTION OF THE SUPPORTS
C THIS ROUTINE USES LINEAR INTERPOLATION BETWEEN DEFINED POINTS IN TIME.
  DIMENSION TY(20,2)
  LOGICAL LSTART
  IF(.NOT.LSTART)GO TO 1
C READ IN THE HISTORY OF THE MOTION
  READ 2,1,((TY(J,K),K=1,2),J=1,I)
  2 FORMAT(12,/, (BF10.5))
  PRINT 2,1,((TY(J,K),K=1,2),J=1,I)
  N=1
  1 IF(T.GE.TY(N,1))GO TO 3
  DEF=SLP*(T-TY(N-1,1))-TY(N-1,2)
  RETURN
  3 N=N+1
  SLP=(TY(N-1,2)-TY(N,2))/(TY(N,1)-TY(N-1,1))
  GO TO 1
END

```









MICHIGAN STATE UNIV. LIBRARIES



31293108164090